NORTHWESTERN UNIVERSITY

Structural and Functional Analyses of Herpes Simplex Virus Type1
Glycoproteins B and L, Two Essential Components of the
Viral Fusogenic Complex

A DISSERTATION

SUBMITTED TO THE GRADUATE SCHOOL
IN PARTIAL FULFULLMENT OF THE REQUIREMENTS

for the degree

DOCTOR OF PHILOSOPHY

Field of Microbiology and Immunology

Integrated Graduate Program in Life Sciences

By

Erick Lin

CHICAGO, ILLINOIS

DECEMBER 2008

ABSTRACT

Structural and Functional Analyses of Herpes Simplex Virus Type 1 Glycoprotein B and

L, Two Essential Components of the Viral Fusogenic Complex

Erick Lin

Herpes simplex virus (HSV) infection of host cells requires virus attachment to

the cell surface and subsequent membrane fusion between the virus envelope and host

cell membrane to deliver the nucleocapsid containing the viral genome into the host cell.

A proposed mechanism for HSV glycoprotein-induced membrane fusion is gD binding to

one of its cellular receptors, induces gD to undergo a conformational change, resulting

in interactions with gH-gL and/or gB to trigger membrane fusion. Recently, gH-gL,

along with gD and a gD receptor, were shown to induce hemifusion (Subramanian and

Geraghty, 2007), mixing of the outer leaflets of two lipid bilayers. However, gB was

required in addition for formation of a fusion pore to permit mixing of cytoplasmic

contents in cell fusion or virion contents with cytoplasm in viral entry. The results

suggest a sequential model of gD:gH-gL:gB for HSV-induced membrane fusion.

The overall goal of this study was to identify and characterize regions of gB, gH

and gL critical for membrane fusion. Random linker-insertion mutagenesis was

performed on HSV-1 gB, gH and gL to identify these regions. For HSV-1 gB, a

homotrimer, analyses of 81 mutants revealed that many insertions prevented proper

folding and transport of gB to the cell surface, other insertions were without consequence on expression or function of gB and a third category of insertions permitted proper folding, oligomerization and cell surface expression but abrogated function in cell fusion and viral entry. The latter insertions were between residues exposed to the surface of the trimer, identifying regions that may be critical for functional interactions with other viral proteins or cellular components or for transitions from the prefusion to postfusion state. For HSV-1 gH, the panel of mutants is being studied by another graduate student. For HSV-1 gL, analyses of 15 mutants identified domains critical for dimerization with gH and for cell fusion activity, demonstrated that gL has differentiable roles in cell fusion and viral entry, both of which are dissociable from its role in mediating transport of gH to the cell surface, and showed that gL, which can be secreted from cells in the absence of gH, binds to the cell surface.

AKNOWLEDGEMENTS

I would like to express my gratitude and appreciation to everyone who supported me during this work. First and foremost, I would like to thank my thesis advisor, Dr. Patricia Spear, who has provided me invaluable scientific insight, guidance and support throughout my time in her lab. I truly enjoyed the freedom to explore projects ranging from structure-function studies of viral glycoproteins to pathogenesis studies in mice. I have learned how to be a successful scientist by having Pat as a role model and teacher. I have greatly benefited from her perspectives and would feel fortunate to have even a fraction of the success that she has had in her illustrious scientific career in the future.

I would also like to thank the past and present members of the Spear Lab, including Nanette Susmarski, Sharmila Manoj, Craig Steffel, Joann Taylor, Anna Zago, Miri Yoon, Cheryl Jogger, Robert Geraghty, Nancy Ruel, Vonia Thompson, Karen Illing, Wanda Martinez, Deepak Shukla, and Dawn Myscofski. Special thanks to Joann and Nanette for all of your hard work and dedication as we spent years working together as a team to finish up the animal study. I also wanted to thank all the members of the Longnecker lab for your kindness and support.

Thank you to all of my committee members, Dr. Adriana Ferreira, Dr. Alan Hauser, Dr. Richard Longnecker and Dr. Greg Smith for their mentorship and guidance. I truly appreciate the time and effort that you have all put into my graduate experience. I am very grateful for your insights and suggestions during our committee meetings.

I would like to acknowledge the NIH F30- NS049726 pre-doctoral fellowship grant and the Medical Scientist Training Program at Northwestern University for financial support, and the large number of faculty and staff in the Microbiology-Immunology Department.

Last, but certainly not least, thank you to my wife and family for all of your patience and support as I study far away from Southern California. You are all in my thoughts and I hope to return home in the not too distant future.

DEDICATION

I want to dedicate this dissertation to my wife, Katty Hsu Lin, for all of her support and patience as I make my long journey through the Northwestern MSTP Program. Thank you and I love you very much.

I also dedicate this thesis to my family, especially my sister, who is currently battling a very serious illness. You inspire me to continue on my path and I am very thankful to have a chance to help you in your time of need.

TABLE OF CONTENTS

LIST OF TABLES

LIST OF FIGURES

CHAPTER 1: INTRODUCTION

General principles of virus-induced membrane fusion

For enveloped viruses, the viral envelope surrounds and protects a proteinaceous nucelocapsid encasing the viral genome. The viral envelope, derived from the lipid membrane of the host cells, is studded with proteins encoded by the viral genome and possibly the host genome as well. Membrane fusion induced by viral glycoproteins permits virus entry into a host cell to deliver the viral genome, and in permissive cells allows for a productive infection with formation of progeny virus. The viral glycoproteins that mediate fusion of the viral envelope with host cell plasma membrane can also mediate cell-to-cell spread of the virus by inducing membrane fusion between adjacent cells.

Virus-induced membrane fusion for enveloped viruses typically begins with the binding of a viral ligand to a receptor expressed on the host cell. This initial attachment, or binding, step localizes the viral fusion machinery in close proximity to the plasma membrane of the host cell where the membrane fusion occurs, in cases where fusion occurs on the cell surface (Jahn et al., 2003). For viruses where membrane fusion occurs with endosomal membranes, the initial attachment step induces endocytosis of the virus and subsequent fusion with the endosomal membrane, which in some cases is triggered by the low pH within the endosome.

The minimal steps required for membrane fusion to occur are: (1) bridging of the two opposing membranes (i.e. viral envelope/cell membrane or infected cell membrane/uninfected cell membrane) and (2) mixing of the outer leaflets of the

opposing membrane with formation of the fusion pore. The initial step of bridging opposing membrane requires viral fusion proteins containing two domains, a transmembrane domain (TM) and fusion peptide. The TM anchors fusion proteins to the viral envelope (or infected cell membrane) while the fusion peptide, upon induction of a fusion event, inserts into the opposing uninfected cell membrane. As the fusion proteins refold, the outer leaflets of the lipid bilayers are brought into close proximity and begin mixing resulting in an intermediate hemifused state, characterized by lipid mixing without content mixing between the two compartments (virus/cell cytoplasm or infected cell/uninfected cell cytoplasm). During the final stage, the fusion proteins complete their refolding, resulting in complete fusion of the opposing membranes and formation of a fusion pore to permit content mixing. It is believed that the energy released from the transition of a metastable pre-fusion form to a stable post-fusion form of the fusion proteins provides the driving force for membrane fusion(Heinz et al., 2004; Stiasny et al., 2001).

The current understanding of the mechanism of virus-induced membrane fusion is derived in part from the x-ray structures of known virus fusion proteins. Two distinct classes of virus fusion proteins have thus far been identified. The fusion proteins are categorized as class I or class II fusion proteins based on properties of the proteins. Table 1.1 lists the virus family, specific virus and name of the fusion protein for known class I and class II fusion proteins(Kielian and Rey, 2006).

Table 1.1. Class I and class II virus fusion proteins.

Virus family	Examples

Class I	
Orthomyxoviridae	Influenza virus (HA2 protein)
Paramyxoviridae	Simian virus 5 (F1 protein)
Filoviridae	Ebola virus (GP2 protein)
Retroviridae	Moloney murine leukemia virus (TM protein) HIV-1 (gp41 protein)
Coronaviridae	Mouse hepatitis virus and SARS virus (S2 proteins)

Class II	
Flaviviridae	(E proteins) of flaviviruses tick-borne encephalitis and dengue viruses
Togaviridae	(E1 protein) of alphavirus Semliki Forest virus

HA, haemagglutinin; SARS, severe acute respiratory syndrome;

TM, transmembrane; gp/GP, glycoprotein.

Reference: Kielian and Rey, Nature Reviews Microbiology, 2006 (Kielian and Rey, 2006).

Although the steps for membrane fusion induced by class I and class II fusogenic glycoproteins appear to be similar, there are distinct differences between these two classes in the pre-fusion conformation, secondary structures, post-fusion conformation, maturation to the pre-fusion form and location of the fusion peptide. Class I fusogenic machinery may require only a trimeric cleavage-activated fusion protein containing both a receptor-binding domain and fusion peptide or a 2-component system with a separate trimeric cleavage-activated fusion protein in complex with a separate receptor-binding protein. The class II machinery may also require both a fusion protein and separate receptor-binding protein (Kielian and Rey, 2006).

Figure 1.1 illustrates membrane fusion carried out by influenza virus hemagglutinin (HA), the prototype of class I fusion proteins. HA is translated as a single polypeptide but has its receptor-binding and fusion-inducing domains separated on the two subunits generated by proteolytic cleavage. In the native prefusion state, HA exists as a trimer, composed primarily of α-helices. HA binding to its receptor induces endocytosis while a subsequent decrease in pH within the endosomal compartment triggers release of a buried N-terminal fusion peptide and its insertion into the opposing membrane (Skehel and Wiley, 2000).   As HA undergoes a conformational change, the outer lipid bilayers first mix, then the inner lipid bilayers mix and finally a fusion pore is formed allowing for content mixing. The post-fusion conformation consists of a trimer of hairpins with an α-helical coiled core.

Figure 1.1. Schematic diagram of class I – mediated membrane fusion.

Influenza virus hemagglutinin (HA) is depicted in its trimeric pre-fusion conformation (dotted bracket). Asterisks (*) indicate differences observed between class I and class II fusion proteins. [1] After the HA receptor binding domain (yellow) interacts with its cell surface receptor, the influenza virus is taken into the cell by endocytosis. After exposure to the low pH in the endosomal compartment, the sequestered N-terminal fusion peptide (red), buried within the trimer, is released and inserts into the opposing cell membrane. Only one chain of the trimer is shown for clarity. [2] As the HA trimer refolds, the fusion peptide and transmembrane anchor (orange) are brought towards each other and the outer leaflets of the opposing membranes begin to mix, resulting in hemifusion. [3] Mixing of the inner leaflets results in formation of a fusion pore and content mixing. The post-fusion form of HA, in a "trimer of hairpins" conformation, is stabilized by an α-helical coiled core indicated by the dashed circles.

Figure 1.1. Schematic diagram of class I – mediated membrane fusion.
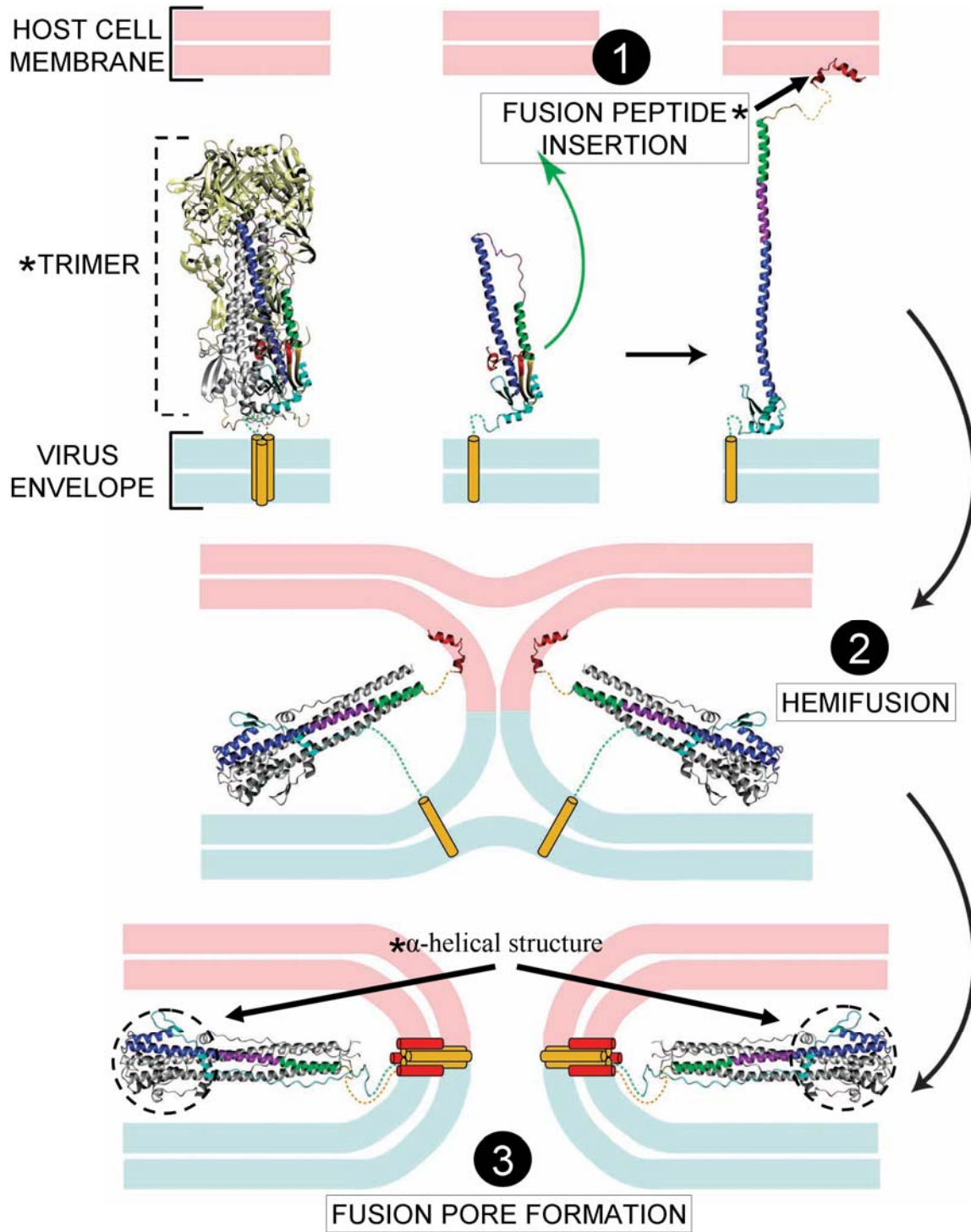
Adapted from (Schibli and Weissenhorn, 2004)

For class II fusion proteins, an internal fusion loop is sequestered through formation of class II fusion protein homo-dimers or formation of hetero-dimers with a receptor-binding glycoprotein partner (Kielian and Rey, 2006). Once homo- or hetero-dimers are exposed to a signal for triggering fusion, such as receptor binding or a decrease in pH, a fusion loop located at the ends of a β-sheet is exposed, allowing for insertion of the fusion loop into the opposing membrane (Wahlberg et al., 1989; Wahlberg et al., 1992; Wahlberg and Garoff, 1992). Figure 1.2 illustrates membrane fusion carried out by Semliki forest virus E1 (SFV E1), a prototype of class II fusion proteins. In the native pre-fusion state, SFV E1 forms a hetero-dimer with its receptor-binding glycoprotein (E2) partner, composed primarily of β-structures. Interaction of E2 with its receptor induces endocytosis while a subsequent decrease in pH within the endosomal compartment triggers dissocation of the E1-E2 hetero-dimer. The E1-E2 dissociation results in trimerization of E1 and exposes an internal fusion loop that then inserts into the opposing membrane. Under low pH conditions, E1 undergoes conformational changes and rearranges into a "trimeric hairpin" post-fusion state composed of β-structures resulting in hemifusion and fusion pore formation with content mixing.

Figure 1.2. Schematic diagram of class II – mediated membrane fusion.

Semliki forest virus E1 (SFV E1) is depicted in its heterodimeric pre-fusion conformation

with the receptor-binding glycoprotein E2 (dotted bracket). Asterisks (*) indicate

differences observed between class I and class II fusion proteins. [1] After E2 interacts

with its cell surface receptor and endocytosis occurs along with a drop in pH, the

internal fusion loop (green loop in yellow domain), is released from sequestration as the

E1-E2 heterodimer dissociates. The released fusion loop then inserts into the opposing

membrane. [2] As E1 refolds, the fusion loop and transmembrane anchor (orange) are

brought towards each other and the outer leaflets of the opposing membranes begin to

mix resulting in hemifusion. [3] Mixing of the inner leaflets results in formation of a

fusion pore and content mixing. The post-fusion form of E1, in a "trimer of hairpins"

conformation, is stabilized by a β-structured core indicated by the dashed circles.

Figure 1.2. Schematic diagram of class II – mediated membrane fusion.
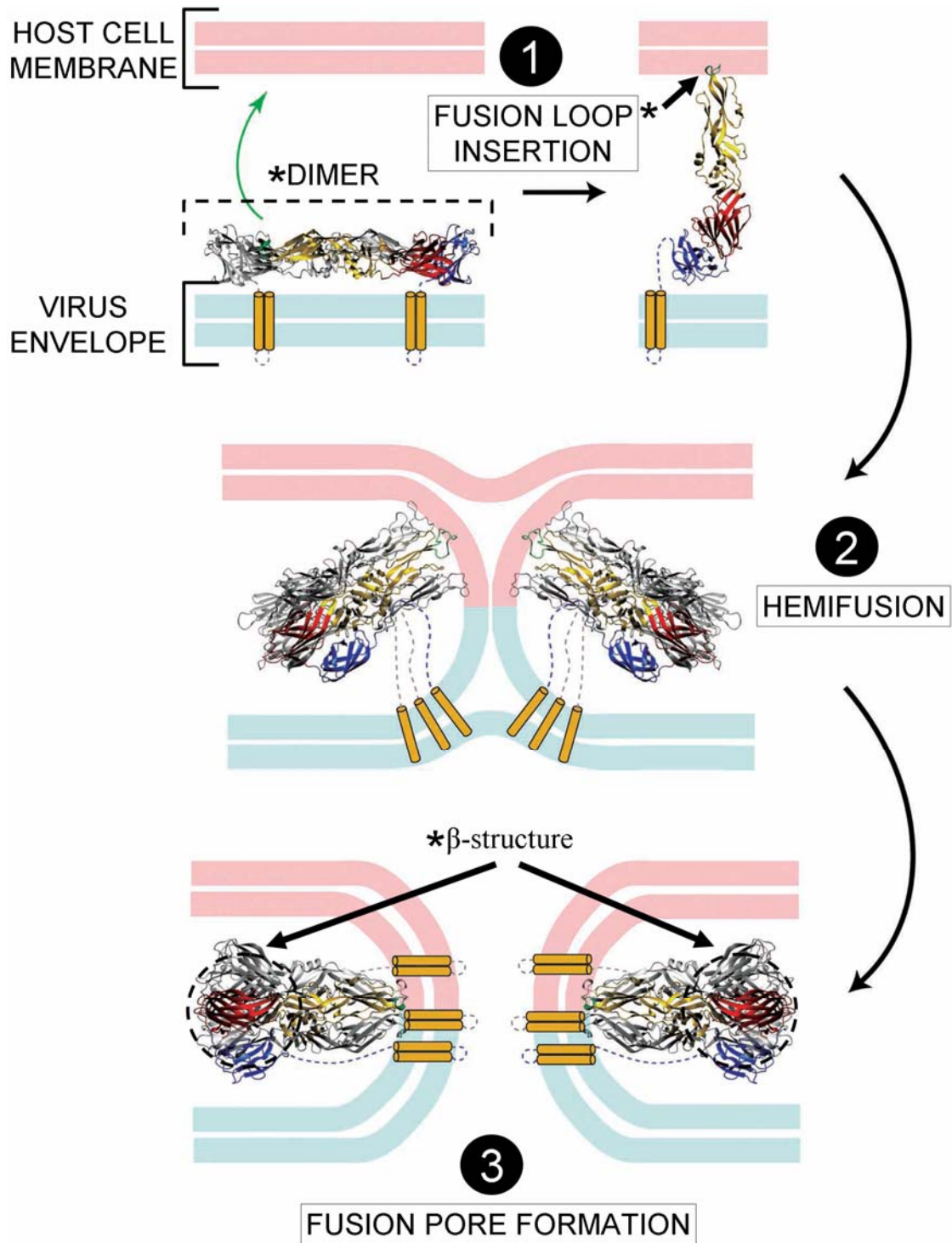
Adapted from (Schibli and Weissenhorn, 2004)

Comparisons between the prototypes for class I (influenza HA) and class II (SFV E1) fusion proteins indicate that, although their structures are very different, they both undergo refolding during fusion that results in a post-fusion trimeric hairpin conformation, one composed largely of α-helices and the other of β-sheets or strands. Both classes of fusion proteins require a trigger such as interaction with a binding receptor or decrease in pH. In addition, the general mechanism for membrane fusion appears to be the same, with bridging of the opposing membranes, hemifusion intermediate and, finally, fusion pore formation.

Table 1.2 summarizes the differences between HA and SFV E1, showing that, in their pre-fusion forms, HA assumes a trimer conformation composed mostly of α-helices while E1 assumes a hetero-dimer conformation composed mostly of β-helices. Class I fusion proteins typically have N-terminal fusion peptides while class II fusion proteins have internal fusion loops. Even though both class I and class II fusion proteins bend into trimeric hairpin structures post-fusion, class I trimeric hairpins are stabilized by an α-helical coiled core while β-structures stabilize class II trimeric hairpins.

Table 1.2. Comparison of class I and class II virus membrane-fusion proteins.

Feature	Class I (influenza HA)	Class II (SFV E1)
Conformational change during fusion	Metastable fusion protein trimer to stable fusion protein trimer	Metastable dimer to stable fusion protein trimer
Predominant secondary structure of fusion protein	α-helix	β-sheet
Post-fusion structure	Trimer of hairpins with central α-helical coiled coil	Trimer of hairpins composed of β structure
Maturation to prefusion state through:	Proteolytic processing of fusion protein	Proteolytic processing of companion protein
Fusion peptide location in metastable structure	N-terminal peptide buried in trimer interface	Internal loop at fusion protein tip, capped by dimer interaction

HA, haemagglutinin; SFV, Semliki Forest virus.

Reference: Kielian and Rey, Nature Reviews Microbiology, 2006 (Kielian and Rey, 2006).

Herpesviridae family and human diseases

The family *Herpesviridae* comprises a large family of enveloped DNA viruses that infect humans and a broad range of animal hosts.   The family is divided into 3 subfamilies (*Alphaherpesvirinae*, *Betaherpesvirinae*, and *Gammaherpesvirinae*) based on distinct biological properties. The alphaherpesviruses are neurotropic viruses with a broad host range, *in vivo* and *in vitro,* and a short replicative cycle in cell culture. They are destructive to host cells during lytic infections and have the capacity to establish latent infections within neurons of sensory and autonomic ganglia. The betaherpesviruses are viruses with a more restricted host range, long reproductive cycles and the capacity to establish latent infections in secretory glands, lynphoreticular cells, kidneys and lymphoid tissues. Lastly, the gammaherpesviruses are lymphotropic viruses with a very restricted host range that do not replicate well in cell culture. Of the *Herpesviridae* family, 8 are known to infect the human host. Table 1.3 summarizes the subfamily and diseases caused by each human herpesvirus.

Table 1.3. Human Herpesvirus (HHV) classification.

Type	Synonym	Subfamily	Pathophysiology
HHV-1	Herpes simplex virus-1 (HSV-1)	α (Alpha)	Oral and/or genital herpes (predominantly orofacial), keratitis, encephalitis
HHV-2	Herpes simplex virus-2 (HSV-2)	α	Oral and/or genital herpes (predominantly genital), meningitis, neonatal herpes
HHV-3	Varicella zoster virus (VZV)	α	Chickenpox and shingles
HHV-4	Epstein-Barr virus (EBV), lymphocryptovirus	γ (Gamma)	Infectious mononucleosis, Burkitt's lymphoma, CNS lymphoma in AIDS patients, post-transplant lymphoproliferative syndrome (PTLD), nasopharyngeal carcinoma
HHV-5	Cytomegalovirus (CMV)	β (Beta)	Infectious mononucleosis-like syndrome, retinitis, congenital deafness and mental retardation
HHV-6, -7	Roseolovirus	β	*Sixth disease (roseola infantum or exanthem subitum)*
HHV-8	Kaposi's sarcoma-associated herpesvirus (KSHV), a type of rhadinovirus	γ	Kaposi's sarcoma, primary effusion lymphoma, some types of multicentric Castleman's disease

Reference: Fields Virology (5th edition), 2007.

Herpes simplex viruses and human diseases

Herpes simplex viruses 1 and 2 (HSV-1 and HSV-2) are two distinct serotypes but more closely related to each other than to other human herpesviruses. Worldwide, the prevalence of HSV-1 and HSV-2 infections differs based on geographic area and subpopulations. In the United States, the US population-based NHANES III study showed a consistent increase of HSV-1 prevalence with age, increasing from 44% in young adults (12–19 years) to 90% among those >70 years old. For HSV-2, the study found that the overall prevalence of HSV-2 seropositivity was 21.9% with a higher prevalence in females than males (overall 26% vs. 18%) (Smith and Robinson, 2002).

For initial, or primary, infection of humans, a range of clinical symptoms is observed, including mucocutaneous lesions of the oral epithelium ("cold sores," "fever blisters") or genital epithelium, lesions on the cornea and, in rare cases, encephalitis. During primary infection, the virus enters nerves innervating the site of infection and is transported in the retrograde direction along axons. HSV then establishes latency, during which the viral genome is stably maintained in the cell bodies of the neurons in sensory ganglia innervating the area of the original outbreak. Although the molecular mechanisms are not well understood, certain factors such as stress or exposure to UV radiation, can cause reactivation of the virus leading to recurrent outbreaks. During reactivation, the virus is produced within the cell body of neurons innervating the site of infection and transported in the anterograde direction down the axon to the skin surface.

No cure is available for HSV-1 and HSV-2 infections, but treatment with anti-viral medications such as acyclovir reduces the frequency of clinically evident reactivation and viral shedding.

Herpes simplex virus infection of host cells and membrane fusion

Infection of host cells occurs through virus attachment to the cell surface and subsequent membrane fusion to deliver the nucleocapsid containing the viral genome into the host cell. Virus attachment is mediated by binding of glycoproteins gC or gB to cell surface glycosaminoglycans (GAGs), primarily heparan sulfate (Shukla and Spear, 2001). Subsequent fusion between the virion envelope and a host cell membrane requires glycoproteins gB, gD, and the heterodimer gH-gL and one of the cellular receptors for gD. These receptors include HVEM, a member of the TNF receptor family; nectin-1 and nectin-2, cell adhesion molecules of the immunoglobulin superfamily; and specific sites in heparan sulfate generated by 3-O-sulfotransferases (Spear et al., 2000). It has been proposed that binding of gD to one of its cellular receptors induces gD to undergo a conformational change, resulting in interactions with gB and/or the gH-gL complex to trigger membrane fusion (Krummenacher et al., 2005; Rey, 2006).

The exact roles for gB and gH-gL in the membrane fusion process have yet to be elucidated. Recently, it was shown (Subramanian and Geraghty, 2007) that gH-gL, along with gD and a gD receptor, were sufficient to induce hemifusion, mixing of the

outer leaflets of two lipid bilayers. However, gB was required in addition for formation of a fusion pore to permit mixing of cytoplasmic contents in cell fusion or mixing of virion contents and cytoplasm in viral entry.
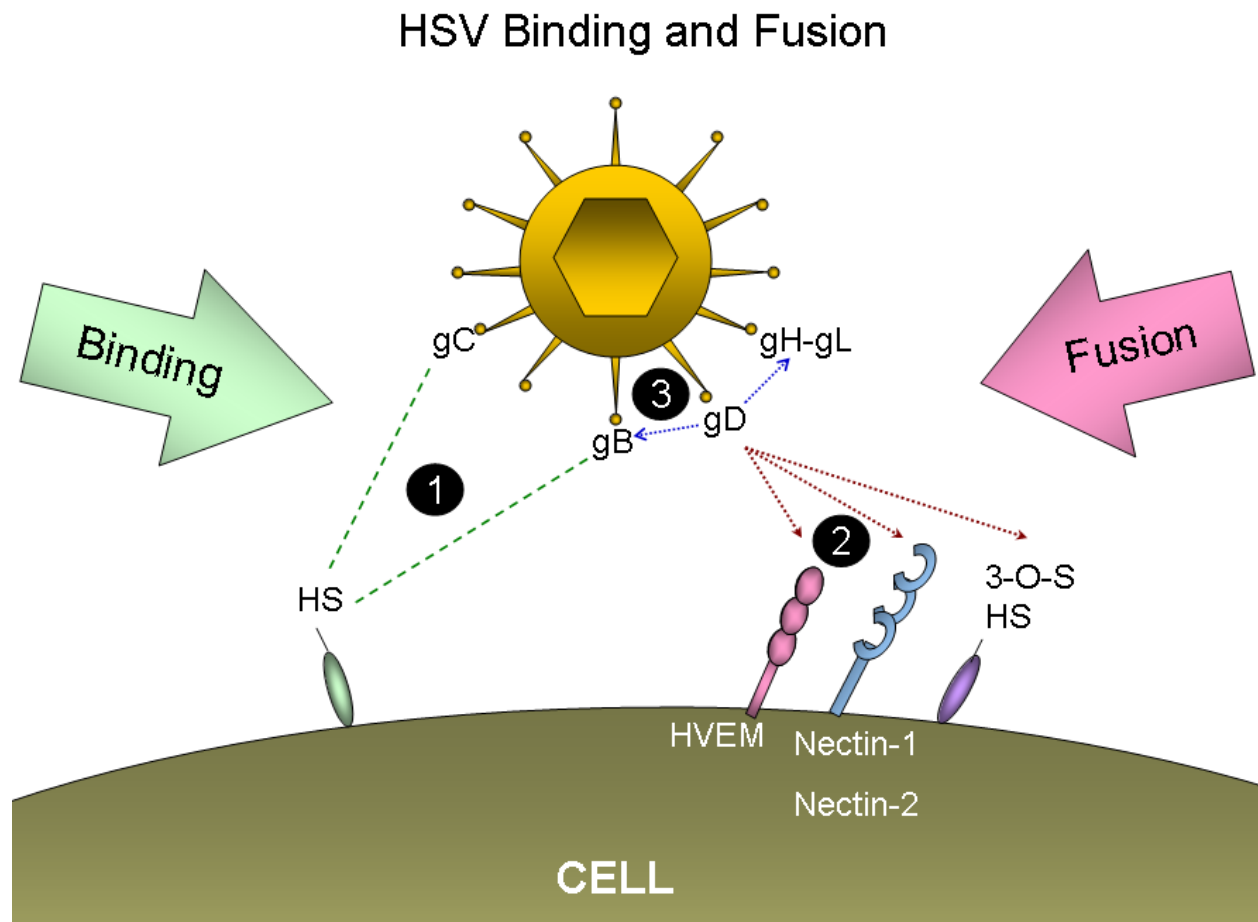
Figure 1.3. HSV binding and fusion to host cells. This diagram illustrates the steps of HSV entry into host cells. [1] Initial binding (green dashed lines) of HSV is mediated by gC or gB binding to cell surface heparan sulfate (HS). [2] gD binds to one of its cell surface receptors (red dashed arrows). [3] Upon binding to a gD-receptor, gD undergoes a conformational change resulting in interactions (blue dotted arrows) with gB and/or gH-gL complex to trigger membrane fusion.

Herpes simplex virus glycoprotein B

HSV type1 (HSV-1) gB is the most highly conserved entry glycoprotein (Norton et al., 1998). HSV-1 gB is initially translated as a 904 amino acid (a.a.) precursor protein containing a signal peptide, a large ectodomain, a single transmembrane domain, and a long cytoplasmic tail. After signal peptidase cleavage, gB is expressed on the cell surface as a 874 a.a. type I membrane protein. Currently, several lines of evidence exist to support the role of gB as a fusion glycoprotein. Deletions or amino acid substitutions in the gB cytoplasmic tail were shown to modulate (enhance or reduce) cell fusion activity (described and reviewed in Ruel et al., 2006), a property also observed with the certain class I viral fusion proteins. In addition, a recent x-ray structure of most of the ectodomain of gB reveals that it exists as a trimer and has characteristics of both class I and class II viral membrane fusion proteins (Heldwein et al., 2006). Figure 1.1 shows the surprising structural homology between HSV-1 gB and glycoprotein G of the unrelated vesicular stomatitis virus (VSV), the glycoprotein solely responsible for entry of VSV. These findings strongly suggest that gB may be the key effector glycoprotein in HSV-1 glycoprotein-mediated membrane fusion.

.
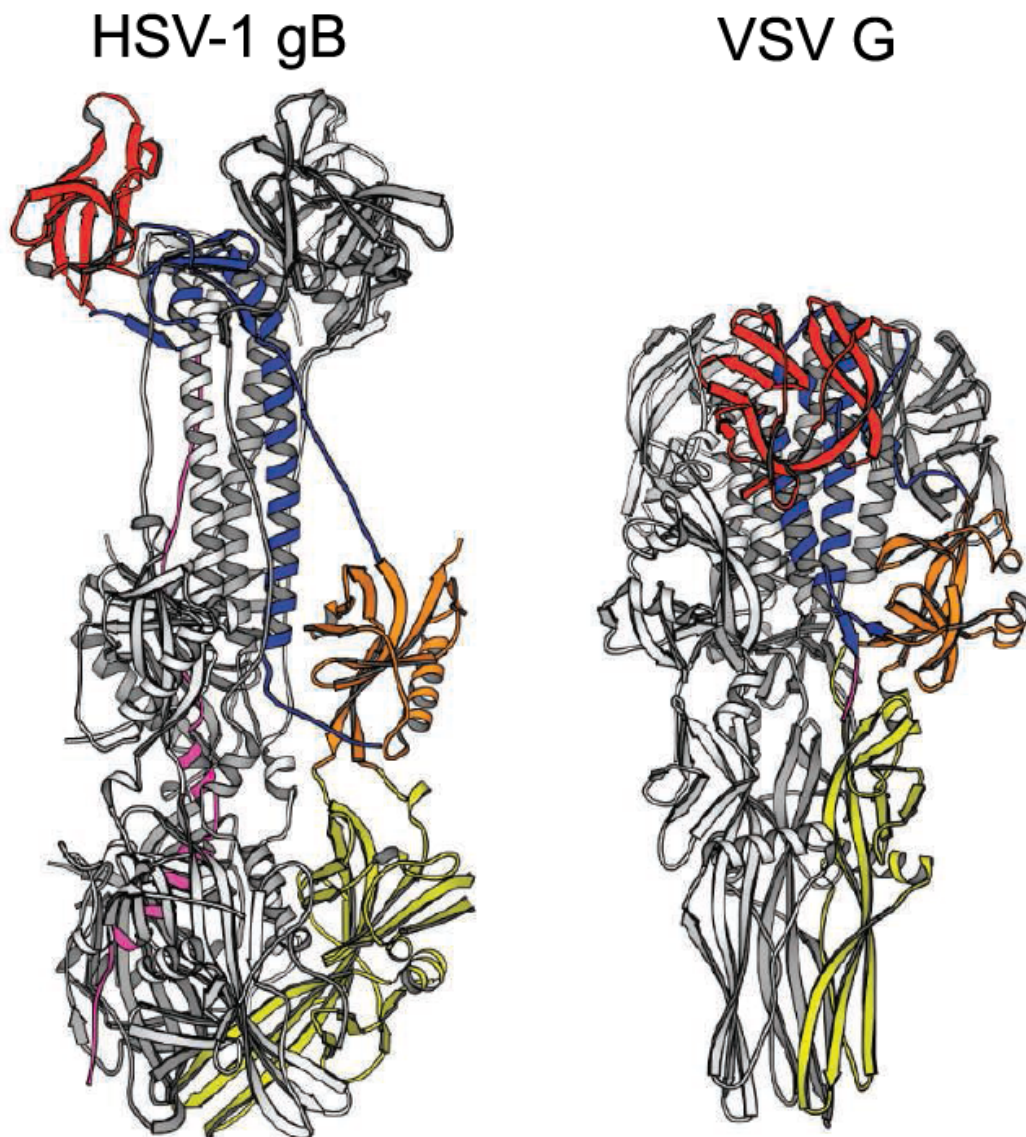
HSV-1 gB

VSV G

Adapted from Steven and Spear, Science 2006.

Figure 1.4. Comparison between the x-ray structures of HSV-1 gB and VSV G.

The x-rays structures of HSV-1 gB (left) and VSV-G (right) are shown. Four of the color-coded regions (red, blue, orange and yellow) indicate homologous structural domains of the two proteins. HSV-1 gB contains a fifth structural domain (pink) that is not found in VSV-G.

Herpes simplex virus glycoproteins H and L

HSV-1 gL and gH have previously been shown to associate stably to form

heterodimers (Hutchinson et al., 1992). In the absence gL, gH is not transported to the

Golgi apparatus or cell surface and remains in the endoplasmic reticulum (ER) as an

immature form (Foa-Tomasi et al., 1991). In the presence of gL, gH heterodimerization

with gL permits its transport out of the ER for maturation of N-linked glycans and for the

addition of O-linked glycans in the Golgi prior to transport to the cell surface (Hutchinson

et al., 1992). Previous and recent studies have shown that the gH-gL heterodimer

forms a functional unit necessary for cell fusion and virus entry (Cairns et al., 2007;

Davis-Poynter et al., 1994; Roop et al., 1993).

It has been proposed that certain regions in gH might function as a fusion peptide

and as heptad repeats that fold up into 6-helix bundles (Gianni et al., 2005a; Gianni et

al., 2005b; Gianni et al., 2006). A recent study of N-terminal truncations of HSV-2 gH

demonstrated that gH2 deleted for the first 48 amino acids (after the signal peptide)

could be transported to the cell surface in the absence of gL but was not functional in

cell fusion unless co-expressed with gL (Cairns et al., 2007). Therefore, transport and

expression of gH on the cell surface was not sufficient for cell fusion demonstrating that

the functional complex is the gH-gL heterodimer.

Of the four glycoproteins involved in cell fusion and viral entry, the role of gL is

least well-defined. In the absence of gH, HSV-1 gL was secreted from cells and was

not detectable on the cell surface (Dubin and Jiang, 1995). HSV-1 gL does not contain

a transmembrane domain but can be retained on the cell surface through its association with gH (Hutchinson et al., 1992). The retention of gH in the ER in the absence of gL demonstrated that gL, at the very least, has a chaperone-function for gH folding and transport. However, it was shown that anti-gL monoclonal antibodies (mAbs) could inhibit cell fusion but not viral entry, despite demonstrable binding of the mAbs to virus, suggesting that gL also has a functional role, at least in cell fusion (Novotny et al., 1996).

The regions involved in dimerization of gH and gL have been mapped to residues between positions 19 and 323 of HSV-1 gH and residues between positions 23 and 147 of gL (Klyachkin et al., 2006; Peng et al., 1998). Although the first 147 aa of gL are sufficient for association with gH, the gH-gL heterodimer formed was not transported to the cell surface. Transport of the gH-gL heterodimer to the cell surface required the first 161 aa of gL (Klyachkin et al., 2006). For HSV-1, the role of gL in gH transport has not been separated from its potential role in cell fusion. However, certain deletion mutants of HSV-2 gH can be transported to the cell surface in the absence of gL but are not functional in the absence of gL (Cairns et al., 2007).

Recently, a study showing that gH-gL, along with gD and a gD receptor, were sufficient to induce hemifusion (Subramanian and Geraghty, 2007) provided the first insights into the functional role of gH-gL in cell fusion. The interactions between gL and gH necessary to obtain the "functional conformation" (Cairns et al., 2007) and the role of each glycoprotein in cell fusion have yet to be determined.

Purpose

The focus of my research was to perform extensive mutagenesis of HSV-1 gB and gH-gL in order to identify domains required for proper processing, oligomerization and intracellular transport and for membrane fusion as assessed in cell fusion and viral entry assays. At the start of this project, little was known about the events of cell fusion induced by HSV glycoproteins downstream of gD interactions with one of its gD-receptors. Given that most viruses can induce membrane fusion through the action of one or two glycoproteins, it was an intriguing puzzle to investigate how and why four glycoproteins were necessary in the case of HSV-1. I decided to undertake a large-scale random linker-insertion mutagenesis study to identify functional domains of HSV-1 gB and gH-gL necessary for membrane fusion. During the course of the study, another graduate student began analyzing gH mutants while I continued my work with gB and gL.

The goals of this dissertation work were to:

1) Identify regions of HSV-1 gB critical for fusion activity

2) Identify regions of HSV-1 gB critical for trimer conformation

3) Relate regions identified in the gB mutagenesis study to the x-ray structure

4) Identify regions of HSV-1 gL critical for gH binding

5) Determine whether the transport and cell fusion functions of gL can be dissociated from one another

6) Determine how alterations to the conformation of the gH-gL heterodimer affects hemifusion and cell fusion activities

CHAPTER 2: Random linker-insertion mutagenesis to identify functional domains of herpes simplex virus type 1 glycoprotein B. *

* Citation: Lin and Spear, 2007. Random linker-insertion mutagenesis to identify functional domains of herpes simplex virus type 1 glycoprotein B. Proc Natl Acad Sci 104(32):13140-5.

SUMMARY

Herpes simplex virus gB is one of four glycoproteins essential for viral entry and cell fusion. Recently, an X-ray structure of the nearly full-length trimeric gB ectodomain was determined. Five structural domains and two linker regions were identified in what is probably a postfusion conformation. To identify functional domains of gB, we performed random linker-insertion mutagenesis. Analyses of 81 mutants revealed that only 27 could fold to permit processing and transport of gB to the cell surface. These 27 mutants fell into three categories. Insertions into two regions excluded from the solved structure (the N-terminus and the C-terminal cytoplasmic tail) had no negative effect on cell fusion and viral entry activity, identifying regions that can tolerate altered structure without loss of function. Insertions into a disordered region in domain II and the adjacent linker region also permitted partial cell fusion and viral entry activity. Insertions at 16 other positions resulted in loss of cell fusion and viral entry activity, despite detectable levels of cell surface expression. Four of these insertion sites were not included in the solved structure. Two were between residues exposed to a cavity that is too small to accommodate the 5-amino acid insertions, consistent with the solved structure being different from the native prefusion structure. Ten were between residues exposed to the surface of the trimer, identifying regions that may be critical for interactions with other viral proteins or cellular components or for transitions from the prefusion to postfusion state.

INTRODUCTION

Herpes simplex virus gB is one of four glycoproteins essential for viral entry and cell fusion. It has been demonstrated that gB is required for formation of a fusion pore to permit mixing of cytoplasmic contents in cell fusion or mixing of virion contents and cytoplasm in viral entry (Subramanian and Geraghty, 2007). Also, mutations in the cytoplasmic tail of gB have been shown to modulate (enhance or reduce) cell fusion activity (described and reviewed in Ruel et al., 2006), as has also been observed with the class I viral fusion proteins, HIV gp41 (Abrahamyan et al., 2005) and paramyxovirus F protein (Tong et al., 2002). An X-ray structure of a portion of the HSV type1 (HSV-1) gB ectodomain exhibits characteristics of both class I and class II viral membrane fusion proteins (Heldwein et al., 2006).

Surprisingly, HSV-1 gB is structurally homologous to glycoprotein G of vesicular stomatitis virus (VSV), the glycoprotein solely responsible for entry of this virus. The solved structure of gB resembles the postfusion form of G rather than the prefusion form (Roche et al., 2006; Roche et al., 2007). Similar to the postfusion forms of class I fusion proteins, gB has a central coiled coil. Like class II fusion proteins, and by analogy with VSV G protein, the presumed fusion domain of gB is a very elongated, 3-stranded beta sheet with the putative bipartite fusion loops at the tip. Overall, the crystal structure of gB reveals 5 distinct structural domains (I, II, III, IV, and V) and 2 linker regions in each monomer of the trimeric ectodomain. The apparent sequential roles of gH-gL and gB in

HSV-induced membrane fusion and properties of each protein suggest a novel paradigm for fusion mediated by the herpesviruses.

Previous mutagenesis studies of HSV gB to identify functional domains have had limited success due to protein misfolding and aberrant processing of most mutants (Cai et al., 1988; Li et al., 2006; Norton et al., 1998). The fraction of mutants that were expressed on the cell surface and incorporated into virions could be increased by targeting mutations to regions predicted to lack secondary structure but, as a result, most mutants retained significant function or were misfolded despite the targeting. The study presented here was designed to identify functional domains of HSV-1 gB by utilizing a transposon-based random linker-insertion mutagenesis strategy to generate a large library of mutants spanning the entire length of HSV-1 gB, a 904-amino-acid type I membrane protein.

A panel of 81 unique linker-insertion mutants was generated. Characterization of these mutants permits conclusions that (i) the N-terminus and distal cytoplasmic tail of gB (neither included in the X-ray structure) tolerate 5-amino acid insertions without loss of cell surface expression or function, indicating flexibility in structural requirements in these regions; (ii) a disordered region and adjacent linker region within the ectodomain also tolerate insertions but with some loss of function; (iii) all other insertions that permitted cell surface expression were in regions exposed to the trimer surface or to an internal cavity of the trimer (or were outside the solved structure) and were non-functional. These results permit predictions about the prefusion form and functional domains of gB.

RESULTS AND DISCUSSION

Cell Surface Expression, Conformation and Processing of the gB Mutants. To assess expression levels on the cell surface, plasmids encoding each of the mutants were transfected into Chinese hamster ovary (CHO) cells, along with plasmids expressing gD, gH and gL, and the live cells were incubated with an anti-gB rabbit antiserum R74, for detection of gB by a cell-based ELISA (CELISA). The position of each insertion is denoted by the name and number of the amino acid 5' of the 5 amino acid-insertion, counting from the first Met of the gB precursor. Figure 2.1 shows the levels of cell surface gB detected for each mutant, as a percentage of wild-type (WT) gB, in relation to the amino acid position of the insertion. A linear representation of gB is shown below the X-axis and color-coded to identify regions comprising the 5 structural domains (I, II, III, IV, and V) and 2 linker regions identified in the X-ray structure (Heldwein et al., 2006). Mutants detectable on the cell surface were clustered at several distinct regions or positions: near the N-terminus in a region not included in the X-ray structure; at two regions in domain I; at one position in domain II; at 1 position in the disordered central region; at 2 positions in the adjacent linker 2; at 3 positions in the small C-terminal segment of domain III; at 2 adjacent positions in domain V; in a region just downstream of domain V outside the solved X-ray structure and at the membrane-distal region of the cytoplasmic tail. All other insertions abrogated cell surface expression of the mutant gBs or rendered them unrecognizable by the rabbit antiserum.

Table 2.1 summarizes the positions of mutations that were expressed on the cell

surface and indicates domains and secondary structures into which they were inserted.

Table 2.1. Positions of HSV-1 gB linker-insertion mutations relative to structural domains and elements and listing of the mutants expressed on cell surfaces.

Region *	Expressed mutants/Total †	Position of insertion for expressed mutants	Secondary Structure *
N-terminus	4 / 4 ‡	K70, K76, P80, P81	–
Linker 1	0 / 2	–	–
Domain I	4 / 22	I185, E187	β5
		A261, Y265	β11
Domain II	1 / 8	D408	–
Disordered	1 / 1 ‡	R470	–
Linker 2	2 / 2 ‡	I495, T497	Linker 2
Domain III	3 / 9	D663	β36 (proximity)
		T665, V667	β36
Domain IV	0 /10	–	–
Domain V	4 / 8	I671, L673	–
		T690	αE
		A725	–
Membrane-proximal	4 / 8	A730, F732, M742, S772	–
TM	0 / 1	–	–
C-terminal tail	4 / 6 ‡	T868, N886, N894, N894	–
TOTAL	**27 / 81**		

* Domains and secondary structure from Heldwein et. al. (Heldwein et al., 2006)

† Mutants expressed on cell surfaces at levels = or > 10% of WT gB levels, as assessed by CELISA with rabbit antiserum R74.

‡ Expressed mutants that retained cell fusion and viral entry activities.
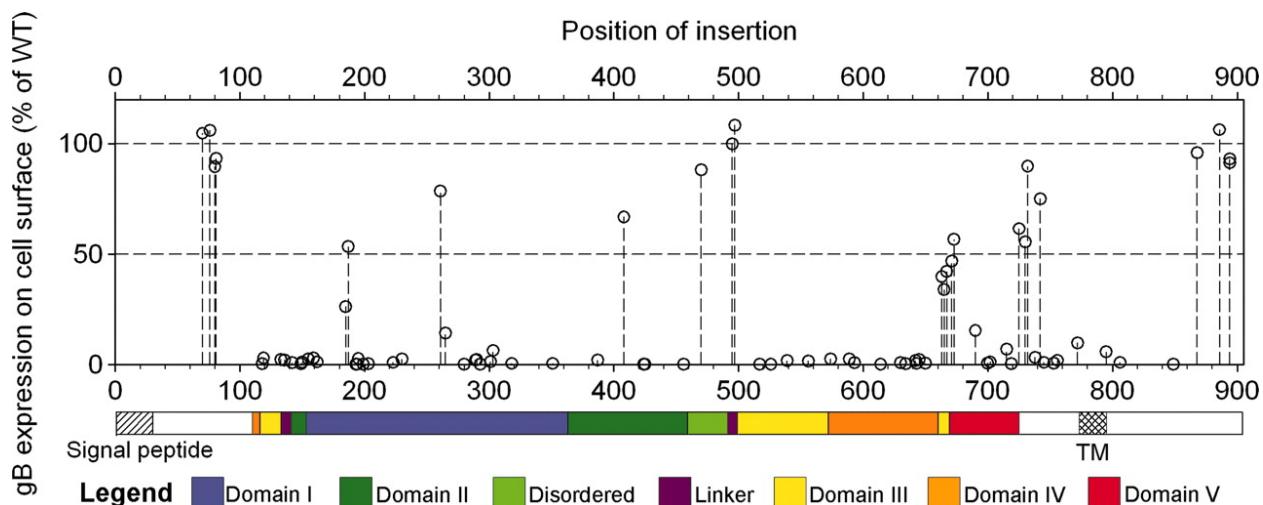
Figure 2.1. Effects of insertional mutations on HSV-1 gB cell surface expression.

CHO cells were transfected as for use as effector cells in cell fusion assays (with plasmids expressing the T7 RNA polymerase, gD, gH, and gL, and plasmids expressing either WT or mutant gB) but not mixed with target cells. Cell surface expression of gB or gB mutant was quantified by CELISA. A linear representation of the gB polypeptide is shown below the graph. The colored bars represent the structural domains of a crystallized portion of the gB ectodomain (Heldwein et al., 2006); the signal peptide and transmembrane (TM) domain are indicated by hatched regions on uncolored portions of gB not included in the crystal structure. The values presented for cell surface expression of each mutant gB are means from three independent experiments expressed as % of WT gB values (after subtraction of background values obtained in the absence of gB expression) and as a function of position of the insertion. Standard deviations (SD) are presented in Figure 2.4 and Table 2.3.

Previously it was shown that certain 2-amino acid insertions into HSV-1 gB or the closely related HSV-2 gB (85% identity) also permitted cell surface expression (Cai et al., 1988; Li et al., 2006). These insertions map to the N-terminal region outside the solved structure (S48, A104: insertion sites in HSV-2 gB at positions equivalent to HSV-1 gB T53 and T109) and to the small N-terminal segment of domain III (P130), linker 1 (R136), domain I (R189, Y254, R304, T313, P358), domain II (G381, S403, G437), the disordered region between domain II and linker 2 (P483), domain V (D680) and the cytoplasmic tail (E816). (The numbering for HSV-1 gB is used for HSV-1 and HSV-2 mutants unless indicated otherwise.) In these other studies and the one described here, all insertions into the central portion of domain III and into domain IV abrogated cell surface expression. Presumably these domains and large portions, but not all, of domains I, II and V cannot contribute to proper folding of gB if disrupted by insertions.

To assess whether mutant gBs expressed on the cell surface were grossly altered in conformation, the CELISA was repeated with a panel of conformation-dependent anti-gB mAbs (Table 2.2). For most mutants, the ratio of mAb binding to polyclonal antibody (R74) binding was essentially equivalent to that observed for WT gB, indicating retention of at least some aspects of WT conformation. Exceptions included T665, V667 and L673, which exhibited reduced or no binding of most or all of the mAbs, relative to binding of R74, and whose insertions are located in the smallest segment of domain III and in the adjacent region of domain V. Also, insertional mutations into the cytoplasmic tail of gB (T868 and N886) resulted in reduced binding of

some or all of the mAbs, indicating that these mutations can alter conformation of the

ectodomain.

Table 2.2. Binding of monoclonal antibodies to selected gB mutants.

Region *	Position of insertion †	Monoclonal antibodies ‡					
		II-105	I-84-5	II-125-4	I-I-7	I-144-2	I-252-4
N-terminus	P80	+++	+++	+++	+++	+++	++
Domain I	I185	+++	+++	+++	+++	++	+++
	E187	+++	+++	+++	+++	++	++
	A261	+++	+++	+++	+++	++	++
Domain II	D408	+++	+++	+++	++	++	++
Disordered	R470	+++	+++	+++	+++	+++	+++
Linker 2	I495	+++	+++	+++	++	++	+++
	T497	+++	+++	+++	+++	+++	+++
Domain III	D663	+++	+++	+++	+++	+++	++
	T665	+	+	–	+	–	++
	V667	+	–	–	–	–	–
Domain V	I671	+++	+++	++	+++	+	++
	L673	+++	+	+	–	–	+
	A725	+++	+++	+++	+++	+++	+++
Membrane-proximal	A730	+++	+++	+++	+++	+++	+++
	F732	+++	+++	+++	+++	+++	+++
	M742	+++	+++	+++	+++	+++	+++
C-terminal tail	T868	++	+++	+	++	+	+++
	N886	++	++	++	++	++	++

* From Heldwein et. al. (Heldwein et al., 2006).

† List includes mutants for which rabbit antiserum R74 binds at > 25% of WT gB levels by CELISA.

‡ CELISA data were normalized to the reactivity of each mAb to WT gB. The normalized values for each mAb were then compared to values obtained using rabbit antiserum R74 for each gB mutant to determine relative changes in reactivity. The symbols represent >80% (+ + +), 50–80 % (++), 20–50% (+), and < 20% (–) reactivity of each mAb compared to R74 values for each gB mutant.

HSV-1 gB is synthesized and released into the ER as a 110-kDa high-mannose, precursor form (pgB), which associates into heat-labile oligomers (Claesson-Welsh and Spear, 1986). Transport of this trimeric precursor through the Golgi apparatus is associated with the addition of O-linked glycans and processing of N-linked glycans and with an increase in apparent MW of the monomer to a 120-kDa mature form (mgB) (Johnson and Spear, 1983).

To test effects of the linker-insertion mutations on the processing of gB, Western blot analysis using rabbit serum R74 was performed for all of the mutants. Lysates of transfected CHO cells were prepared, either heated to dissociate oligomeric forms or not heated, and then fractionated by SDS-PAGE. Levels of the two monomeric species (pgB and mgB) produced by each mutant, relative to WT gB, were assessed using the heated samples (Figure 2.2). Oligomeric forms could be detected in the unheated samples (Figure 2.3) and, in some cases, in the heated samples. For all but 3 mutants detectable on cell surfaces by CELISA, both of the monomeric forms (pgB and mgB) as well as oligomeric forms could be detected, as expected, indicating relatively normal processing and transport to the cell surface (Table 2.3). Two of the exceptions (V667 and L673) were not detected at all by Western blot with the rabbit antiserum despite detection on the cell surface by CELISA using the same antiserum. These mutants exhibited reduced or no binding to all the mAbs (Table 2.2), indicating disruption of multiple epitopes. Probably, epitopes retained by the unfixed and undenatured cell surface protein were able to bind to a subset of antibodies in the rabbit serum but these epitopes were not retained by the proteins after denaturation for western blotting. The

third exception (T665) was detected on Western blots as pgB and mgB, but not as oligomers, and was impaired for binding to several mAbs (Table 2.2).

It is perhaps not surprising that these insertions had such a large effect on conformation because they are targeted within or near residues that form many of the essential trimer contacts. Residues R661 to T669 in one protomer donate one strand to a four-strand mixed β sheet comprised mostly of strands from another protomer (Heldwein et al., 2006). Although oligomers of mutants T665, V667 and L673 could not be detected on Western blots, perhaps because of instability to detergent or loss of epitopes, presumably they must form to enable transport of gB to the cell surface. All mutants that failed to be detected on the cell surface by CELISA produced pgB but not mgB and, in some cases, also failed to produce oligomers, indicating significant disruption of gB folding and/or processing (summarized in Table 2.3).
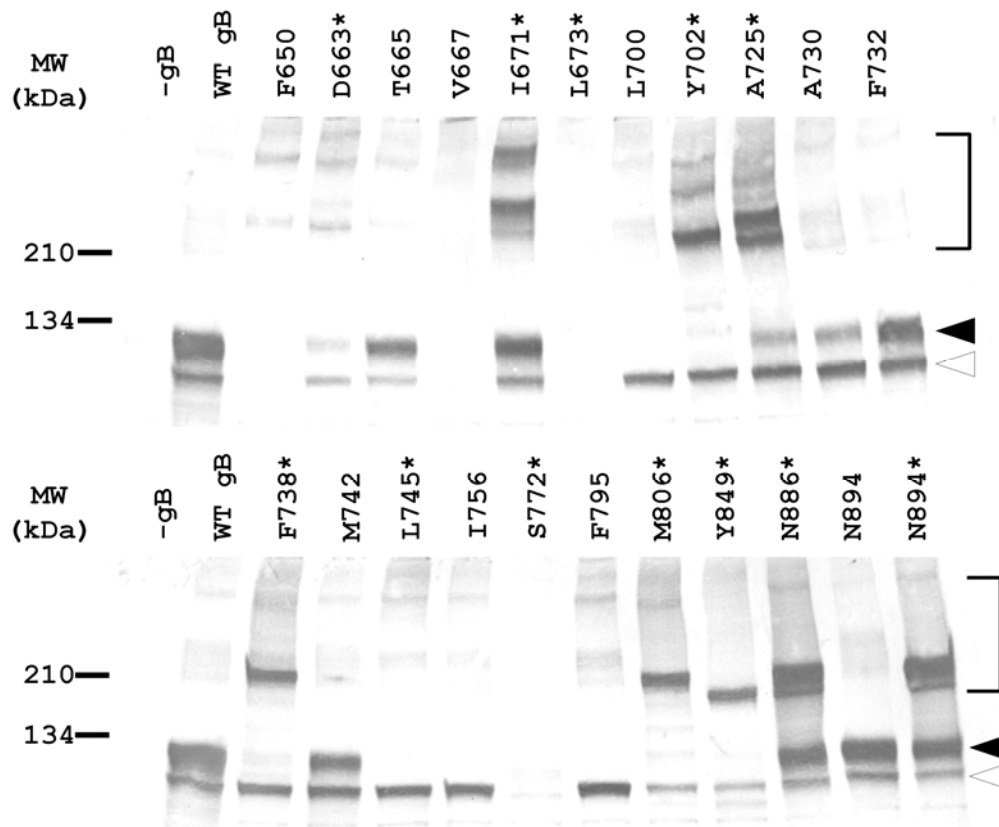
Figure 2.2. Western blot analysis of representative gB mutants (boiled samples).
CHO cells seeded in 24-well plates were transfected with 400 ng of empty vector
(pCAGGS) or a plasmid expressing wild-type gB (pPEP98) or a gB mutant. Proteins in
the cell lysates (boiled samples) were separated by electrophoresis on 4–15 %
polyacrylamide gels under non-reducing conditions and western blots were performed
using the rabbit anti-gB antiserum R74. Brackets--high-molecular weight oligomers of
gB; solid arrowheads--mature gB (mgB); open arrowheads--precursor gB (pgB). The
asterisks identify mutants in which the insertions included a Cys (Table 2.3), perhaps
accounting for the presence of gB oligomers even after boiling of the unreduced
samples.
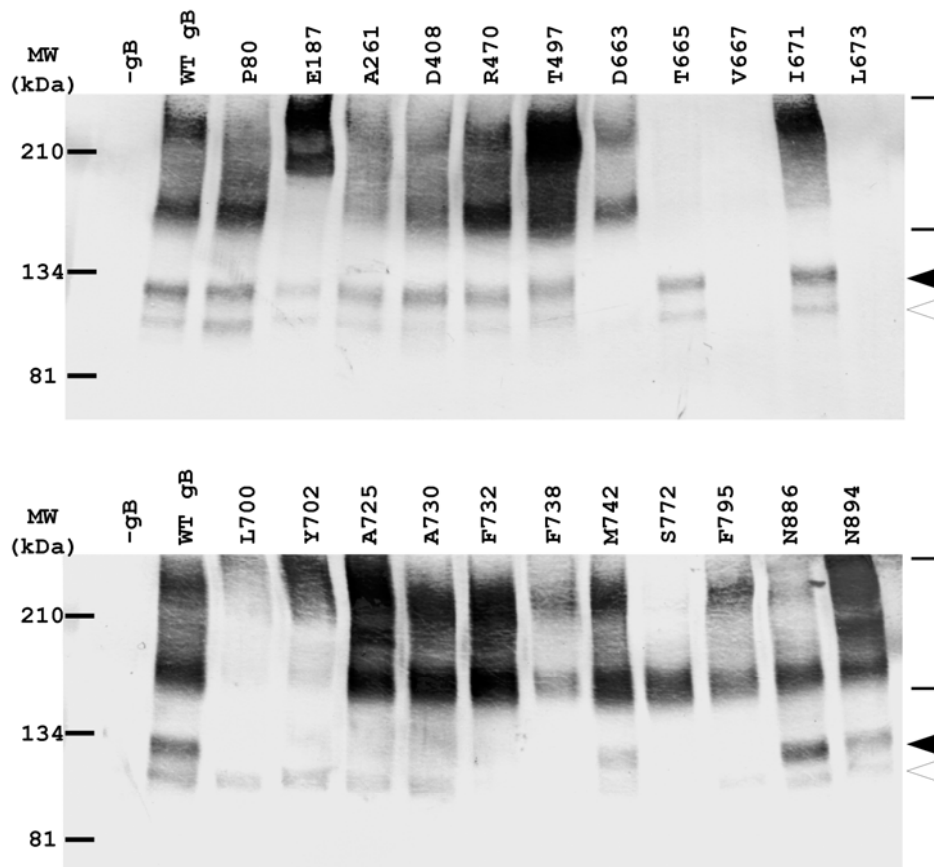
Figure 2.3. Western blot analysis of representative gB mutants (unheated samples). CHO cells seeded in 24-well plates were transfected with 400 ng of empty vector (pCAGGS) or a plasmid expressing wild-type gB (pPEP98) or a gB mutant. Proteins in the cell lysates were separated by electrophoresis on 4–15 % polyacrylamide gels under non-reducing conditions and western blots were performed using the rabbit anti-gB antiserum R74. Brackets--high-molecular weight oligomers of gB; solid arrowheads--mature gB (mgB); open arrowheads--precursor gB (pgB).

Table 2.3. Summary of HSV-1 gB linker-insertion mutants and phenotypes

Position of insertion	Secondary structure *	Amino acids inserted	Western blot †			CELISA	Cell fusion	Viral Entry
			Precursor gB (pgB)	Mature gB (mgB)	HMW Oligomers	Mean±SD (% of WT)	Mean±SD (% of WT)	Mean±SD (% of WT)
K70		MFKQK	+ + +	+ + +	Y	105 ± 20	94 ± 22	
K76	_	NCLNK	+ + +	+ + +	Y	106 ± 26	120 ± 29	89 ± 18
P80		LFKQP	+ + +	+ + +	Y	90 ± 14	86 ± 20	
P81		LFKQP	+ + +	+ + +	Y	93 ± 17	90 ± 5	92 ± 10
P118	_	PCLNT	– / +	-	N	0 ± 0	0 ± 0	
P119		TCLNT	– / +	-	Y	3 ± 2	2 ± 2	
C133	Linker 1	PCLNS	+	-	Y	2 ± 2	0 ± 0	0 ± 0
R136		VFKQP	+	-	Y	2 ± 2	1 ± 1	
Y142		VFKHT	+	-	Y	1 ± 1	0 ± 1	
V149	β3	MFKHF	– / +	-	N	0 ± 1	0 ± 0	
F150		KCLNI	+	-	Y	1 ± 1	0 ± 0	
A155		LFKHP	+ +	-	Y	2 ± 3	1 ± 1	0 ± 1
F159		KCLNI	-	-	N	3 ± 1	1 ± 1	
T162	β4	MCLNT	-	-	N	1 ± 1	0 ± 1	0 ± 0
I185		LFKQI	+ +	+	Y	26 ± 9	0 ± 0	
E187		DCLNK	+ + +	+ +	Y	53 ± 13	0 ± 0	1 ± 0
P193		FCLNT	– / +	-	Y	0 ± 0	0 ± 0	0 ± 0
F194		ECLNI	– / +	-	Y	0 ± 0	0 ± 0	
E195	αA	VFKHE	– / +	-	Y	3 ± 2	0 ± 0	0 ± 0
D199		MFKHK	– / +	-	Y	0 ± 0	0 ± 0	
A203		KCLNT	-	-	N	0 ± 0	0 ± 0	
F223	β8	VFKHR	-	-	N	1 ± 1	0 ± 0	0 ± 0
T230	β9	DCLNT	+	-	Y	2 ± 3	0 ± 0	0 ± 0
A261		LFKQF	+ + +	+ + +	Y	78 ± 8	0 ± 0	0 ± 1
Y265	β11	GCLNN	+ +	+	Y	14 ± 8	0 ± 0	1 ± 1
S280		VFKHS	-	-	N	0 ± 0	1 ± 1	

Position of insertion	Secondary structure *	Amino acids inserted	Western blot †			CELISA	Cell fusion	Viral Entry
			Precursor gB (pgB)	Mature gB (mgB)	HMW Oligomers	Mean±SD (% of WT)	Mean±SD (% of WT)	Mean±SD (% of WT)
L289	β12	VFKQL	+	-	N	2 ± 2	0 ± 0	
A290		TCLNT	-	-	N	2 ± 2	2 ± 1	0 ± 0
D293	β13	FCLNN	-	-	N	0 ± 0	0 ± 0	
Y301		VFKHY	-	-	N	1 ± 2	1 ± 3	
Y303	–	RCLNN	-	-	N	6 ± 6	2 ± 2	0 ± 0
R318		LFKHR	-	-	N	0 ± 1	3 ± 2	
T351	β16	VCLNT	-	-	N	0 ± 1	1 ± 1	
S387	β19	SCLNT	+	-	Y	2 ± 2	0 ± 0	0 ± 0
D408		LFKQD	+ +	+ +	Y	67 ± 13	1 ± 1	
I424		FCLNI	– / +	-	Y	0 ± 0	0 ± 0	0 ± 0
F425	αB	VFKHF	– / +	-	Y	0 ± 0	0 ± 0	0 ± 0
L456	β23	SCLNI	+	-	Y	0 ± 0	0 ± 0	
R470	Disordered	ECLNR	+ + +	+ + +	Y	88 ± 12	56 ± 7	54 ± 8
I495		KCLNI	+ + +	+ + +	Y	100 ± 21	10 ± 4	48 ± 14
T497	Linker 2	TCLNT	+ + +	+ + +	Y	108 ± 3	11 ± 6	45 ± 9
V517		NCLNI	– / +	-	Y	0 ± 0	1 ± 1	0 ± 0
I526	αC	VFKHI	+	-	Y	0 ± 0	1 ± 0	
W539	αC	NCLNR	+	-	Y	2 ± 2	0 ± 1	
G556	–	RCLNS	+	-	Y	2 ± 1	1 ± 1	
V574	β26	PVFKQ	+	-	Y	2 ± 2	2 ± 2	0 ± 0
I589	β27	SCLNI	– / +	-	Y	2 ± 1	1 ± 1	
P593	–	GCLNT	+	-	Y	1 ± 1	0 ± 0	
E614	β30	VFKHE	+	-	Y	0 ± 0	0 ± 0	
I630	β32	ECLNI	– / +	-	Y	1 ± 1	0 ± 0	0 ± 0
T634		VCLNT	– / +	-	Y	0 ± 1	0 ± 1	
T642	β33	FCLNT	– / +	-	Y	2 ± 1	1 ± 1	0 ± 0

| Position of insertion | Secondary structure * | Amino acids inserted | Western blot † | | | CELISA | Cell fusion | Viral Entry |
			Precursor gB (pgB)	Mature gB (mgB)	HMW Oligomers	Mean±SD (% of WT)	Mean±SD (% of WT)	Mean±SD (% of WT)
F643		GCLNI	– / +	-	Y	0 ± 1	1 ± 1	
G645	–	VFKHG	– / +	-	Y	2 ± 1	2 ± 0	
F650	β34	VFKHF	– / +	-	Y	1 ± 0	1 ± 1	
D663	–	ICLNN	+ +	+	Y	40 ± 7	1 ± 1	0 ± 0
T665	β36	MFKHT	+ +	+ +	N	34 ± 11	0 ± 0	0 ± 0
V667		MFKHV	-	-	N	42 ± 20	0 ± 0	0 ± 0
I671	–	DCLNI	+ + +	+ + +	Y	47 ± 3	1 ± 1	0 ± 0
L673		NCLNI	-	-	N	57 ± 10	0 ± 0	0 ± 0
T690	αE	LFKHT	+ + +	-	Y	15 ± 2	1 ± 1	0 ± 0
L700	–	VFKQL	+ + +	-	Y	1 ± 0	1 ± 1	
Y702	αF	TCLNN	+ + +	-	Y	1 ± 0	0 ± 0	
R715		FCLNS	– / +	-	Y	7 ± 2	1 ± 1	0 ± 0
I719	–	VFKHI	+	-	Y	0 ± 0	0 ± 0	0 ± 0
A725		DCLNT	+ + +	+ +	Y	61 ± 14	0 ± 0	0 ± 0
A730		MFKHA	+ + +	+ +	Y	55 ± 5	1 ± 1	0 ± 1
F732		VFKQF	+ + +	+ + +	Y	90 ± 11	1 ± 0	0 ± 0
F738		FCLNI	+ + +	-	Y	3 ± 4	0 ± 0	
M742		VFKQM	+ + +	+ +	Y	75 ± 7	3 ± 1	0 ± 0
L745	–	GCLN M	+ + +	-	Y	1 ± 1	0 ± 1	
V753		MFKQV	+ + +	+	Y	1 ± 0	0 ± 0	
I756		VFKHI	+ + +	-	Y	2 ± 2	0 ± 0	
S772		NCLNT	– / +	+	Y	10 ± 8	0 ± 0	
F795	–	LFKHF	+ + +	-	Y	6 ± 3	0 ± 0	
M806		KCLNM	+ +	-	Y	1 ± 1	0 ± 0	
Y849	–	MCLNN	+ +	-	Y	0 ± 0	0 ± 0	
T868		SCLNT	+ +	+ +	Y	96 ± 5	170 ± 41	71 ± 9
N886		TCLNN	+ + +	+ + +	Y	106 ± 35	89 ± 30	87 ± 2

Position of insertion	Secondary structure *	Amino acids inserted	Western blot †			CELISA	Cell fusion	Viral Entry
			Precursor gB (pgB)	Mature gB (mgB)	HMW Oligomers	Mean±SD (% of WT)	Mean±SD (% of WT)	Mean±SD (% of WT)
N894		MFKHN	+ + +	+ + +	Y	93 ± 9	76 ± 35	
N894		KCLNN	+ + +	+ + +	Y	91 ± 22	70 ± 37	

* From Heldwein et al. (Science 313:217-220, 2006).

† Western blots were performed as described in the text. Detection of pgB and mgB was scored as a percentage of WT gB levels: >80% (+++), 50-80% (++), 20-50% (+), 0-20% (-/+), undetectable (-). High molecular weight (HMW) oligomers were scored as detectable (Y) or not (N).

Functional Activities of the gB Mutants. To assess cell fusion activity by a quantitative luciferase-based assay, all 81 gB mutants were co-expressed with HSV-1 gD, gH and gL in CHO cells (effectors), which were mixed with nectin-1-expressing or HVEM-expressing CHO cells (targets). CELISAs were performed in parallel to quantitate cell surface expression of gB in the effector cell populations. The results obtained with HVEM as the fusion receptor did not differ from those obtained with nectin-1 and therefore only the latter results are presented here. Failure of a mutant to be detected on the cell surface by rabbit serum R74 correlated with absence of activity in the cell fusion assay (Table 2.3), as expected. These mutants were not studied further.

Figure 2.4 presents the cell fusion results for all mutants that were detected on the cell surface, in comparison with the CELISA results obtained with the rabbit antiserum. Category 1 mutants (insertions in the N-terminus or C-terminus of gB) were nearly indistinguishable from WT gB in both cell fusion activity and cell surface expression, with the exception of T868 which had enhanced cell fusion activity. Category 2 mutants were located centrally in the gB ectodomain and had slightly or severely reduced cell fusion activity but nearly WT levels of cell surface expression. Category 3 mutants had little or no detectable cell fusion activity and variable levels of cell surface expression.

Figure 2.4. Cell fusion activities of the gB insertion mutants in relation to cell surface expression. CHO cells were transfected with plasmids expressing WT gB or each of the gB mutants capable of cell surface expression, other HSV-1 glycoproteins (gD, gH and gL) and T7 polymerase (effector cells). CHO-nectin-1 cells were transfected with a plasmid carrying the firefly luciferase gene under control of the T7 promoter (target cells). One set of effector cells was used for CELISA (results shown also in Figure 2.1) and the other set was mixed with the target cells for assessment of cell fusion activity by quantification of luciferase activity. Positions of the mutations with respect to structural domains are indicated across the top. Categorization of the mutants with respect to phenotype is indicated across the bottom: Category 1--indistinguishable from WT gB or with enhanced fusion activity; Category 2--normal levels of cell surface expression but reduced fusion activity; Category 3—normal or reduced levels of cell surface expression but no fusion activity. The results are expressed as % of WT gB activity, after subtraction of background values obtained in the absence of gB expression, and are means and SD of three independent experiments.

Figure 2.4. Cell fusion activities of the gB insertion mutants in relation to cell surface expression.
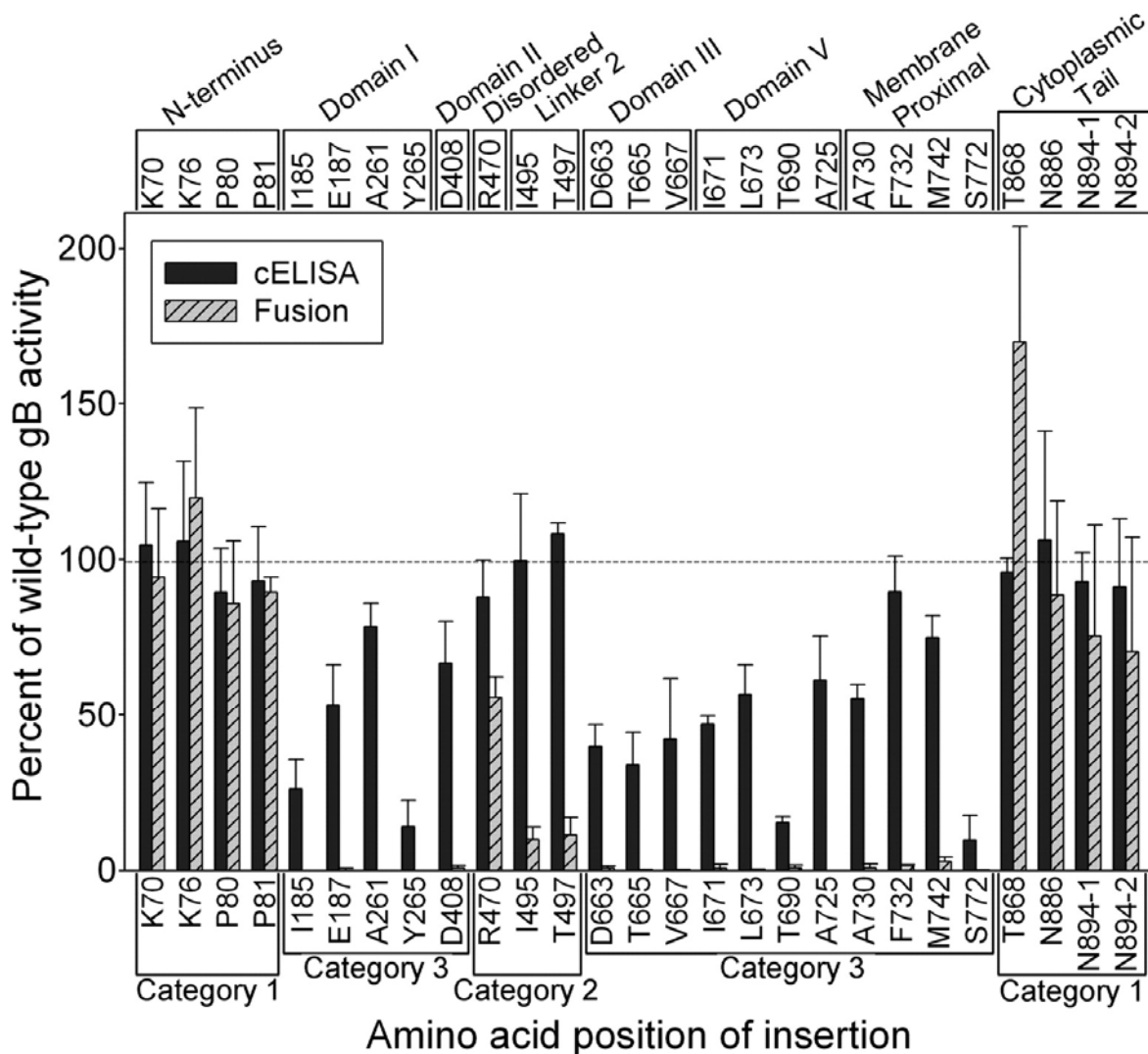
Most of the mutants shown in Figure 2.4 were also co-expressed with WT gB (twice the amount of gB-expressing-plasmid total) in the fusion assay to determine whether they had dominant-negative effects on cell surface expression or cell fusion. Figure 2.5 shows that the functional gB mutants (categories 1 and 2) exhibited slightly enhanced levels of cell surface expression and cell fusion activity as did samples with twice the amount of WT gB. Most of the non-functional category 3 mutants caused reduced cell fusion activity, to various levels, and also caused reduced cell surface expression in a subset of cases. A notable exception was mutant A730, in which the insertion is downstream of the last ordered residue in the X-ray structure (A725). It appears that WT gB may have rescued the reduced cell surface expression and undetectable activity of this mutant whereas most of the non-functional mutants had dominant-negative effects on WT gB cell surface expression and function.

Selected mutants were tested for ability to complement the entry deficiency of a gB-negative viral mutant (Table 2.3). The only mutants that exhibited any viral entry activity were those that were expressed on the cell surface and had detectable levels of cell fusion activity. The two category 2 mutants with cell fusion activity reduced to 10% of WT gB levels (I495 and T497) were more active in viral entry (54% and 48% activity, respectively).
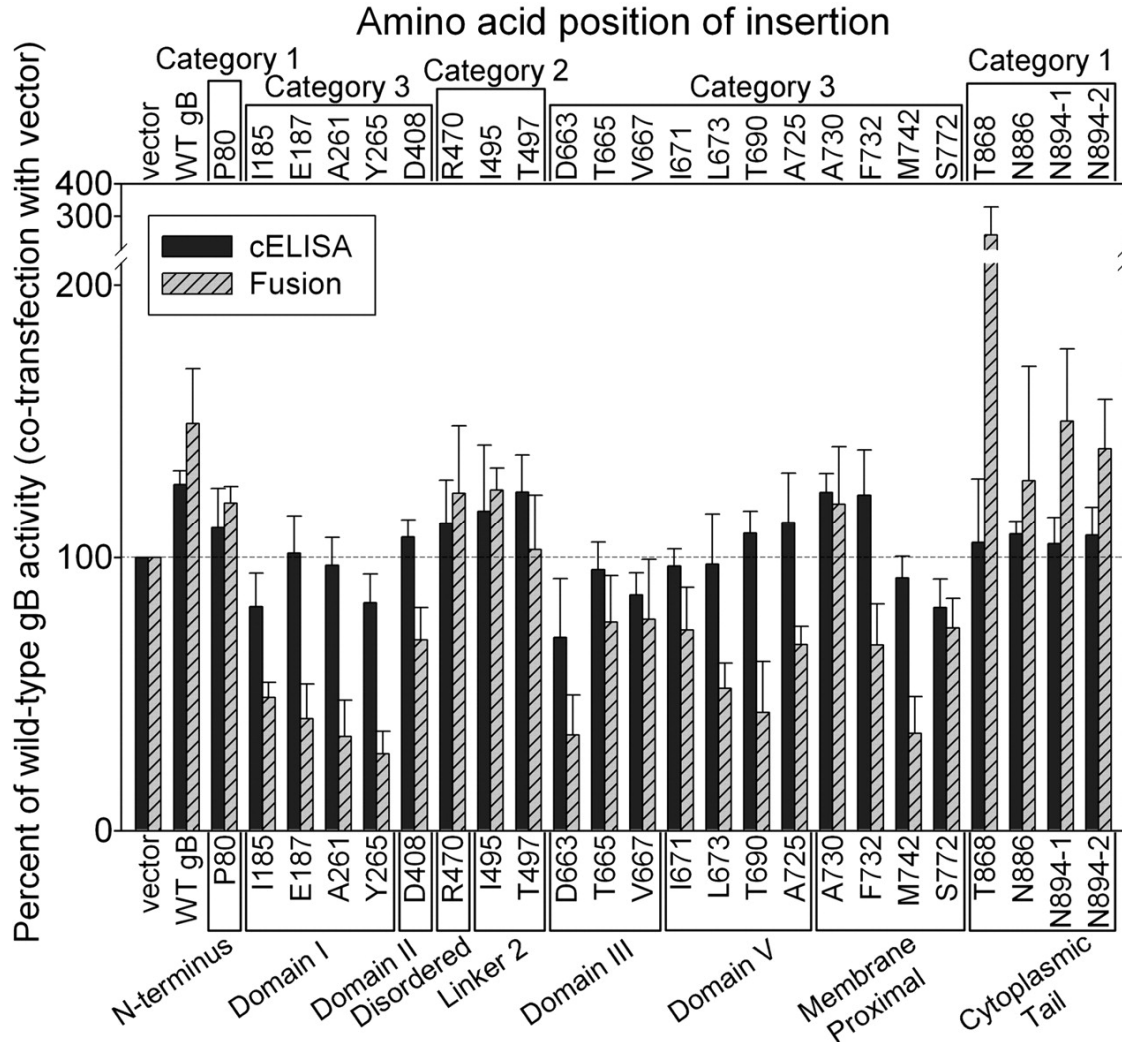
Figure 2.5. Effects of gB insertion mutants on cell surface expression and cell fusion activity of WT gB. The CELISA and cell fusion assays were performed as described in Figure 2.2 except that the transfection mixtures for each sample of effecter cells contained an additional 30 ng of plasmid expressing WT gB. Positions of the mutations with respect to structural domains are indicated across the bottom. Categorization of the mutants with respect to phenotype is indicated across the top. The results are expressed as % of WT gB activity (1X dose of gB plasmid mixed with added empty vector).

Locations of insertions on gB structure in relation to effects on function. The only

insertions without negative consequences on cell surface expression of gB and function

were outside the solved structure, in the N-terminus and distal portion of the C-terminal

cytoplasmic domain. The N-terminal region from A31 to D110 appears to be quite

flexible. To obtain well-ordered crystals for the high resolution structure, the N-terminus

up to D103 was removed by trypsin from the expressed form of gB, A31 to A730. In a

lower resolution structure of uncleaved gB (A31 to A730), the N-terminal residues from

A31 to N108 remained disordered (Heldwein et al., 2006). The results presented here

and elsewhere show that this region is also tolerant of insertions and deletions.

Insertions after K70, K76, P80 and P81 had no effect on expression or function of gB,

as assessed here. Similarly, insertions into HSV-2 gB at positions equivalent to HSV-1

gB T53 and T109 (S48 and A104 in HSV-2) had no effect on expression and only the

insertion at A104 partially reduced function (Li et al., 2006). Insertions K70 and K76

targeted a Lys-rich region from K68 to K76 shown to be critical for the binding of gB to

heparin (Laquerre et al., 1998). Deletion of these amino acids impaired the binding of

gB to heparin and also to heparan sulfate-expressing cells but had relatively minor

effects on viral infectivity (Laquerre et al., 1998).

It is not surprising that insertions into the distal part of the cytoplasmic tail of gB

had no negative effect of gB expression and function. Deletions of up to about 40

amino acids from the C-terminus of HSV-1 or HSV-2 gB had either no effect on, or

enhanced, function in cell fusion whereas larger deletions inhibited cell fusion (Fan et

al., 2002; Foster et al., 2001). The insertion that enhanced cell fusion activity (T868)

also altered epitopes in the ectodomain, suggesting both that conformation of the cytoplasmic tail can influence conformation of the ectodomain and that this altered conformation in the ectodomain may have a role in the enhanced cell fusion activity.

Membrane-proximal insertions into the cytoplasmic tail (M806 and Y849) abrogated cell surface expression. This was found also for certain amino acid substitutions into conserved positions in the membrane-proximal region of the cytoplasmic tail of HSV-2 gB, although adjacent substitutions permitted cell surface expression and enhanced cell fusion activity (Ruel et al., 2006). Amino acid substitutions at various positions in the cytoplasmic tails of HSV-1 and HSV-2 gB have been shown to enhance cell fusion (reviewed in ref. Ruel et al., 2006). The mechanistic basis for the positive and negative effects of the various mutations is not understood.

Only two of the insertions that map to the crystallized portion of the gB ectodomain (Figure 2.6) permitted expression on the cell surface at WT levels *and* retention of cell fusion activity. Category 2 mutants I495 and T497 in the second linker region had significantly reduced cell fusion activity (10%) but higher complementing activity (~50%). A third category 2 mutant, insertion R470, retained the highest level of fusion activity (50%) and maps to a disordered loop between domain II and linker 2 (Figure 2.1). This loop was cleaved by trypsin in preparing the recombinant protein for crystallization and is a poorly conserved region where posttranslational cleavage occurs for members of the gB family encoded by other herpesviruses. Nine 2-amino acid insertions into HSV-1 or HSV-2 gB have been described previously to permit cell surface expression and at least partial function in cell fusion or viral entry (Cai et al.,

1988; Li et al., 2006). With the exception of one in the cytoplasmic tail and one in the disordered central loop, all map to the surface of the crystallized portion of gB, in domain I (Y254, R304, T313), domain II (G381, G437), the N-terminal-most segment of domain III (P130) and linker 1 (R136).

Sixteen other insertions that permitted cell surface expression of gB (greater than 10% of WT levels) were non-functional (category 3 mutants). Four map outside the solved structure just downstream of domain V (A730, F732, M742 and S772). The remainder were insertions between residues on the surface of the trimer or of an internal cavity (Figure 2.6). Of these, only 3 mutants (T665 and V667 in the C-terminal-most segment of domain III and L673 in domain V) exhibited global alterations in conformation, as discussed above. The remainder could not be distinguished from WT gB in conformation and yet are non-functional. Four 2-amino acid insertions into HSV-1 or HSV-2 gB have been described previously to permit cell surface expression but with loss of function (Cai et al., 1988; Li et al., 2006). These map to domain I in the internal cavity (R189) or to the trimer surface in domains I (P358), II (S403) and V (D680).

Insertions A261 and Y265 are located in or near one of the two loops at the lower tip of domain I (Figure 2.6), loops analogous to the bipartite fusion loops of VSV G (Roche et al., 2006). Loss of function caused by these insertions is consistent with recent findings that certain amino acid substitutions at W174, Y179, V259 and A261 also abrogated function in cell fusion; only V259R prevented cell surface expression of gB (Hannah et al., 2007). It remains to be determined whether the two loops at the ends of domain I actually serve as internal fusion peptides. If so, it appears to be important

that all protomers of the trimer have intact fusion loops because mutants A261 and Y265 were among those exerting the strongest dominant-negative effects when co-expressed with WT gB. The only other expressed insertions in domain I (I185 and E187) point toward a small cavity inside the trimer (Figure 2.6). Similar cavities are also found in the postfusion forms of VSV G (Roche et al., 2006) and flavivirus protein E (Bressanelli et al., 2004; Modis et al., 2004). In gB this cavity is not large enough to accommodate three 5-amino acid insertions, supporting the idea that the solved structure of gB is different from the prefusion structure.

Insertion D408 is located within domain II which, as is also the case for a part of domain I and for an analogous domain in VSV G, resembles a canonical pleckstrin-homology (PH) domain (Heldwein et al., 2006; Roche et al., 2006). PH domains in cytoplasmic molecules can serve as scaffolds for phosphoinositide and peptide binding, but it is unclear what roles the PH domains in the ectodomains of gB and VSV G may play.
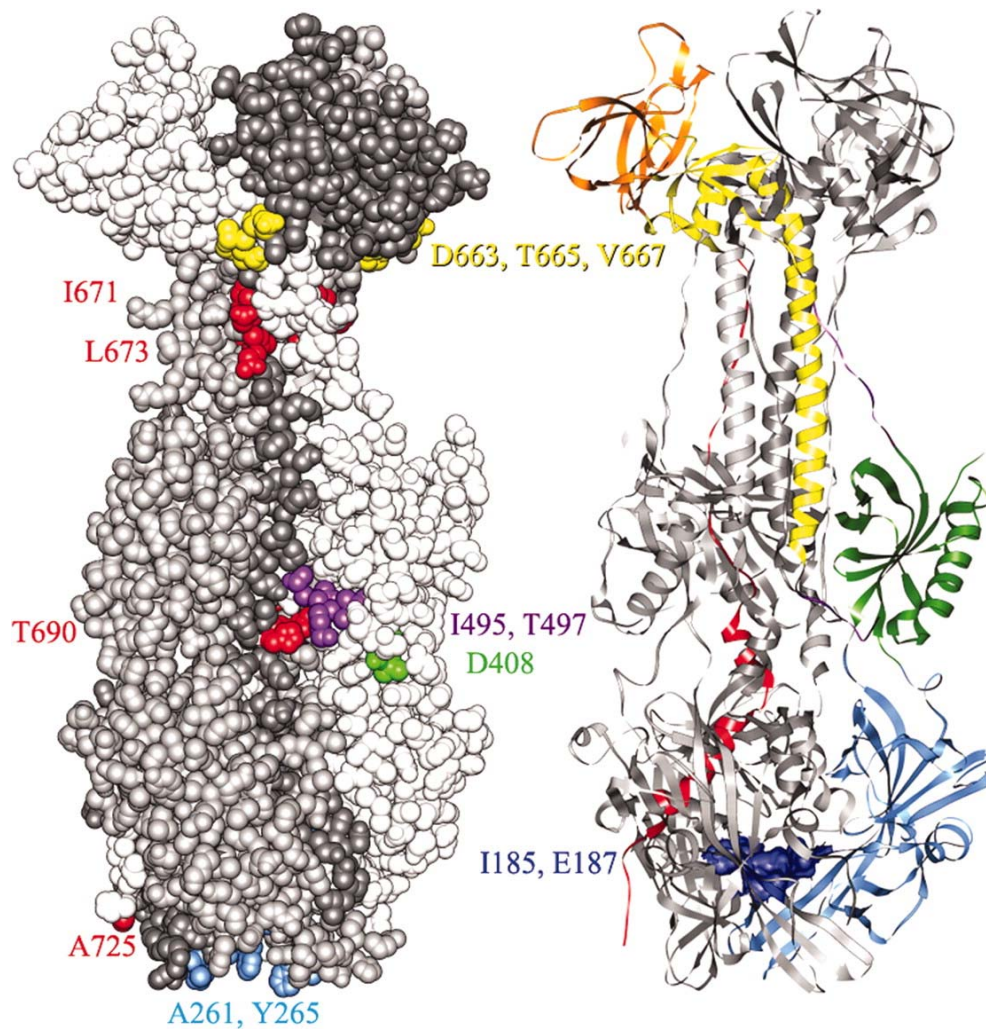
Figure 2.6. Mapping of insertion mutations on the structure of gB. Left – Space-filling model with each protomer colored a different shade of grey. The amino acids bounding each insertion site are colored according to the domain or region to which each maps, using the color code shown in Figure 2.1. Insertion sites in all three protomers are colored so that all surface insertion sites can be seen in one view. Right – Ribbon model with the domains and regions of one protomer colored according to the code in Figure 2.1. The insertion sites into the cavity of the trimer are indicated by dark blue coloring of the residues displayed in space-filling mode.

HSV gB and VSV G. Although gB cannot act alone to mediate membrane fusion, as VSV G does, it is clearly essential for HSV-induced membrane fusion. Its structural homology with VSV G invites comparisons in relating the effects of insertions in gB on function in cell fusion. Three domains of G (equivalent to domains I, II and IV of gB) retain their folded structure in both the prefusion and postfusion forms, in spite of large rearrangements in their relative orientations (Roche et al., 2006; Roche et al., 2007). Of interest, the G domain equivalent to domain II of gB is at the top of the prefusion structure but is relocated to the side of the trimer in the postfusion form, also the location for domain II in the solved structure of gB. Assuming this structure of gB is equivalent to the postfusion form of G, insertion D408 in domain II is likely to be at a site exposed also on the prefusion form, a site available for interactions with cell receptors or other viral proteins required for fusion. Insertions A261 and Y265, in one of the putative fusion loops of domain I, would presumably interfere with insertion of these loops into the target membrane but would point toward the virion envelope in both the prefusion and postfusion forms of gB, by analogy with VSV G. The VSV G monomers in the region of domain IV (elongated three-stranded β sheet with internal fusion loops equivalent to a similar region of gB domain I) are close together in the postfusion form (as in the solved gB structure) but separated in the prefusion form. Such separation would permit accommodation of insertions I185 and E187 in a prefusion structure. Insertions into gB that would likely affect hinge regions involved in reorientation of domains I, II and IV include those in linker 2 (I495, T497) and those near the junction of domains III and V (D663, T665, V667, I671, L673). By analogy with VSV G, domain III

in the postfusion form of gB is likely to differ in conformation from that in the prefusion form.

In summary, the results presented here provide support for the notion that the solved structure of gB is a postfusion form; identify regions of gB that are critical for function in membrane fusion and require further study using assays that can assess relevant protein-protein or protein-lipid interactions; and identify regions of gB that tolerate insertions without loss of function and may tolerate insertions of probes for fusion-associated alterations in conformation.

CHAPTER 3: Random linker-insertion mutagenesis to identify functional domains of herpes simplex virus type 1 glycoprotein L.

SUMMARY

Herpes simplex virus gL is one of four glycoproteins essential for viral entry and cell fusion. To identify functional domains of gL, we performed random linker-insertion mutagenesis. Analyses of 15 gL mutants revealed that 11 bound and transported gH to the cell surface. Of the 4 remaining mutants, 2 were processed properly and secreted from cells but failed to bind gH and define the gH-binding domain. The remaining 2 mutants were not detected on the cell surface identifying two regions critical for transport and processing. Some mutants that bound and transported gH were found to have partial or complete dissociation of transport and cell fusion activity. Monoclonal antibody studies showed altered gH-gL heterodimer conformations with certain gL mutants. Loss of monoclonal antibody epitopes did not affect cell fusion activity.

INTRODUCTION

Of the four glycoproteins involved in cell fusion and viral entry, the role of gL is least well-defined. HSV-1 gL is the only fusion glycoprotein that does not contain a transmembrane domain, and when expressed in the absence of gH, is secreted from cells. It has been previously postulated that gL merely has a chaperone role necessary for the proper folding and transport of gH. The regions involved in dimerization of gH and gL are located between residues 19 and 323 of HSV-1 gH and residues 23 and 147 of gL (Klyachkin et al., 2006; Peng et al., 1998). The 4 conserved cysteines in gL were also found to be essential for gH binding and function (Cairns et al., 2005). Mutational analyses of gL by C-terminal deletions showed that the first 147 aa of gL are required for association with gH (Klyachkin et al., 2006) but that the first 161 aa are necessary for co-transport of gH and gL to the cell surface (Klyachkin et al., 2006; Peng et al., 1998) and for gL activity in cell fusion and viral entry (Klyachkin et al., 2006). A recent study of N-terminal deletions in HSV-2 gH demonstrated that gH2 deleted for the first 48 amino acids (after the signal peptide) could be transported to the cell surface in the absence of gL but was not functional in cell fusion unless co-expressed with gL. These results indicate that the role of gL in HSV-induced cell fusion is probably not limited to its putative chaperone role in mediating transport of gH to the cell surface. Although a corresponding internal deletion mutant in HSV-1 (gH1Δ48) did not demonstrate gL-independent transport, it is possible that some other mutant forms of gH1 not yet identified would allow for the same gL-independent transport observed with gH2.

Lastly, an early study of gL found that anti-gL monoclonal antibodies (mAbs) could inhibit cell fusion but not viral entry, despite demonstrable binding of the mAbs to virus, suggesting that gL may play a different role in each process (Novotny et al., 1996).

The complex interactions between gL and gH required for proper intracellular transport, processing and cell surface expression have complicated previous attempts to study the functional role of each glycoprotein in cell fusion and viral entry. To study the role gL in fusion, I generated a panel of gL linker-insertion mutants to identify regions critical for gH binding and transport and regions essential for cell fusion and viral entry. Furthermore, the recent development of the lipid transfer assay provided the means to study the intermediate hemifusion state mediated by gD and gH-gL and allowed for characterization of the role of gL in the intermediate hemifusion step in addition to cell fusion and viral entry.

Characterization of 15 unique gL linker-insertion mutants permited conclusions that (i) a conserved region near the middle of gL is critical for dimerization with gH, (ii) wild-type (WT) and most mutant gLs can be detected on the cell surface in the absence of gH, (iii) some gL mutations caused altered conformation of the gH-gL heterodimer, (iv) the gH-trafficking and cell fusion activities of gL are separable functions, (v) gL plays a role in fusion downstream of hemifusion, and (vi) the roles of gL in cell fusion and viral entry are different.

RESULTS

Cell Surface Expression, Conformation and Heterodimerization with gH of the gL Mutants.

Each of the 15 linker-insertion mutants generated for this study is named for the position of the insertion, denoted by the name and number of the amino acid 5' of the 5 amino acid-insertion, counting from the first Met of the gL precursor. To assess expression levels on the cell surface, plasmids encoding each of the gL mutants were transfected into Chinese hamster ovary (CHO) cells, along with a plasmid expressing wild-type (WT) gH. The live cells were incubated with an anti-gL rabbit antiserum R88 for detection of gL and the mAb 52S for detection of gH, by a cell-based ELISA (CELISA).

Figure 3.1 shows the level of cell surface gL detected for each mutant, as a percentage of WT gL, in relation to the amino acid position of the insertion. In addition, the level of cell surface gH detected with the anti-gH mAb 52S, as a percentage of gH levels co-expressed with WT gL, is also shown. A linear representation of gL is shown below the X-axis and coded to identify specific features of gL. All but two of the gL mutants (V017 and K146) were detected on the cell surface.

Figure 3.1. Effects of insertional mutations on HSV-1 gL cell surface expression.
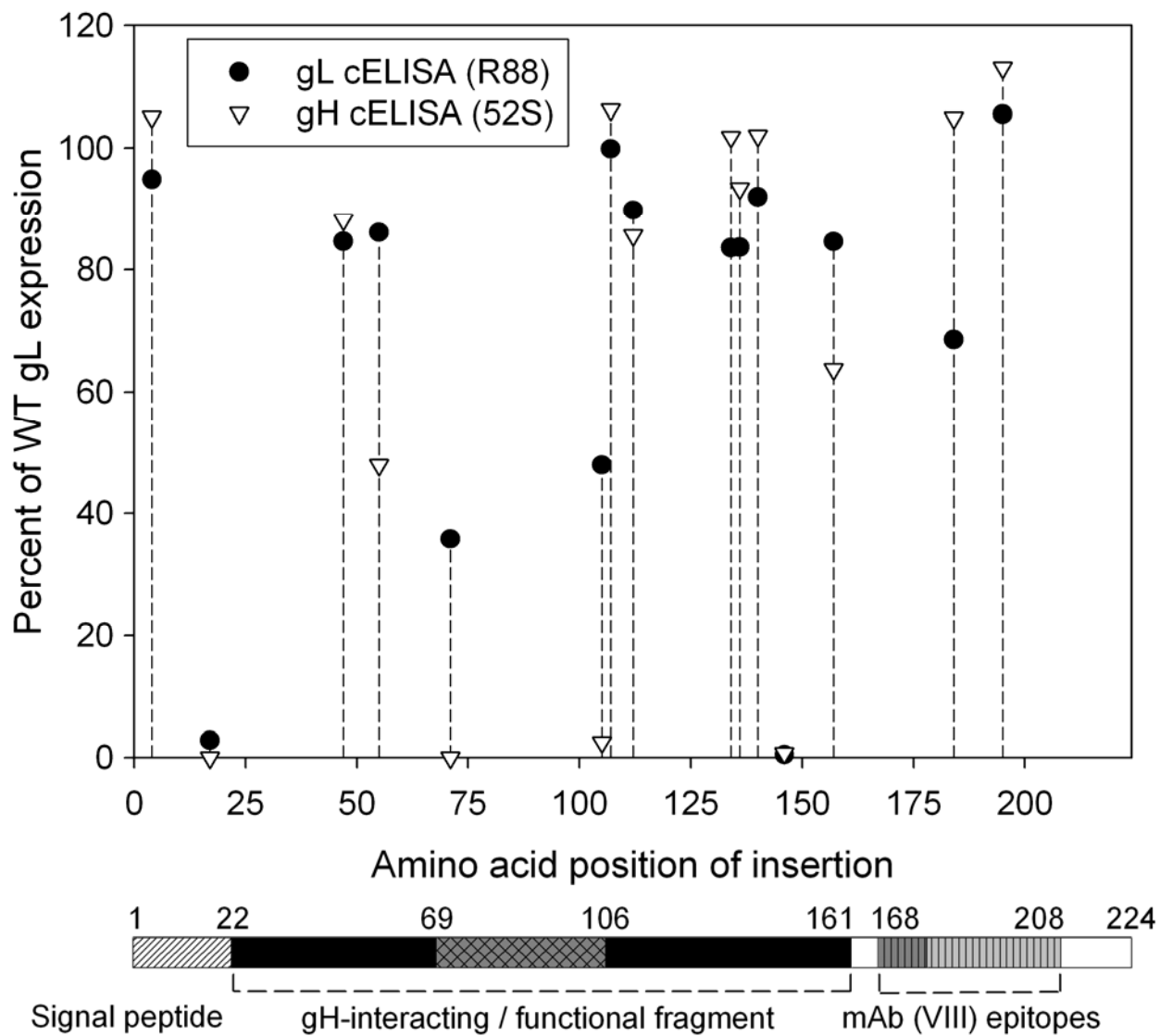
Figure 3.1. Effects of insertional mutations on HSV-1 gL cell surface expression.

CHO cells were transfected with plasmids expressing gH and WT gL or gL mutant. Cell surface expression of gL and gH was quantified by CELISA using R88 and 52S, respectively. A linear representation of the gL polypeptide is shown below the graph with coded bars identifying features of gL. The bars represent the signal peptide (uncolored hatched), the N-terminal 161 a.a. fragment necessary for formation of functional gH-gL complexes (black bars) and highly conserved residues within this fragment (crossed dark grey bar), and epitopes recognized by a panel of anti-gL mAbs (dark and light grey vertical striped bars). The values presented for cell surface expression of each mutant gL (and co-transfected WT gH) are means from three independent experiments expressed as % of WT gL (or gH co-transfected with WT gL) values (after subtraction of background values obtained in the absence of gL expression) and as a function of position of the insertion. Standard deviations are presented in Table 3.2.

Table 3.1 summarizes the results of the gL and gH CELISAs and places each mutant

into one of five categories based on gL and gH expression patterns. Category 1

comprises a group of 8 mutants for which levels of gL and gH expression were

comparable to those observed for wild-type gL (and gH). Category 2 contains mutant

E184 for which gL expression, but not gH expression, appeared to be reduced relative

to WT levels. In contrast, Category 3 mutants, R055 and T157, were expressed at near

WT levels but their insertions caused reduced levels of gH expression or reduced

recognition of gH. Category 4 mutants, F071 and E105, were detected on the cell

surface at reduced levels and in the absence of any measurable expression of gH.

Lastly, cells transfected with Category 5 mutants, V017 and K146, exhibited no

detectable levels of either gL or gH on the cell surface.

Table 3.1. Categorization of gL mutants by gL and gH expression levels.

Category	Detection on cell surface [a]		gL Mutants
	gL	gH	Position of insertion
1	+++[a]	+++	L004, L047, L107, F112, D134, R136, A140, P195
2	++	+++	E184
3	+++	++	R055, T157
4	+	–	F071, E105
5	–	–	V017, K146

[a] (+++) > 80% of WT, (++) 45 - 79% , (+) 25 - 44% , (–) < 5%

The insertions in Category 2, 3 and 4 mutants altered the relative ratios of gL and gH detected on the cell surface, compared to that observed for WT gH-gL hetero-dimers. Most strikingly, the results showed that Category 4 mutants are detected on the cell surface in the apparent absence of gH. Previous studies demonstrated that, in the absence of gH, gL is secreted by transfected cells into the medium but it was not determined whether this secreted gL could bind to the cell surface. To determine whether some gL (WT or mutant) can associate with the cell surface in the absence of gH and also to assess the effects of gH on gL cell surface expression, gL CELISAs were performed on CHO cells expressing WT gL and each gL mutant in the presence and absence of gH. Additionally, a gL-GFP construct with GFP fused to the C-terminus of gL was tested as an additional control.

Figure 3.2 shows the levels of gL detected on cell surfaces in the presence and absence of gH, presented as a percentage of WT gL co-transfected with gH. The amount of WT gL detected on the cell surface in the absence of gH was approximately 68% that of levels in the presence of gH. For most of the gL mutants, presence of gH increased the levels of gL detected on the cell surface, as for WT gL, consistent with the formation of stable gH-gL heterodimers that were transported to the cell surface. However, Category 4 mutants F071 and E105 showed no increase in gL detectable on the cell surface resulting from co-expression with gH. This finding, coupled with the failure to detect gH on the cell surface when F071 and E105 were co-expressed with gH (Figure 3.1), suggests that these mutants failed to dimerize with gH and to mediate its transport to the cell surface. Consistent with Figure 3.1, Category 5 mutants V017 and

K146 were not detected on the cell surface in the presence or absence of gH. These mutants may be defective for post-translational processing and transport to the cell surface. Interestingly, Category 2 mutant E184 and the gL-GFP fusion protein both exhibited significantly reduced levels on the cell surface in the absence of gH but cell surface expression was to a large extent restored in the presence of gH, indicating that the presence of gH could compensate for their impaired transport to the cell surface or impaired recognition by the antibodies used. In summary, although gL was detected on the cell surface in the absence of gH, co-expression with gH, and presumably dimerization with gH, enhanced the levels of cell surface gL or its recognition by the antibodies used, for WT protein and most of the mutants. For the Category 4 and 5 mutants, there is no evidence from the data presented in Figures 3.1 and 3.2 that these mutants are capable of interacting with gH. Moreover, the insertions in V017 and K146 (Category 5) abrogated cell surface detection of gL whether gH was expressed or not.

.
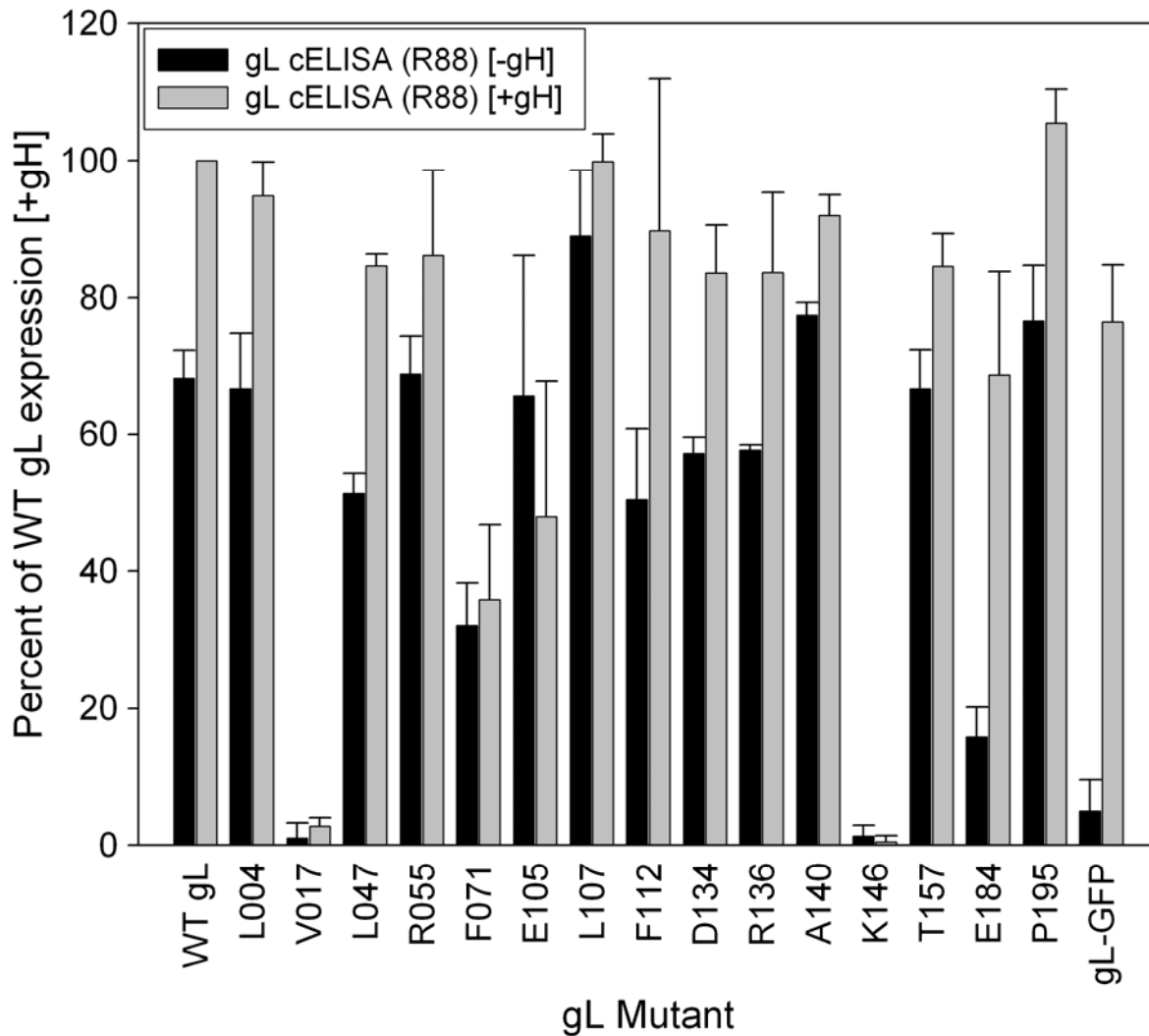
Figure 3.2. Cell surface expression of WT and gL mutants in the absence and presence of gH. CHO cells were transfected with plasmids expressing WT gL or gL mutant and either a plasmid expressing gH or empty vector. Cell surface expression of gL was quantified by CELISA using R88. The values presented for cell surface expression of each mutant gL are means from three independent experiments expressed as % of WT gL values (otained in the presence of gH after subtraction of background values obtained in the absence of gL expression). Standard deviations are presented here as error bars and also in Table 3.2.

To assess effects of the insertions on conformation of the gH-gL complexes, CELISAs were performed on CHO cells expressing WT gL or each of the gL mutants along with gH, using a mAb that recognizes the gH-gL heterodimer but not gH or gL alone (53S). The results are presented in Figure 3.3 along with parallel results obtained using mAb 52S, which recognizes gH alone. Most mutants showed approximately WT levels of gH and gH-gL on the cell surface as detected by 52S and 53S, respectively. All Category 4 and 5 mutants failed to bind to either of these mAbs. Category 3 mutant T157 showed an overall decrease in cell surface binding with both the 52S and 53S but to the same relative degree. Interestingly, Category 1 mutant L047 and Category 3 mutant R055 both exhibited reduced binding by 53S compared to 52S, indicating that the gH-gL complexes formed with these gL mutants are altered in conformation compared to WT complexes.
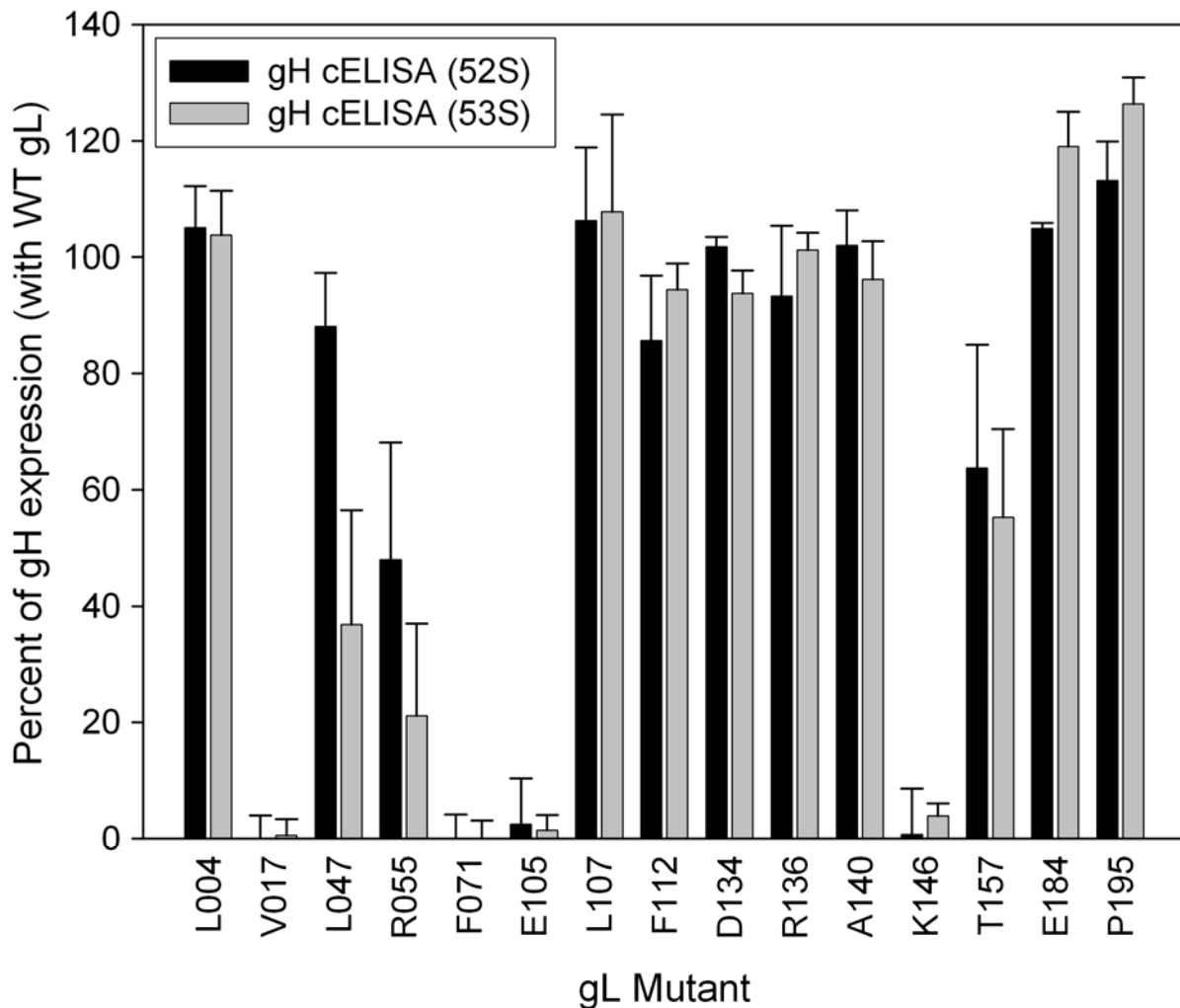
Figure 3.3. Binding of 52S and 53S to cell surface gH co-expressed with gL mutants. CHO cells were transfected with plasmids expressing gH and WT gL or gL mutant. Cell surface expression of gH and gH-gL complex was quantified by CELISA using 52S and 53S, respectively. The values presented for binding of 52S and 53S to gH are means from three independent experiments expressed as % of values obtained when gH was co-expressed with WT gL(after subtraction of background values obtained in the absence of gL expression). Standard deviations are presented here as error bars and in Table 3.2.
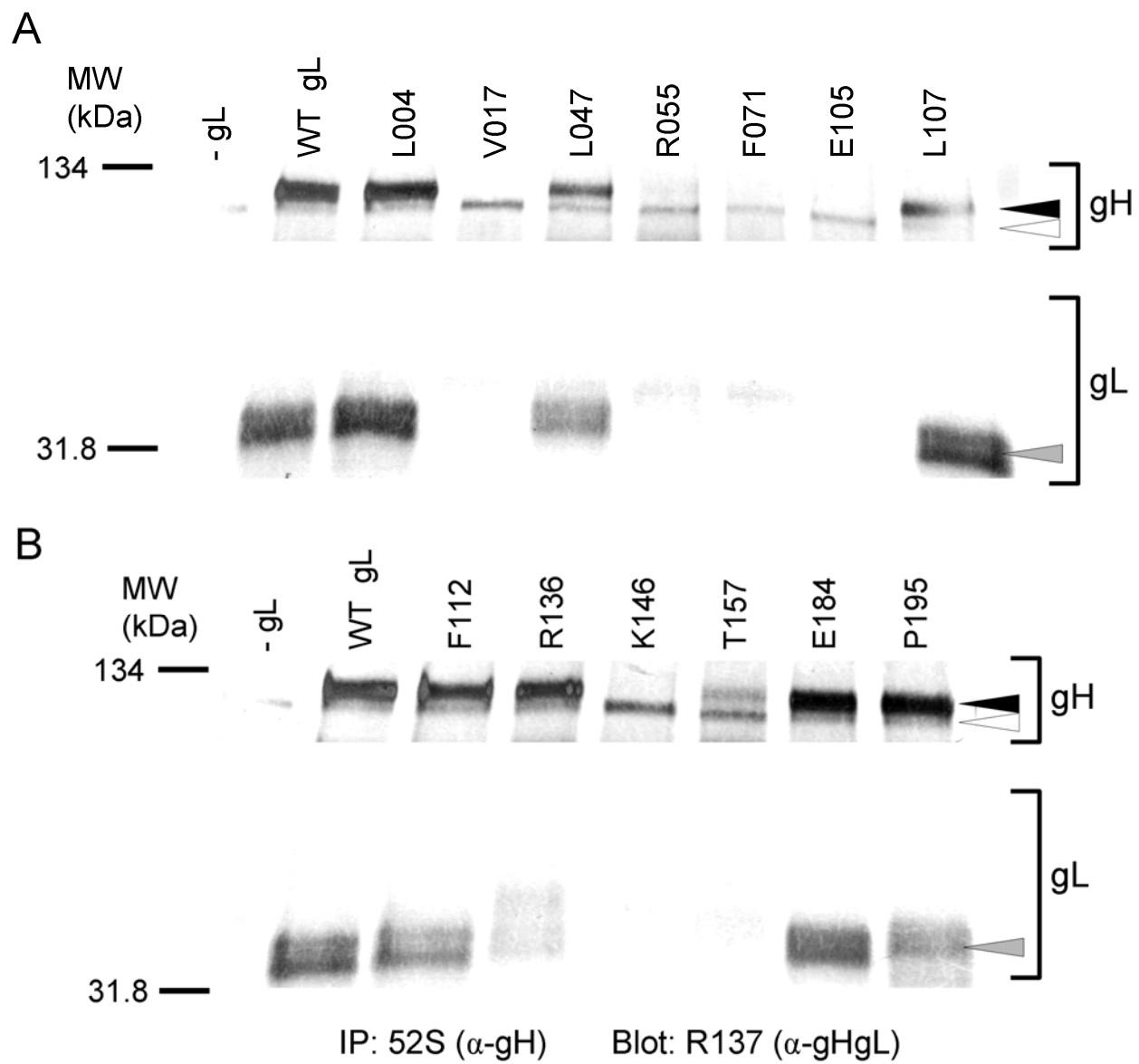
To test effects of the linker-insertion mutations on gL heterodimerization with gH, co-immunoprecipitation and Western blot analyses were performed for WT gL and the mutants. Lysates of transfected CHO cells were incubated with the anti-gH mAb 52S for immunoprecipitation. The recovered immunoprecipitates were fractionated by SDS-PAGE and Western blot analysis was done using rabbit serum R137 which recognizes both gH and gL. Figure 3.4 shows the results of the Western blot analysis. For all Category 1 mutants tested, mgL co-precipitated with gH and significant levels of mgH were detected in the immunoprecipitates, indicating that these mutant gLs heterodimerized with gH and moved through the Golgi for processing, consistent for their detection at WT levels on the cell surface. The same results were obtained for Category 2 mutant E184, despite its reduced detection on the cell surface both in the presence and absence of gH. Category 3 mutants, R055 and T157, exhibited significantly reduced levels of mgH relative to pgH in immunoprecipitates and very little gL was co-precipitated, indicating impairment in gH-gL dimerization and post-translational processing. These effects were more pronounced for R055 than for T157, consistent with a lower level of gH detected on cell surfaces for R055 (Figures 3.1 and 3.3). Immunoprecipitates obtained with the Category 4 mutants, F071 and E105, contained little or no detectable mgH and very little if any gL, consistent with severely reduced gH-gL oligomer formation and inability to detect any gH on cell surfaces with either 52S or 53S (Figures 3.1 and 3.3). Lastly, Category 5 mutants (V017 and K146), not detected on the cell surface in the presence or absence of gH, also failed to heterodimerize with gH and to promote maturation of gH to mgH.

Figure 3.4. Co-immunoprecipitation of gL mutants with WT gH. CHO cells seeded in 24-well plates were co-transfected with a plasmid expressing gH and a plasmid expressing WT gL or a gL mutant or an empty-vector control. Proteins in cell lysates were immunoprecipitated with anti-gH mAb 52S and separated by electrophoresis on 4–20 % polyacrylamide gels under non-reducing conditions and western blots were performed using the rabbit anti-gH-gL serum R137. HSV-1 gH is synthesized and released into the ER as a 100-kDa precursor form (pgH) (white arrow heads). Hetero-dimerization of pgH with pgL allows transport of the complex to the Golgi where addition of O-linked and N-linked glycans increases the apparent molecular mass of mature gH (mgH) to 110-kDa (black arrow heads) (Hutchinson et al., 1992). Heterodimerization of gL with gH results in a fully processed form of gL with an apparent molecular mass of 33-kDa (grey arrowheads).

Figure 3.4. Co-immunoprecipitation of gL mutants with WT gH.

IP: 52S (α-gH)   Blot: R137 (α-gHgL)

Table 3.2. Effects of HSV-1 gL linker-insertion mutations on gH and gL cell surface expression and gH-gL interactions.

| Position of insertion | Amino acids inserted | Mutant Category | Cell surface expression (% of WT)[a] (Mean±SD) | | | Immunoprecipitated with anti-gH (52S)[b] | | |
			gL	gH	gH (in complex wth gL)	Precursor gH	Mature gH	Mature gL
L004	GCLNM	1	95 ± 5	105 ± 7	104 ± 8	+	+ + +	+ + +
V017	RCLNM	5	3 ± 1	0 ± 4	1 ± 3	+	–	–
L047	PCLNI	1	85 ± 2	88 ± 9	37 ± 19 *	+	+ +	+ +
R055	LFKQR	3	86 ± 12	48 ± 20	21 ± 16 *	+	– / +	–
F071	LFKQF	4	36 ± 11	0 ± 4	0 ± 3	+	–	–
E105	VFKQE	4	48 ± 20	2 ± 8	1 ± 3	+	–	–
L107	MFKHL	1	100 ± 4	106 ± 13	108 ± 17	+	+ +	+ + +
F112	LFKQF	1	90 ± 22	86 ± 11	94 ± 4	+	+ + +	+ +
D134	SCLNN	1	84 ± 7	102 ± 2	94 ± 4	ND[c]	ND	ND
R136	KCLNS	1	84 ± 12	93 ± 12	101 ± 3	+	+ + +	+
A140	MFKHA	1	92 ± 3	102 ± 6	96 ± 7	ND	ND	ND
K146	VFKQK	5	0 ± 1	1 ± 8	4 ± 2	+	–	–
T157	LFKHT	3	85 ± 5	64 ± 21	55 ± 15	+	+	–
E184	ACLNK	2	69 ± 15	105 ± 1	119 ± 6	+	+ + +	+ + +
P195	LFKQP	1	106 ± 5	113 ± 7	126 ± 5	+	+ + +	+ +

[a] Quantified by CELISA using R88 to detect gL, mAb 52S to detect gH and mAb 53S to detect gH in complex with gL.

[b] See Figure 3.4

[c] ND = not determined

Table 3.2 summarizes the results of all the experiments done to assess the effects of insertions in gL on cell surface expression of gH and gL and dimerization of gH with gL. All Category 1 and 2 mutants can dimerize with gH and were expressed on the cell surface at levels at least 75% that of wild-type gL, presumably as heterodimers with gH and perhaps also as gL alone. Category 3 mutants exhibited WT levels of gL expression on cell surfaces but some impairment in dimerization with gH (Fig. 3.4), indicating that the reduced detection of gH (Figure 3.1) and gH-gL (Figure 3.3) on cell surfaces reflected actual reduced levels of gH-gL. Category 4 mutants were expressed at reduced levels on cell surfaces but probably not in association with gH inasmuch as dimerization was greatly impaired (Fig. 3.4). Category 5 mutants were not detected on cell surfaces at all. Mutant V017 (Category 5) has its insertion near the signal peptidase cleavage site (Fig. 3.1), which may account for its severe impairment in dimerization with gH and post-translational processing. The other severely impaired mutant (K146) has its insertion near the border of the gH-gL interaction domain. The insertions in mutants L047 (Category 1) and R055 (Category 3) alter the conformation of gH-gL dimers (Figure 3.3) although only R055 exhibited reduced efficiency of this dimerization (Figure 3.4). Both F071 and E105 (Category 4) significantly impaired the dimerization of gH-gL and appearance of dimers on the cell surface. These four insertions define a domain that is critical for gH-gL dimerizaton (F071 and E105) and WT conformation of these heterodimers (L047 and R055), within the larger region identified by truncation mutations.

To assess whether mutant gLs expressed on the cell surface were grossly altered in conformation, the CELISA was repeated with a panel of conformation-dependent anti-gL mAbs (Table 3.3). The anti-gL mAbs used in this study are from the VIII series of anti-gL mAbs that were found to map to a C-terminal fragment (168–208) of gL (Novotny et al., 1996; Peng et al., 1998). One of these studies (Peng et al., 1998) concluded that major epitopes for these mAbs are located between amino acids (a.a.) 168 to 178, but did not exclude the possibility that additional a.a. beyond 178 contributed to these epitopes. For most mutants, the ratio of mAb binding to polyclonal antibody (R88) binding was essentially equivalent to that observed for WT gL, indicating retention of at least some aspects of WT conformation. Category 2 mutant E184, located within the C-terminal 168–208 domain, showed a complete loss of binding by all of the VIII mAbs indicating disruption of their epitopes. This disruption probably explains the reduced binding of the rabbit anti-gL serum R88, as shown in Figure 3.1. Category 3 mutant, R055, and Category 4 mutants, F071 and E105, all showed somewhat reduced binding of several of the anti-gL mAbs, relative to R88 binding. Insertions in these mutants appear to affect conformation of the mAb epitopes, which are clearly located downstream of the insertions. Since these insertions also partially or completely impaired the heterodimerization of gL with gH and altered an epitope dependent on gH-gL heterodimerization (Figure 3.3), it seems likely that conformation of the epitopes recognized by the anti-gL antibodies is in part dependent on gH-gL heterodimerization. Not surprisingly, Category 5 mutants, V017 and K146, which were not detected on the cell surface by R88, were also not detected by any of the mAbs.

Table 3.3. Binding of monoclonal antibodies to gL mutants.

Position of insertion	Mutant Category	Monoclonal antibodies *				
		VIII-62-15	VIII-82-24	VIII-87-1	VIII-200-1	VIII-820-8
L004	1	+ + +	+ + +	+ + +	+ + +	+ + +
V017	5 †	X	X	X	X	X
L047	1	+ + +	+ + +	+ + +	+ + +	+ + +
R055	3	+ +	+ +	+ +	+ + +	+ +
F071	4	+	+ +	+ +	+ + +	+ +
E105	4	+	+ +	+ +	+ +	+
L107	1	+ + +	+ + +	+ + +	+ + +	+ + +
F112	1	+ + +	+ + +	+ + +	+ + +	+ + +
D134	1	+ + +	+ + +	+ + +	+ + +	+ + +
R136	1	+ + +	+ + +	+ + +	+ + +	+ + +
A140	1	+ + +	+ + +	+ + +	+ + +	+ + +
K146	5 †	X	X	X	X	X
T157	3	+ + +	+ + +	+ + +	+ + +	+ + +
E184	2	–	–	–	–	–
P195	1	+ + +	+ + +	+ + +	+ + +	+ + +

* CELISA data were normalized to the reactivity of each mAb to WT gL. The

normalized values for each mAb were then compared to values obtained using rabbit

antiserum R88 for each gL mutant to determine relative differences in reactivity. The

symbols represent >80% (+ + +), 50–80 % (++), 20–50% (+), and < 20% (–) reactivity of

each mAb compared to R88 values for each gL mutant.

† For Category 5 mutants, the symbol (X) indicates lack of binding by R88 and all mAbs

tested.

Functional Activities of the gL Mutants.

To assess cell fusion activity by a quantitative luciferase-based assay, all 15 gL mutants were co-expressed with HSV-1 gB, gD and gH in CHO cells (effectors), which were mixed with nectin-1-expressing or HVEM-expressing CHO cells (targets). CELISAs were performed in parallel to quantitate cell surface expression of gL in the effector cell populations (results were not significantly different from those shown in Fig. 3.1 for CHO cells co-transfected with gH and gL only). Fig. 3.5 presents the cell surface expression for all gL mutants in comparison with cell fusion results obtained with both the HVEM and nectin-1 target cell populations.

Of the 15 gL mutants tested, all Category 1 and 2 mutants had cell fusion activity detected with both HVEM and nectin-1 as the fusion receptor. Cell fusion activity was impaired for three of the Category 1 mutants, severely for L047 and minimally for L107 and F112. The impaired function of L047 is consistent with results indicating that the conformation of the gH-gL oligomer was altered (Fig. 3.3). It may be relevant that the insertions of L047, L107 and F112 flank a region critical for gH-gL oligomerization as defined by the impaired heterodimerization of mutants R055, F071 and E105. Given that HVEM and nectin-1 are both gD receptors capable of triggering cell fusion activity, it was somewhat surprising that, for four Category 1 mutants (L004, L047, L107 and P195), fusion activity was higher with cells expressing HVEM than nectin-1. The Category 2 mutant E184 did not differ from WT gL in cell fusion activity, indicating that the disruption of mAb epitopes (Table 3.3) was without effect on this activity.

Of the remaining 6 mutants, only the category 3 mutants, R055 and T157, permitted expression of cell surface gH-gL dimers (Fig. 3.3), with T157 permitting higher levels of gH than R055. However, only T157 had detectable cell fusion activity, and only with HVEM. None of the category 4 or 5 mutants had cell fusion activity as expected.

Figure 3.5. Cell fusion activities of gL mutants in relation to cell surface expression. CHO cells were transfected with plasmids expressing WT gL or one of the gL mutants, other HSV-1 glycoproteins (gB, gD and gH) and T7 polymerase (effector cells). CHO-HVEM and CHO-nectin-1 cells were transfected with a plasmid carrying the firefly luciferase gene under control of the T7 promoter (target cells). One set of effector cells was used for CELISA and the other set was mixed with the target cells for assessment of cell fusion activity by quantification of luciferase activity. The results are expressed as % of WT gL activity, after subtraction of background values obtained in the absence of gL expression. The final values represent the means and SD of three independent experiments.

Figure 3.5. Cell fusion activities of gL mutants in relation to cell surface expression.
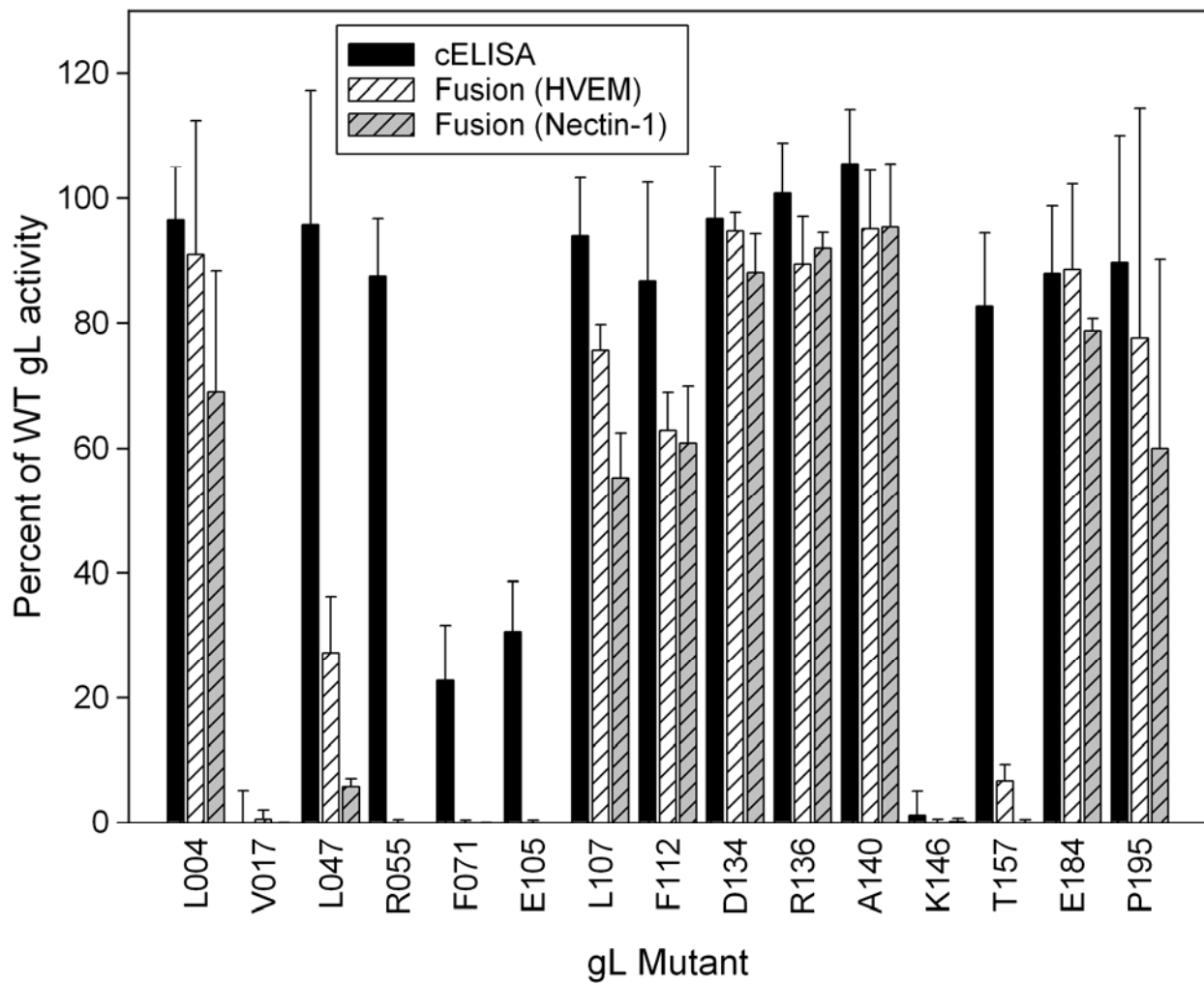
To assess fusion and hemifusion activity by a lipid transfer assay, gL mutants were co-expressed with HSV-1 gB, gD, gH and EGFP in CHO cells (effectors), which were mixed with Vero-BG20 cells (targets) expressing the glycolipid GM1 and engineered to overexpress HVEM. CHO cells do not express GM1. After 12 hours of co-cultivation, the CHO and Vero-BG20 cells were fixed, stained with anti-GM1 and imaged on a Zeiss UV LSM 510 confocal microscope. If hemifusion occurs, GM1 transfer from Vero-BG20 cells to the membranes of adjacent GFP-positive CHO cells is detected in the absence of syncytium formation. Complete fusion is evident when multiple nuclei are present in a GFP-positive syncytium bounded by the GM1-positive plasma membrane, indicating both cytoplasmic and lipid mixing. Fig.6A shows a representative fusion event (white arrow), defined as a syncytium with $\geq$ 2 DAPI-stained nuclei (blue) and cytoplasmic GFP (green) surrounded by GM1-positive membrane (red) [GFP+/GM1+ w/ > 2 nuclei]. Fig.6B shows representative hemifusion events. The white arrowheads point to hemifused CHO cells with a single DAPI-stained nucleus and cytoplasmic GFP surrounded by GM1-positive membrane.

Figure. 3.6. Representative fusion and hemifusion events from the lipid transfer assay. CHO cells were transfected with plasmids expressing WT gL or selected gL mutants, other HSV-1 glycoproteins (gB, gD and gH) and EGFP (effector cells) and overlayed on Vero-BG20 cells previously seeded onto glass coverslips. After 12 hours of co-cultivation, fusion and hemifusion events were imaged on a Zeiss UV LSM 510 confocal microscope. A representative fusion event (Panel A, white arrowhead) and hemifusion events (Panel B, white arrowheads) are shown.

Figure. 3.6. Representative fusion and hemifusion events from the lipid transfer assay.
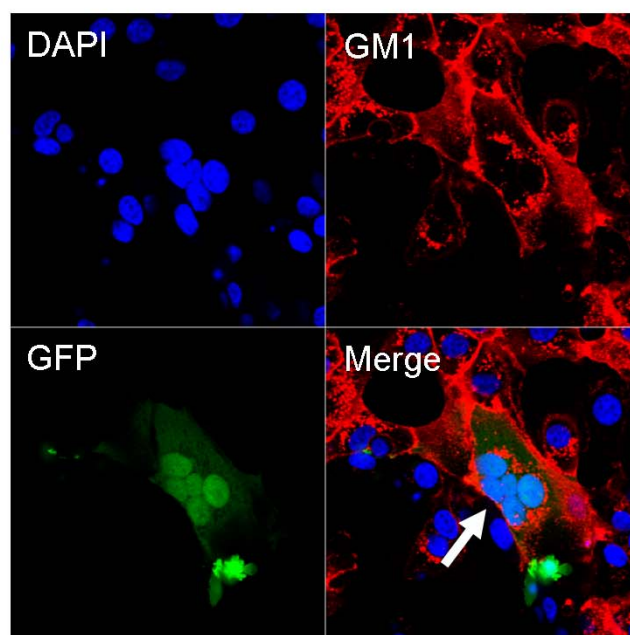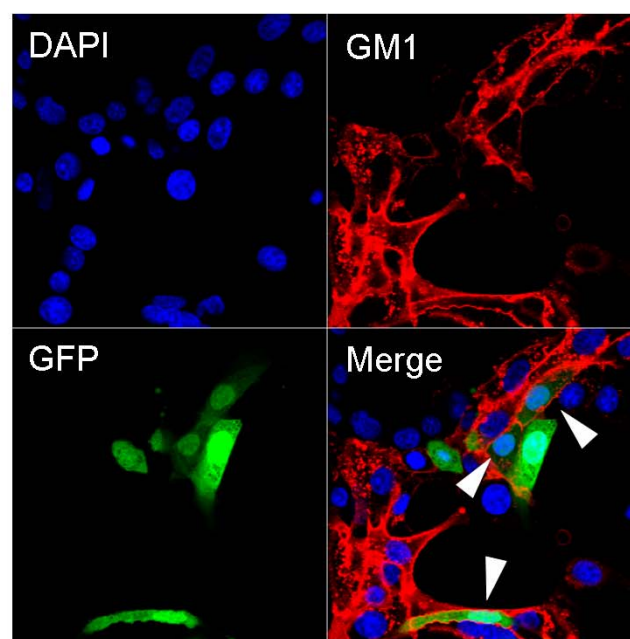
The gL mutants selected for the lipid transfer assay included two Category 1 mutants, L047 with reduced fusion activity and R136 with WT fusion activity, and all Category 3, 4 and 5 mutants. For each control and mutant, multiple sets of chambered coverslips were prepared for the lipid transfer assay. Between 8 to 10 high-powered fields per coverslip were randomly imaged for examination. Table 3.4 summarizes the data collected from quantitation of the images. On average, 8 to 11% of the cells per field were GFP-positive. For fusion events, the average number of nuclei per syncytium was 3.

Table 3.4. Effects of HSV-1 gL linker-insertion mutations on hemifusion and full fusion.

Position of insertion	Mutant Category	Events (%) or number of nuclei (Mean + SD)			
		% GFP+	Hemifusion as % of GFP+ cells	Full fusion as % of GFP+ cells	# of Nuclei / syncytium
pCAGGS		7.6 ± 1.3	8.5 ± 10.3	0.0 ± 0.0	–
WT gL		10.0 ± 3.6	27.6 ± 8.9	43.0 ± 21.0	3.1 ± 0.4
V017	5	9.8 ± 0.4	14.2 ± 7.6	5.3 ± 6.1	2.2 ± 0.2
L047	1	10.0 ± 1.9	32.7 ± 5.7	14.1 ± 4.6	2.8 ± 0.6
R055	3	11.4 ± 2.8	19.9 ± 3.7	2.2 ± 3.8	–
F071	4	11.1 ± 2.6	8.2 ± 8.7	1.2 ± 2.1	–
E105	4	8.4 ± 0.9	21.8 ± 0.4	4.2 ± 3.8	3.0 ± 1.4
R136	1	8.1 ± 1.9	33.9 ± 4.3	31.4 ± 18.3	3.1 ± 0.6
K146	5	8.6 ± 0.7	19.5 ± 6.2	1.1 ± 2.0	–
T157	3	9.9 ± 2.4	32.7 ± 7.0	4.9 ± 5.7	3.3 ± 0.5

Figure 3.7 presents the results of the lipid transfer assay in graphical format. In gL-negative control cells expressing only gD, gH and gB, a low-level (~8%) of hemifusion was observed but fusion events were not detectable. In comparison, with WT gL and the other fusion glycoproteins, hemifusion events increased 3.5-fold to ~28% while fusion events were detected for ~43% of GFP-positive cells. For Category 1 mutant L047, which exhibited reduced activity in the luciferase-based cell fusion assay, hemifusion activity was similar to that of WT gL but full fusion activity was reduced 3.0-fold. This indicates that gL has a role in formation of the fusion pore necessary for cytoplasmic mixing. Category 1 mutant R136 did not differ significantly from WT gL for hemifusion or full fusion activity. Category 3 mutants, R055 and T157, were both functional in hemifusion, with reduced and WT levels of hemifusion, respectively. However, both mutants had severely reduced full fusion activity, as expected. All four Category 4 and 5 mutants exhibited little if any full fusion activity as expected, but two of them (E105 and K146) had intermediate levels of hemifusion activity despite the effects of these mutations on cell surface expression of gH. Because mutants with the lowest levels of cell surface expression of gH-gL dimers, such as V017 and F071, exhibited the greatest reduction in hemifusion activity, it is difficult to assess whether gL has a role in hemifusion activity other than its role in gH transport to the cell surface.
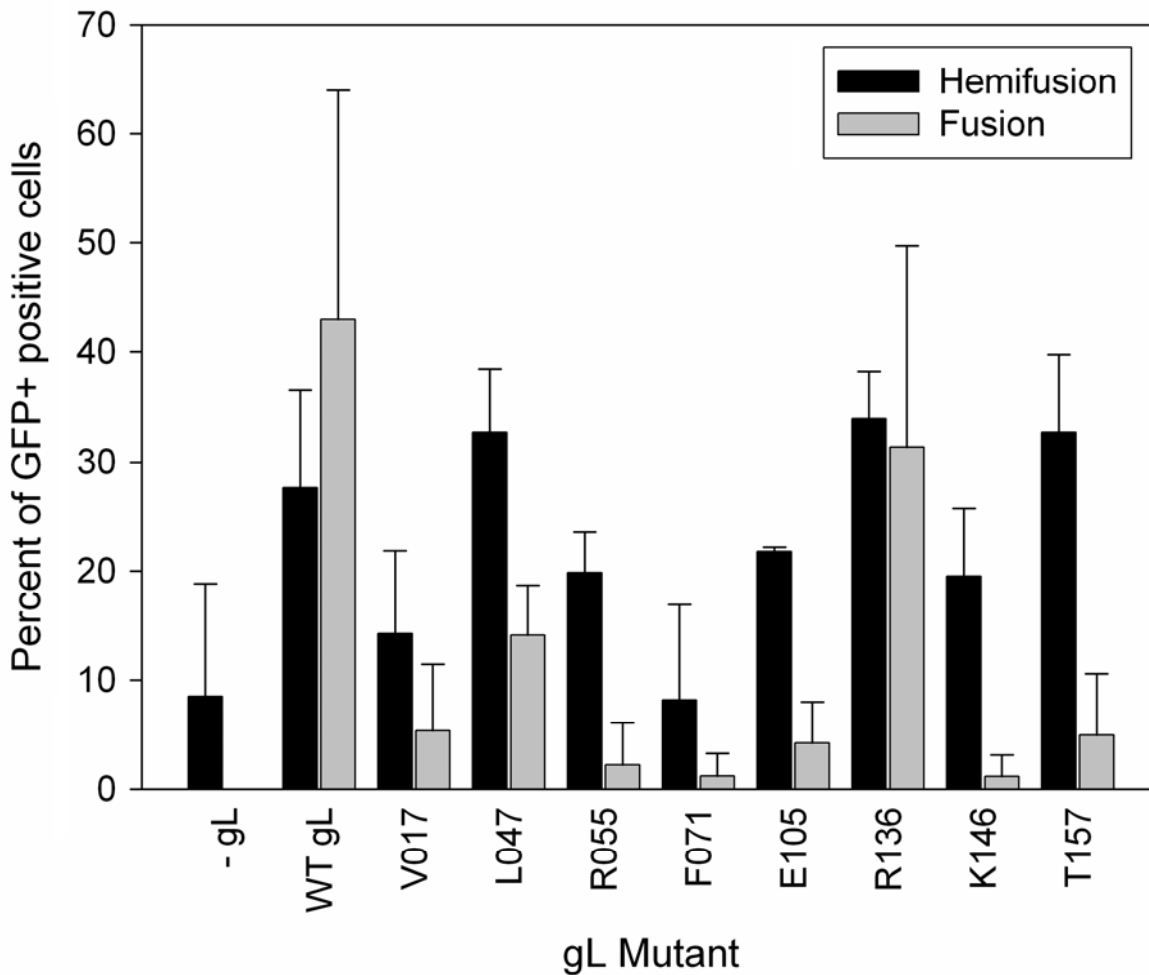
Figure 3.7. Hemifusion and fusion activities associated with WT gL and gL mutants as determined by the lipid transfer assay. The results of the hemifusion and fusion activities using the lipid transfer assay are expressed as % of GFP-positive cells for each control and selected gL mutants.

To address whether the mutant forms of gL were functional for viral entry, the mutants were tested using a virus complementation assay. Vero cells were transfected with a plasmid expressing vector alone, wild-type gL or one of the mutant forms of gL. At 24 h post-transfection, the Vero cells were infected with a gL-negative HSV- mutant, gL86. Complemented virus was harvested 24 h post-infection and titrated on the gL-complementing Vero cell line, Vero-gL, to determine the PFU/mL harvested for each gL mutant.

Figure 3.8 shows the titers (PFU/mL) of complemented virus for each gL mutant. Table 5 summarizes, for each mutant, the results of cell surface expression, cell fusion activity from the luciferase-based fusion assay, and viral entry activity from the complementation assay. For some of the mutants, the complementation results paralleled the cell fusion results although a greater range of differences in activity were observed for complementation than for cell fusion. For the gL-negative control, the virus titer obtained was $\sim 10^2$ PFU/ml whereas the virus titer for WT gL was $> 10^7$ PFU.ml. With the exception of L047, Category 1 and 2 mutants complemented viral infectivity to WT levels. L047, with cell fusion activity at 27% and 6% of WT gL values, for HVEM and nectin-1 respectively, had about 20% of WT gL complementing activity. For Category 3 mutants, R055 and T157, the differences in degree of their impairments were evident for complementation as well as for cell fusion. T157 permitted higher levels of gH expression on the cell surface (Figure 3.1), exhibited detectable cell fusion activity whereas R055 did not (Figure 3.5) and complemented the gL-negative virus >100 times better than did R055 but 100 times less well than did WT gL. Category 4

mutants F071 and E105 did not traffic gH to the cell surface to detectable levels (Figs. 3.1 and 3.3) but complemented the gL-negative virus better than did R055, which was able to interact with gH to promote some cell surface expression. Unexpectedly, Category 5 mutant V017 complemented the defective virus almost as well as did L047 and K146 complemented as well as did T157. Thus, for these mutants, the cell fusion activities (nil, except for hemifusion) and viral entry activities are totally incongruent.
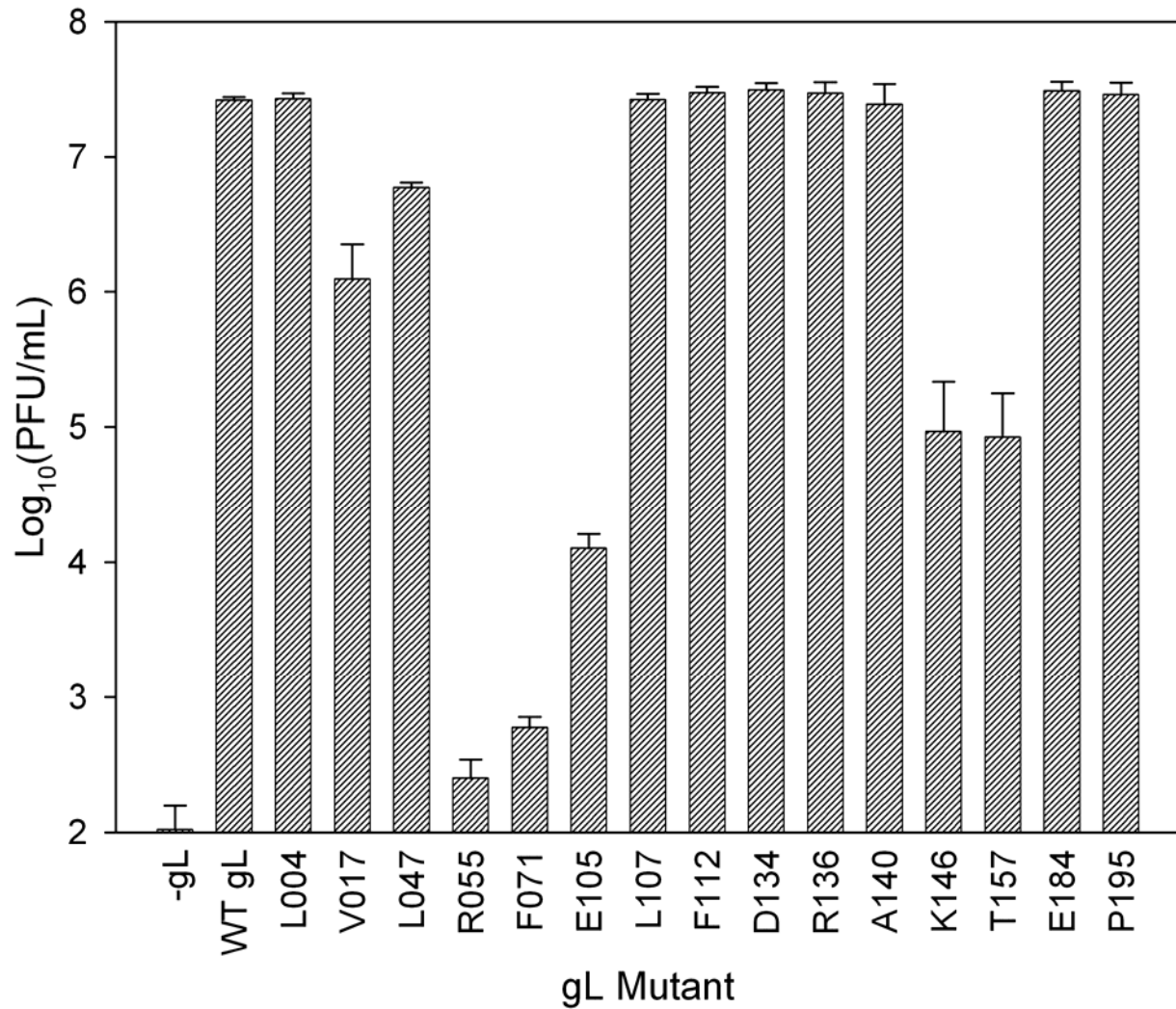
Figure 3.8. Complementation of gL-negative virus entry by gL mutants.

Vero cells, transfected with a plasmid expressing vector alone, wild-type gL or one of the mutant forms of gL, were infected with the gL-negative virus, gL86, at 24 hours post-transfection. Complemented virus was harvested 24 hours post-infection and titrated on the gL-complementing Vero cell line, Vero-gL, to determine the PFU/mL harvested for each gL mutant. The results show the Log_{10}(PFU/mL) of complemented virus for each gL mutant.

Table 3.5. Effects of HSV-1 gL linker-insertion mutations on cell surface expression, cell fusion activity, and viral entry.

Position of insertion	Mutant Category	cELISA (R88 α-gL) Mean±SD (% of WT)	Cell fusion (HVEM) Mean±SD (% of WT)	Cell fusion (Nectin-1) Mean±SD (% of WT)	Complementation Log$_{10}$(PFU/mL) ± SD	ΔLog$_{10}$(PFU/mL)
L004	1	96 ± 9	91 ± 21	69 ± 19	7.43 ± 0.04	+ 0.01
V017	5	0 ± 5	1 ± 1	0 ± 0	6.09 ± 0.26	− 1.33
L047	1	96 ± 22	27 ± 9	6 ± 1	6.77 ± 0.04	− 0.65
R055	3	88 ± 9	0 ± 1	0 ± 0	2.40 ± 0.14	− 5.02
F071	4	23 ± 9	0 ± 1	0 ± 0	2.77 ± 0.08	− 4.64
E105	4	31 ± 8	0 ± 0	0 ± 0	4.10 ± 0.11	− 3.32
L107	1	94 ± 9	76 ± 4	55 ± 7	7.42 ± 0.04	+ 0.00
F112	1	87 ± 16	63 ± 6	61 ± 9	7.47 ± 0.04	+ 0.05
D134	1	97 ± 8	95 ± 3	88 ± 6	7.49 ± 0.05	+ 0.08
R136	1	101 ± 8	89 ± 8	92 ± 3	7.47 ± 0.08	+ 0.05
A140	1	106 ± 9	95 ± 9	95 ± 10	7.39 ± 0.15	− 0.03
K146	5	1 ± 4	0 ± 1	0 ± 0	4.97 ± 0.36	− 2.45
T157	3	83 ± 12	7 ± 3	0 ± 0	4.92 ± 0.32	− 2.49
E184	2	88 ± 11	89 ± 14	79 ± 2	7.49 ± 0.07	+ 0.07
P195	1	90 ± 20	78 ± 37	60 ± 30	7.46 ± 0.09	+ 0.04

DISCUSSION

The goals of this study were to identify regions of HSV-1 gL critical for gL interactions with and transport of gH, assess the effects of insertions in gL on gH-gL heterodimer conformation, and relate any alterations in gH-gL dimerization, conformation and transport to the cell surface to gL function in cell fusion and viral entry. CELISA results for the co-expression of gH with gL linker-insertion mutants permited several conclusions about regions of gL critical for binding to gH and expression of gL and gH on the cell surface.

The data show that insertions in the region from residues 47 to 105 either abrogated gL binding to gH or altered the conformation of the gH-gL heterodimer, as determined by 53S binding. Insertions at F071 and E105 appear to define the principal gH-binding domain in gL, given that these mutants failed to dimerize with gH, failed to mediate transport of gH to the cell surface, and were non-functional in cell fusion and severely impaired in virus entry. The gH-binding domain identified in this study correlates well with the boundaries of a conserved region identified by an amino acid sequence alignment of gLs from various alphaherpesviruses (Figure 3.9). The alignment shows that, although the overall sequence identity between different gLs is low, the region between residues 69 to 106 in HSV-1 gL is relatively well conserved. Identification of the gH-binding domain for HSV-1 gL in this study suggests that this region may be the gH-binding domain for the other alphaherpesvirus gLs.

Other mutations impaired the dimerization of gL with gH and/or altered the conformation of these dimers.   Mutant R055, located N-terminal to the gH-binding domain near a highly conserved Pro residue, was impaired for dimerization with gH; formed dimers that were altered in conformation, according to the ratios of 52S/53S binding; and was severely impaired for both cell fusion and viral entry. Interestingly, mutant L047, which appeared to dimerize normally with gH, formed dimers with altered conformation and was severely impaired in cell fusion but not in viral entry. This region from aa 47 to 105 is not the only region critical for the formation of functional gH-gL dimers. The insertion in mutant T157 also impaired dimer formation and functional activity of gH and gL in cell fusion and viral entry (cell fusion was more severely reduced than viral entry). One possibility is that, in the 3-dimensional structure of gH-gL, residues around aa 157 are in close proximity to residues 47 to 55. The region between residues 155 to 161 was previously shown to be critical for gH-gL transport, which is consistent with our results and would also help to explain the impairment in function in cell fusion. Mutants V017 and K146 failed to dimerize with gH, as well as failing to be transported to the cell surface in the presence or absence of gH, and had no detectable function in cell fusion. Surprisingly, these mutants exhibited significant, but not WT levels of, viral entry activity (to be discussed below). The results presented here with all of the functionally-impaired gL mutants are consistent with the idea that gH-gL heterodimers are necessary for function, at least in cell fusion, and that these heterodimers must adopt a very specific "functional conformation(Cairns et al., 2007)." Consistent with my findings, an N-terminal deletional analysis of HSV-2 gH that showed gH can be expressed on the cell

surface independent of gL but is non-functional, and that function can be only restored if

gL is present.

```
                                                             *      +                          *
HSV-1     1 -----MGILGWV-GLIAVGVLCVRGGL---PSTEYVIR----------SRVAR-----------EVGDILKVPCVP-----------LPSDDLDWRYETPSAINYA---
HSV-2     1 -----MGFVCLF-GLVVMGAWGAWGGS---QATEYVLR----------SVIAK-----------EVGDILRVPCMR-----------TPADDVSWRYEAPSVIDYA---
VZV       1 -----MASHKWLLQIVFLKTITIAYCLHLQDDTPLFFG----------AKPLS-----------DVSLIITEPCVS-----------SVYE--AWDYAAPPVSNLSE--
GHV       1 -----MKIY-----RVLVHLSFVLGMF---TKTDTVLAWSKYDLVHGFMRVA------------NISSIMRLDCLPNLLSSNAGYAALPSDDI------PT--------
EHV       1 MY---QILIGCV-WQKSPYINQCTEFQ---PPLSFVTP----------ERMRRFMRCWARLELVYMLAWIVTTKLVK-----------ATRLDFTWGPGEPKRILEASCG
BHV-1     1 MAPAVARACAWA-LLAALLWLPPAGA--------------------TRRAD-----------SAESILAERCRGNL---------LLADRPQHEEAAPG--------

            **         *       **            +  **    +   +
HSV-1    66 ----------------LID--GIFLRYHCPGLDTVLWDRHAQKAYWVNPFLFVAGFLEDLSYPAFPANTQETETRLALYKEIRQALDSRKQAASHTPVK---AGCV-N
HSV-2    66 ----------------RID---GIFLRYHCPGLDTFLWDRHAQRAYLVNPFLFAAGFLEDLSHSVFPADTQETTTRRALYKEIRDALGSRKQAVSHAPVR---AGCV-N
VZV      69 ----------------ALS---GIVVKTKCPVPEVILWFKDKQMAYWTNPYVTLKGLAQSVG-----EEHKSGDIRDALLDALSGVWVDSTPSSTNIP-E---NGCVWG
GHV      71 ----------------------GIFIKVNCSIPEFILWYEQKAMAAWINPIMGTVLMMNDVLKSGL-----ENSVKVGLLTFLKRIAEK----GPNGPLRNRGSGCI-N
EHV      83 SGPIMKGQLFTSPNIKNLLNRTTGIMVKAHCNPPEAILWVDTPPKPVWVNPFAVVQGLAEDVTNGNMPQDFKE---------KLLFALDDSLSQSQSSP----------
BHV-1    59 ----------------LA---GIFIRGRCSPPEAALWYEDTGETYWANPYAVARGLAED-------------------IRRVL-------ADTPV----------

            +
HSV-1   152 FDYSRTRRCVGRQDLGPTNGTSGRTPVLPPDDEAGLQPKPL-TTPPPIIATSDPTPRRDAATKSRRRRPHSRRL--
HSV-2   152 FDYSRTRRCVGRRDLRPANTTSTWEPPVSSDDEASSQSKPL-ATQPPVLALSNAPPRRVSPTRGRRRHTRLRRN--
VZV     150 ADRLFQRVCQ---------------------------------------------------------------------
GHV     148 LIAPADISCYGSTRLDRFNRDF-------EDDSRGM-------------------PCR--AKAMRRTTSGSRRAGT
EHV     173 ------DEILGPPPLGCFTGPFFLSPPKSKDIAEGL--KDS-CIPASYYANLQKT--------------------
BHV-1   109 ------YRDLAIQVLNSAFG-------LPHEVRAPLPPPPRGCVLPPRYHTTGPCGPGDGIYR------------
```

Symbol	Conservation
*	100%
+	80%

Figure 3.9 Amino acid sequence alignment of alphaherpesvirus gL.

The alignment of alphaherpesvirus gLs begins at the first Met of the gL precursor.

Asterisks (*) indicate residues that are 100% conserved and (+) plus signs indicate

residues that are 80% conserved between species. The bracket indicates the region of

relatively high conservation of amino acid sequence.

The results obtained for the gH-gL expression patterns also provide some insights into the trafficking, processing, cell surface expression of gL. Unexpectedly, all mutants detected on the cell surface in the presence of gH were also detected in the absence of gH. These findings differ from a previous study showing that gL was secreted by cells but was not detected on the cell surface (Dubin and Jiang, 1995). One possible explanation for this discrepancy is that the previous study utilized immunofluorescence as the method to detect gL while CELISA was used in our study. The sensitivity of each assay may differ leading to the conflicting results. An additional possibility is that the antibody used in the immunofluorescence study was unable to detect gL secreted from cells while the rabbit anti-serum used in our study did recognize secreted gL. The results of the mAb antibody binding experiment (Table 3.3) showed that gL mutants detected on the cell surface but unable to dimerize with gH (F071 and E105) were somewhat altered in conformation, consistent with the latter possibility. These results also indicate that gL adopts a different conformation when complexed with gH, providing additional support for the existence of a specific "functional conformation" of the gH-gL heterodimer.

Of all gL mutants generated in this study, only 2 failed to be detected on the cell surface, mutants V017 and K146. Insertions into these 2 regions disrupted movement to and attachment to the cell surface. Furthermore, no gH interaction was detected by co-immunoprecipitation. The results identify two regions critical for processing of gL and trafficking to the cell surface but much less critical for incorporation into virion envelopes. Although mutants V017 and K146 were severely impaired or non-functional

in nearly all assays used, both were still able to complement entry of a gL-negative virus although not at WT gL levels. Insertion V017 is located within the predicted signal peptide. Using a signal peptidase prediction program, it was determined that the insertion likely causes the cleavage site to occur 6 a.a. N-terminal of the WT cleavage site and adds an additional 3 a.a. from the insertion itself. The resulting 9-a.a. addition to the N-terminus of gL may account for difficulty of this gL mutant to traffic to the cell surface. Insertion K146 is located near a conserved Pro residue at position 144 and may fail to traffic to the cell surface because of improper folding of gL, resulting in a less stable protein. The discrepancy between the lack of cell surface expression and the ability to complement entry of a gL-negative virus suggests that gL may be processed differently for incorporation into virions than for transport to the cell surface. It should be noted that envelopment of virions is a complicated process involving budding of nucleocapsids through the inner nuclear envelope, de-envelopment by fusion of primary virions with the outer nuclear envelope and re-envelopment of released nucleocapsids at a cytoplasmic vacuole probably derived from the Golgi apparatus (Mettenleiter, 2004). The possibility exists that gL retained in the endoplasmic reticulum or inner nuclear envelope could be incorporated into primary virions and that production of infectious virus does not require incorporation of gL into mature virions. Future studies should investigate the composition of mature virions produced by complementation with mutants V017 and K146.

CELISA results and functional assays showed that gL is necessary in cell fusion aside from its role in mediating gH transport to the cell surface. Mutants unable to bind

gH can either be secreted from cells and detected on the cell surface (F071 and E105) or retained intracellularly (V017 and K146). However, it has not been excluded that V017 and K146 may be secreted from cells but not be able to bind to the cell surface, a possibility that needs further study. Not surprisingly, all of these mutants had no detectable cell fusion activity, consistent with the essential role for gH in the gH-gL dimer. Mutants that bind and traffic gH to the cell surface exhibited two general phenotypes: WT levels of cell fusion activity or reduced to absent cell fusion activity. Mutants showing the former phenotype include L004, D134, R136, A140, and E184, and do not demonstrate the dissociation between formation and transport of gH-gL dimers and cell fusion activity. In contrast, the remaining mutants showed dissociation of the transport and cell fusion functions of gL. Mutants L107 and F112, located C-terminal to the gH-binding domain, exhibited a moderate reduction in cell fusion activity, as did mutant P195. As previously discussed, mutants L047, R055 and T157 exhibited a near total or total loss of cell fusion activity even though gH-gL heterodimers could be detected on the cell surface, at near WT levels for L047 only. Mutant R055 is the only gL mutant capable of binding gH (with reduced efficiency) that was unable to complement entry of a gL-negative virus. Thus, this current study demonstrates the separation of transport and cell fusion activities for HSV-1 gL and is consistent with the recent HSV-2 gH deletion mutant study demonstrating a separation of transport and cell fusion activities for gH.

The recent development of the lipid transfer (hemifusion) assay permited an additional assessment of the role of gL in the cell fusion process. Selected mutants

were tested in the hemifusion assay. Firstly, full cell fusion events detected with the hemifusion assay correlated fairly well with the data obtained by the luceriferase-based fusion assay, indicating that our modified method for performing the hemifusion assay was suitable. For mutant R136,, the levels of hemifusion and fusion were similar to those of WT gL as expected, inasmuch as R136 resembed WT gL in all other assays performed. Mutants unable to form gH-gL dimers (F071 and E105) had no significant fusion activity but some hemifusion was detected. For mutants with partial dissociation of the transport and cell fusion functions, L047 and T157, hemifusion was detected at WT gL levels but cell fusion activity was significantly reduced. Similarly, mutant R055 had detectable but lower levels of hemifusion activity and essentially no fusion activity. These findings indicate that the alterations in gH-gL heterodimer conformation recognized by the 53S antibody did not necessarily affect the hemifusion process. Therefore, the insertions that had the most deleterious effects on cell fusion, as assessed in the luciferase-based assay, but permitted cell surface expression of gH-gL dimers also permitted hemifusion but not full fusion. This indicates that, although gD and gH-gL were found to be sufficient for hemifusion and gB was required in addition for full fusion, gL also has a post-hemifusion role in cell fusion.

It was somewhat surprising to find that epitopes on gL recognized by mAbs capable of inhibiting cell fusion could be disrupted without any detectable effects on cell fusion activity. An insertion at E184 completely abrogated binding by all the mAbs tested here, indicating that their epitopes are disrupted by this insertion and must include at least a short region downstream of aa 168 to 178, the minimal region

identified in a previous epitope mapping study (Peng et al., 1998). The finding that E184 is detected at lower levels on the cell surface by the R88 polyclonal anti-serum, relative to WT gL, without a corresponding decrease in gH level also suggests that a major epitope for R88 lies within the same region. However, the loss of these epitope(s) for the mAbs and the antiserum did not affect cell fusion activity, despite an earlier study showing that these mAbs could block cell fusion activity in a HSV-strain specific manner but not virus entry, even though the mAbs bound to virions. Based on these findings, one would predict that a mutant virus carrying the E184 insertion would not have its cell fusion activity inhibited by these mAbs. Inhibition of cell-to-cell fusion (using the luciferase-based assay) and hemifusion (lipid transfer assay) have not been studied using these mAbs but could be the topic of future studies to study the mechanism of the block in cell fusion activity.

The apparently low levels of mutant E184 detected by the rabbit antiserum on cell surfaces in the absence of gH and restoration of E184 mutant levels in the presence of gH suggests several possibilities. Given that mutants F071 and E105 are at least somewhat altered in conformation, as detected by reduced binding by the mAbs, it is possible that in the absence of gH, E184 also adopts an altered conformation which abrogates binding of the mAbs and reduces binding of antibodies in the antiserum. The low levels of the E184 mutant detected on the cell surface could also be accounted for by aberrant transport or processing that disrupts entry into the secretory pathway in the absence of gH. A third intriguing possibility is that mutant E184 has greatly reduced ability to bind to the cell surface in the absence of gH. An insertion at position 184 could

theoretically disrupt the region on gL responsible for binding of gL to a putative cell surface receptor.

The findings of this study identify several critical functional regions in HSV-1 gL, including the gH-binding domain, additional domains critical for functional interactions between gL and gH and domains for trafficking of both gL alone and the gH-gL heterodimer. Future studies should be focused on studying mutant gLs in the context of the virus to investigate potential differences in the roles of gL in cell fusion and virus entry. Identification of an as yet unidentified gL receptor is another area for exploration using expression cloning in a cell line that secretes gL is unable to bind gL. Further studies of the gH-gL heterodimer can utilize other anti-gH or anti-gL mAbs to probe how alterations in conformation affect hemifusion or cell fusion.

CHAPTER 4: MATERIALS AND METHODS

Cells and viruses. Cell lines used included CHO cells; CHO cells stably expressing human HVEM (Montgomery et al., 1996) or nectin-1 (Geraghty et al., 1998); Vero cells; Vero-B24 cells carrying the HSV-1 gB gene (Herold et al., 1991) and used for the propagation and titration of the gB-negative mutant HSV-1(KOS)K082 (Cai et al., 1987) and Vero-gL cells carrying the HSV-1 gL gene and used for the propagation and titration of the gL-negative mutant HSV-1 gL86. The CHO cell line and derivatives were grown in Ham's F12 medium supplemented with 10% fetal bovine serum (FBS) and the Vero cell line and derivatives were grown in DMEM-10% FBS.

The complementing cell line, Vero-gL, and the viral mutant, HSV-1(KOS)gL86, were generated by Michael Novotny. To isolate the Vero-gL cell line, Vero cells were stably transfected with plasmid pMN79, which carries the HSV-1(KOS) UL1 (gL) gene (nucleotides 9327-10156 of the HSV-1 genome) driven by the HSV-1(KOS) ICP6 early promoter (nucleotides 85899-86414 of the HSV-1 genome) and both Amp and Neo selectable markers. Nucleotide numbers are based on the sequence of HSV-1(17) (GenBank entry X14112). The transfected cells were maintained in DMEM-10% fetal bovine serum (FBS) and geneticin at 600 µg/ml. The complementing clone Vero-gL was identified and isolated by use of a type-specific anti-gL antiserum to detect HSV-1 gL expression induced by infection of the cells with HSV-2.

The gL-negative mutant, HSV-1(KOS)gL86, was obtained by co-transfection of Vero-gL cells with infectious HSV-1(KOS) DNA and plasmid pMN86, which contains the *lacZ* gene driven by the cytomegalovirus immediate-early promoter inserted between a region upstream of the UL1 (gL) gene (nucleotides 7729-9333) and a region from codon

33 of the gL gene extending to the end of the downstream overlapping UL2 gene

(nucleotides 9434-10639), thus deleting the first 32 codons of the gL gene at the

position of the *lacZ* insertion. Recombination of this plasmid with genomic HSV-1 DNA

yielded a recombinant virus which could not express gL (the only start codon was

deleted) and in which expression of the downstream gene was not affected. This

recombinant was identified by its ability to express β-galactosidase and was plaque-

purified on Vero-gL cells.

Random Linker-Insertion Mutagenesis of HSV-1 gB, gH and gL. The GPS™-LS

linker scanning system (New England Biolabs, NEB) was used, as recommended by the

manufacturer, on the insert excised from pPEP98, pPEP100 and pPEP101 (Pertel et

al., 2001), to generate random linker-insertion mutations of gB, gH and gL. After

religation of the library of inserts into pCAGGS and transformation of bacteria, 81

unique gB and 15 unique gL linker-insertion mutants were isolated and sequenced

using PrimerN (30-mer) and PrimerS (30-mer) provided by the manufacturer. After

removal of the transposon, each mutant plasmid was re-sequenced to verify the position

of each insertion. Insertion mutants for gH were analyzed by another graduate student

in the lab.

Co-immunoprecipitation and Western blotting. CHO cells seeded in 24-well plates

were transfected with 300 ng of a plasmid expressing gH and 300 ng of empty vector

(pCAGGS) or a plasmid expressing WT gL (pPEP101) or a gL mutant and 1.8 µl of

Lipofectamine 2000 (Invitrogen) both diluted in Opti-MEM (Gibco). After 24 h incubation, the cells were washed with phosphate-buffered saline (PBS) and lysed with 300 µl of lysis buffer (50mM Tris pH 8.0, 150 nM NaCl, 1% NP40) containing protease inhibitor cocktail (Roche). Nuclei and debris were removed by centrifugation and the supernatants mixed with 5 µg of anti-gH mAb 52S for 1 h at 4°C. Next, the supernatants were mixed with 20 µl of washed Protein A Sepharose beads (Amersham Pharmacia Biotech) for 1 h at 4°C on a rotator. The beads were centrifuged at 10,000g and washed with 500 µl on lysis buffer 5 times. Sample buffer with 100mM DTT was added to the bead pellet and boiled for 10 minutes. Proteins in the immunoprecipitation were separated by electrophoresis on 4–20 % gels under reducing conditions and western blots were performed using the rabbit anti-gH1/gL1 antiserum R137.

Western blotting. CHO cells seeded in 24-well plates were transfected with 400 ng of empty vector (pCAGGS) or a plasmid expressing WT gB (pPEP98) or a gB mutant and 1.2 µl of Lipofectamine 2000 (Invitrogen) both diluted in Opti-MEM (Gibco). After 24 h incubation, the cells were washed with phosphate-buffered saline (PBS) and lysed with 300 µl of lysis buffer (50mM Tris pH 8.0, 150 nM NaCl, 1% NP40) containing protease inhibitor cocktail (Roche). Nuclei and debris were removed by centrifugation and the supernatants mixed with sample buffer (without reducing agent) for SDS-PAGE and boiled for 5 min to detect monomeric forms of gB or not heated to detect high-molecular weight gB oligomers. Proteins in the cell lysates were separated by electrophoresis on

4–15 % gels under non-reducing conditions and western blots were performed using the rabbit anti-gB antiserum R74 (Herold et al., 1991)

Cell-based ELISA (CELISA). CHO cells seeded in 96-well plates were transfected with 30 ng of empty vector or a plasmid expressing WT gB or a gB mutant and 0.15µl of Lipofectamine 2000 both diluted in Opti-MEM. The cells were washed once with PBS 24 h after transfection and CELISA was performed as described previously (Geraghty et al., 2000), using anti-gB serum R74 at 1:10,000 dilution or one of several anti-gB mAbs (Para et al., 1985). In addition, CHO cells were transfected with all the plasmids used to prepare effector cells for the cell fusion assays as described below, including plasmids expressing mutant or WT forms of gB, so that levels of gB expression could be assessed in replicates of the cell populations used in the fusion assays. The cells were washed once with PBS 16 h after transfection and CELISA was performed with the anti-gB serum R74 as described above.

For gL mutants, CHO cells seeded in 96-well plates were transfected with 20 ng of plasmid expressing WT gH or empty vector and a plasmid expressing WT gL or a gL mutant and 0.13µl of Lipofectamine 2000 both diluted in Opti-MEM. The cells were washed once with PBS 24 h after transfection and CELISA was performed as described previously, using anti-gL serum R88 at 1:5,000 dilution or one of several anti-gL mAbs (VIII-62-15 at 1:5,000, VIII-82-24 at 1:100,000, VIII-87-1 at 1:20,000, VIII-200-1 at 1:2,000, and VIII-820-8 at 1:100,000) . CELISAs for gH were performed using anti-gH

mAbs 52S and 53S at 1:10,000 dilution. In addition, CHO cells were transfected with all the plasmids used to prepare effector cells for the cell fusion assays as described below, including plasmids expressing mutant or WT forms of gL, so that levels of gL expression could be assessed in replicates of the cell populations used in the fusion assays. The cells were washed once with PBS 16 h after transfection and CELISA was performed with the anti-gL serum R88 as described above.

Cell fusion assay. In parallel with CELISA, cell fusion activity of gB was measured using a modification of a quantitative luciferase-based cell fusion assay, along with the plasmids described for that assay (Pertel et al., 2001). CHO cells were seeded in 96-well plates and CHO cells stably expressing human HVEM or nectin-1 were seeded in 6-well plates one day prior to transfection. CHO (effector) cells were transfected with 20 ng each of plasmids expressing the T7 RNA polymerase, gD, gH, and gL, 30 ng of empty vector or plasmid expressing either WT (pPEP98) or mutant gB and 0.4μl of Lipofectamine 2000. For interference assays, 30 ng of pPEP98 expressing WT gB was added to each well in addition. CHO-nectin-1 or CHO-HVEM (target) cells were transfected with 400 ng of a plasmid carrying the firefly luciferase gene under control of the T7 promoter (Okuma et al., 1999), 1.8μg of empty vector (pCAGGS) and 7 μl of of Lipofectamine 2000. Two h post-transfection, effector cells were washed once with Opti-MEM while each target cell population was washed, detached with versene (0.2 g/L EDTA in PBS), and suspended in Opti-MEM. The target cell population was overlayed ($3x10^4$ cells/well) on the effector population. After 10 h, the cells were washed once with

PBS and lysed with 50 µl/well of 1X passive lysis buffer (Promega). Expression of luciferase was quantified by adding 50 µl/well of luciferase substrate (Promega) and measuring light output with a Wallac 1420 plate reader (Perkin-Elmer).

For gL mutants, CHO (effector) cells in 96-well plates were transfected with 20 ng each of plasmids expressing the T7 RNA polymerase, gD and gH, 30ng of gB, and 20 ng of empty vector or plasmid expressing either WT (pPEP101) or mutant gL and 0.4 µl of Lipofectamine 2000. CHO-nectin-1 or CHO-HVEM (target) cells in 6-well plates were transfected with 400 ng of a plasmid carrying the firefly luciferase gene under control of the T7 promoter, 1.8µg of empty vector (pCAGGS) and 7 µl of Lipofectamine 2000. Two h post-transfection, effector cells were washed once with Opti-MEM while each target cell population was washed, detached with versene (0.2 g/L EDTA in PBS), and suspended in Opti-MEM. The target cell population was overlayed ($3x10^4$ cells/well) on the effector population. After 10 h, the cells were washed once with PBS and lysed with 50 µl/well of 1X passive lysis buffer (Promega). Expression of luciferase was quantified by adding 50 µl/well of luciferase substrate (Promega) and measuring light output with a Wallac 1420 plate reader (Perkin-Elmer).

Complementation assay. This assay was done as described for complementation of a gD-negative virus by WT and mutant forms of gD (Manoj et al., 2004) except that Vero cells in 6-well plates were transfected with 1.0 µg of plasmid expressing WT or mutant forms of gB and 3.5 µl of Lipofectamine 2000, and later infected with the gB-negative

mutant, HSV-1(KOS)K082. Virus stocks were prepared and titrations performed on Vero-B24 cells.

For gL mutants, Vero cells in 6-well plates were transfected with 1.0 µg of plasmid expressing WT or mutant forms of gL and 3.5 µl of Lipofectamine 2000, and later infected with the gL-negative mutant, HSV-1(KOS)gL86. Virus stocks were prepared and titrations performed on Vero-gL cells.

Lipid transfer (hemifusion) assay. CHO (effector) cells seed in 24-well plates were transfected with 400 ng each of plasmids expressing HSV-1 gB, gD, gH and EGFP and 400 ng of empty vector (pCAGGS) or a plasmid expressing WT gL (pPEP101) or a gL mutant and 7 µl of Lipofectamine 2000 both diluted in Opti-MEM. After 3 h incubation, effector cells were washed once with Opti-MEM, detached with versene (0.2 g/L EDTA in PBS) and suspended in Opti-MEM. The Vero-BG20 (target) cells, previously seeded on Lab-Tek II 2-Well Chambered Coverglass (Nunc™) coated with poly-ornithine and grown overnight in DMEV, were washed with Opti-MEM and then overlayed with the effector cells. After 12 hours of co-cultivation, the cells were washed with PBS and fixed with 4% paraformaldehyde.   After an additional wash with PBS, the cells were stained using 2 µg/ml TRITC-conjugated cholera toxin (CTX-555; Molecular Probes, Eugene, OR) and 100 ng/ml DAPI in PBS for 30 min at 37°C in the dark. Cells were washed with PBS containing 2% heat-inactivated serum and imaged on a Zeiss UV LSM 510 confocal microscope using the 40X objective. Random fields (8 to 10) were imaged per chambered coverglass and images manually counted.

CHAPTER 5: CONCLUSIONS AND FUTURE DIRECTIONS

To date, the initial virus attachment step and early events for HSV glycoprotein-induced membrane fusion have been well-studied. The HSV glycoproteins requirements (gC or gB) and host cell requirements (heparan sulfate) for attachment have been identified. HSV receptor-binding protein gD interactions with HVEM, nectin-1, nectin-2 or 3-OST HS, serving as the trigger for initiating membrane fusion and virus entry, have also been well-characterized. The complex nature of the HSV fusion machinery requiring 4 different glycoproteins, gD, gB and gH-gL, has made it inherently more difficult to unravel the mechanism of HSV-induced membrane fusion.

In a systematic fashion, I performed extensive mutagenesis of HSV-1 gB and gL and detailed investigation of the phenotypes of the mutants, to study the role of each glycoprotein in the membrane fusion process. For gB, the mutagenesis study demonstrated that disruptions of highly ordered secondary structures prevented the proper folding and expression. Given that gB shares characteristics of class I (α-helical core) and class II (β-structure with fusion loop) fusion proteins, it is perhaps not surprising that gB is intolerant of most insertions. The fusion proteins in class I and class II are in metastable pre-fusion conformations, and transitions to very stable post-fusion conformation is believed to be the energetic driving force to promote membrane fusion. The results of my study suggest that most of the insertions (54 of 81) cause misfolding or aberrant processing by disrupting the metastable pre-fusion conformation of gB.

The gB study also revealed that the N-terminus and cytoplasmic tail are tolerant of insertions and permitted cell surface expression and function, indicating that these

regions were more flexible and/or less-ordered than the majority of the ectodomain.

One group of mutants having insertions within the central part of the gB ectodomain is

expressed on the cell surface while retaining partial fusion activity. These mutants

mapped to a disorderd region and adjacent linker region on the x-ray structure, in more

structurally flexible regions. Insertions into these regions probably alter the dynamics of

the pre-fusion to post-fusion conformational change since the corresponding region in

the structurally homologous VSV G fusion protein was predicted to permit the large

movements of structural domains necessary for the transition.

For expressed gB mutants that were non-functional, insertions were located on

the exposed surface of the gB trimer or within an internal cavity of the trimer (based on

the x-ray structure). The surface exposed insertions likely permitted reduced or near-

normal expression because they did not totally disrupt the tertiary structure of gB

structural domains. Two insertions, mapping to an internal cavity of the solved gB

structure, permit the prediction that the solved structure is the post-fusion form of gB

since the internal cavity seen in the structure is too small to accommodate 3 separate 5

a.a. insertions.

Future studies could focus on the regions of gB where insertions, mapped to the

trimer surface, still permitted cell surface expression but had a complete loss of

function. The regions may critical for protein-protein or protein-lipid interactions. For

protein-protein interactions, new assays would have to be developed that are able to

detect gB interactions with other proteins, presumably either with gD or gH-gL. A

recently reported assay using the split-GFP technology looks promising (Avitabile E,

2007). Additionally, evidence currently exists that gB interacts with another cell surface protein or glycolipid (Bender et al., 2005), however, the protein or glycolipid has yet to be identified. Future work could also be directed towards identifying this unknown gB receptor and studying its role in HSV membrane fusion. In this context, truncated versions of the gB mutants could be generated to assess whether they retain the ability to bind to the as-yet-uknown cell surface receptor for gB.

Of all of the HSV-1 entry glycoproteins, gL remains the least well-characterized. Most of the recent work into HSV-1 entry glycoproteins has focused on gD, gB and gH with few efforts directed towards gL. Several early studies of the gH-gL heterodimer suggested that the role of gL in cell fusion may be merely that of a chaperone for gH folding, processing and transport. Consequently, previous studies on gL relied on C-terminal truncations to identify the regions necessary for gH transport without more comprehensive mutational studies to identify other functional domains. Therefore, I performed the random linker-insertion mutagenesis of gL to define more narrowly the domain(s) responsible for gL dimerization with gH and to identify other potential functional domains.

The findings of the gL mutagenesis study identified several new functional domains in gL. The principal gH-binding domain mapped to a region encompassing residues 69 to 106, a region also conserved among gLs of various alphaherpesviruses, suggesting that this may be the gH-binding domain for the other gLs. Regions adjacent to the gH-binding domain (N-terminal and C-terminal) contribute to gH-gL dimerization or influence gH-gL conformation and are critical for cell fusion activity, indicating that gL

plays at least one additional role for HSV fusion aside from gH transport.   A recent study of gH mutants showed that gH deleted for an N-terminal region transported to the cell surface in the absence of gL but was not functional in the absence of gL, indicating that gL has a distinct role in cell fusion activity. The studies performed here are consistent with the gH findings and also provide direct evidence for the role of gL as a fusion mediator. Given that class I and class II fusion proteins are proteolytically processed before they become fusion-competent, gH-gL might also need to acquire a specific functional conformation in order to carry out its activity. Future work can focus on studying gH-gL and the role that gL plays in formation of the active or primed conformation using different anti-gH and anti-gL mAbs. Other areas for future studies include the identification of the gL cell surface receptor and studying the apparent discrepancies between gL activities in cell fusion versus virus entry to determine if there are different intracellular pathways involved in processing gL for the cell surface and incorporation into virions.

Our current understanding of the HSV fusion machinery have advanced the studies presented here and studies by other groups. An understanding of class I and class II viral fusion proteins forms the foundation for our understanding into the mechanisms of enveloped virus entry into host cells. The increased complexities inherent in the HSV fusion system relative to class I and class II fusion proteins, along with the finding that gB has characteristics of both class I and class II fusion proteins, suggests that the overall HSV fusion machinery may be the prototype for a novel paradigm into virus entry. Currently, infections with HSV lead to lifelong, mostly latent,

infections. However, studies aimed at unraveling the mechanism of HSV fusion can

provide targets for future development of anti-HSV therapeutic agents that can block

virus entry through exploitation of novel aspects of HSV entry yet to be uncovered.

REFERENCES

Abrahamyan, L.G., Mkrtchyan, S.R., Binley, J., Lu, M., Melikyan, g.B., and Cohen, F.S. (2005). The cytoplasmic tail slows the folding of human immunodeficiency virus type 1 Env from a late prebundle configuration into the six-helix bundle. J Virol *79*, 106-115.

Avitabile E, F.C., Campadelli-Fiume G. (2007). Complexes between herpes simplex virus glycoproteins gD, gB, gH detected in cells by complementation of split enhanced green fluorescence protein. J Virol *Aug 1; [Epub ahead of print]*.

Bender, F.C., Whitbeck, J.C., Lou, H., Cohen, G.H., and Eisenberg, R.J. (2005). Herpes Simplex Virus Glycoprotein B Binds to Cell Surfaces Independently of Heparan Sulfate and Blocks Virus Entry. J Virol *79*, 11588-11597.

Bressanelli, S., Stiasny, K., Allison, S.L., Stura, E.A., Duquerroy, S., Lescar, J., Heinz, F.X., and Rey, F.A. (2004). Structure of a flavivirus envelope glycoprotein in its low-pH-induced membrane fusion conformation. EMBO J *23*, 728-738.

Cai, W., Gu, B., and Person, S. (1988). Role of glycoprotein B of herpes simplex virus type 1 in viral entry and cell fusion. JVirol *62*, 2596-2604.

Cai, W., Person, S., Warner, S.C., Zhou, J., and DeLuca, N.A. (1987). Linker-insertion nonsense and restriction-site deletion mutations of the gB glycoprotein gene of herpes simplex virus type 1. JVirol *61*, 714-721.

Cairns, T.M., Friedman, L.S., Lou, H., Whitbeck, J.C., Shaner, M.S., Cohen, G.H., and Eisenberg, R.J. (2007). N-terminal mutants of HSV-2 gH are transported without gL but require gL for function. J Virol, JVI.00097-00007.

Cairns, T.M., Landsburg, D.J., Charles Whitbeck, J., Eisenberg, R.J., and Cohen, G.H. (2005). Contribution of cysteine residues to the structure and function of herpes simplex virus gH/gL. Virology *332*, 550-562.

Carfi, A., Willis, S.H., Whitbeck, J.C., Krummenacher, C., Cohen, G.H., Eisenberg, R.J., and Wiley, D.C. (2001). Herpes simplex virus glycoprotein D bound to the human receptor HveA. Mol Cell *8*, 169-179.

Claesson-Welsh, L., and Spear, P.G. (1986). Oligomerization of herpes simplex virus glycoprotein B. JVirol *60*, 803-806.

Cocchi, F., Menotti, L., Mirandola, P., Lopez, M., and Campadelli-Fiume, G. (1998). The ectodomain of a novel member of the immunoglobulin subfamily related to the poliovirus receptor has the attributes of a bona fide receptor for herpes simplex virus types 1 and 2 in human cells. J Virol *72*, 9992-10002.

Croft, M. (2005). The evolving crosstalk between co-stimulatory and co-inhibitory receptors: HVEM-BTLA. Trends in Immunology *26*, 292-294.

Davis-Poynter, N., Bell, S., Minson, T., and Browne, H. (1994). Analysis of the contributions of herpes simplex virus type 1 membrane proteins to the induction of cell-cell fusion. JVirol *68*, 7586-7590.

Dolan, A., Jamieson, F.E., Cunningham, C., Barnett, B.C., and McGeoch, D.J. (1998). The genome sequence of herpes simplex virus type 2. JVirol *72*, 2010-2021.

Dubin, G., and Jiang, H. (1995). Expression of herpes simplex virus type 1 glycoprotein L (gL) in transfected mammalian cells: Evidence that gL is not independently anchored to cell membranes. JVirol *69*, 4564-4568.

Fan, Z., Grantham, M.L., Smith, M.S., Anderson, E.S., Cardelli, J.A., and Muggeridge, M.I. (2002). Truncation of herpes simplex virus type 2 glycoprotein B increases its cell surface expression and activity in cell-cell fusion, but these properties are unrelated. J Virol *76*, 9271-9283.

Foa-Tomasi, L., Avitabile, E., Boscaro, A., Brandimarti, R., Gualandri, R., Manservigi, R., Dall'Olio, F., Serafini-Cessi, F., and Campadelli-Fiume, G. (1991). Herpes simplex virus (HSV) glycoprotein H is partially processed in a cell line that expresses the glycoprotein and fully processed in cells infected with deletion or ts mutants in the known HSV glycoproteins. Virology *180*, 474-482.

Foster, T.P., Melancon, J.M., and Kousoulas, K.G. (2001). An α-helical domain within the carboxyl terminus of herpes simplex virus type1 (HSV-1) glycoprotein B (gB) is associated with cell fusion and resistance to heparin inhibition of cell fusion. Virology *287*, 18-29.

Fusco, D., Forghieri, C., and Campadelli-Fiume, G. (2005). The pro-fusion domain of herpes simplex virus glycoprotein D (gD) interacts with the gD N terminus and is displaced by soluble forms of viral receptors. Proc Natl Acad Sci USA *102*, 9323-9328.

Geraghty, R.J., Jogger, C.R., and Spear, P.G. (2000). Cellular expression of alphaherpesvirus gD interferes with entry of homologous and heterologous alphaherpesviruses by blocking access to a shared gD receptor. Virology *268*, 147-158.

Geraghty, R.J., Krummenacher, C., Cohen, G.H., Eisenberg, R.J., and Spear, P.G. (1998). Entry of alphaherpesviruses mediated by poliovirus receptor-related protein 1 and poliovirus receptor. Science *280,* 1618-1620.

Gianni, T., Martelli, P.L., Casadio, R., and Campadelli-Fiume, G. (2005a). The Ectodomain of Herpes Simplex Virus Glycoprotein H Contains a Membrane {alpha}-Helix with Attributes of an Internal Fusion Peptide, Positionally Conserved in the Herpesviridae Family. J Virol *79,* 2931-2940.

Gianni, T., Menotti, L., and Campadelli-Fiume, G. (2005b). A Heptad Repeat in Herpes Simplex Virus 1 gH, Located Downstream of the {alpha}-Helix with Attributes of a Fusion Peptide, Is Critical for Virus Entry and Fusion. J Virol *79,* 7042-7049.

Gianni, T., Piccoli, A., Bertucci, C., and Campadelli-Fiume, G. (2006). Heptad Repeat 2 in Herpes Simplex Virus 1 gH Interacts with Heptad Repeat 1 and Is Critical for Virus Entry and Fusion. J Virol *80,* 2216-2224.

Haarr, L., Shukla, D., Rødahl, E., Dal Canto, M.C., and Spear, P.G. (2001). Transcription from the gene encoding the herpesvirus entry receptor nectin-1 (HveC) in nervous tissue of adult mouse. Virology *287,* 301-309.

Hannah, B.P., Heldwein, E.E., Bender, F.C., Cohen, G.H., and Eisenberg, R.J. (2007). Mutational Evidence of Internal Fusion Loops in HSV glycoprotein B. J Virol, JVI.02755-02706.

Heinz, F.X., Stiasny, K., and Allison, S.L. (2004). The entry machinery of flaviviruses. Archives of Virology - Supplementum, 133-137.

Heldwein, E.E., Lou, H., Bender, F.C., Cohen, G.H., Eisenberg, R.J., and Harrison, S.C. (2006). Crystal structure of glycoprotein B from herpes simplex virus 1. Science *313*, 217-220.

Herold, B.C., WuDunn, D., Soltys, N., and Spear, P.G. (1991). Glycoprotein C of herpes simplex virus type 1 plays a principal role in the adsorption of virus to cells and in infectivity. JVirol *65*, 1090-1098.

Honda, T., Sakisaka, T., Yamada, T., Kumazawa, N., Hoshino, T., Kajita, M., Kayahara, T., Ishizaki, H., Tanaka-Okamoto, M., Mizoguchi, A.*, et al.* (2006). Involvement of nectins in the formation of puncta adherentia junctions and the mossy fiber trajectory in the mouse hippocampus. Mol Cell Neurosci *31*, 315-325.

Hsu, H., Solovyev, I., Colombero, A., Elliott, R., Kelley, M., and Boyle, W.J. (1997). ATAR, a novel tumor necrosis factor receptor family member, signals through TRAF2 and TRAF5*. J Biol Chem *272*, 13471-13474.

Hutchinson, L., Browne, H., Wargent, V., Davis-Poynter, N., Primorac, S., Goldsmith, K., Minson, A.C., and Johnson, D.C. (1992). A novel herpes simplex virus glycoprotein, gL, forms a complex with glycoprotein H (gH) and affects normal folding and surface expression of gH. JVirol *66*, 2240-2250.

Inagaki, M., Irie, K., Ishizaki, H., Tanaka-Okamoto, M., Morimoto, K., Inoue, E., Ohtsuka, T., Miyoshi, J., and Takai, Y. (2005). Roles of cell-adhesion molecules nectin 1 and nectin 3 in ciliary body development. Development *132*, 1525-1537.

Jahn, R., Lang, T., and Sudhof, T.C. (2003). Membrane fusion. Cell *112*, 519-533.

Johnson, D.C., and Spear, P.G. (1983). O-linked oligosaccharides are acquired by herpes simplex virus glycoproteins in the Golgi apparatus. Cell *32*, 987-997.

Kielian, M., and Rey, F.A. (2006). Virus membrane-fusion proteins: more than one way to make a hairpin. Nature Reviews Microbiology *4*, 67-76.

Klyachkin, Y.M., Stoops, K.D., and Geraghty, R.J. (2006). Herpes simplex virus type 1 glycoprotein L mutants that fail to promote trafficking of glycoprotein H and fail to function in fusion can induce binding of glycoprotein L-dependent anti-glycoprotein H antibodies
10.1099/vir.0.81563-0. J Gen Virol *87*, 759-767.

Krummenacher, C., Supekar, V.M., Whitbeck, J.C., Lazear, E., Connolly, S.A., Eisenberg, R.J., Cohen, G.H., Wiley, D.C., and Carfi, A. (2005). Structure of unliganded HSV gD reveals a mechanism for receptor-mediated activation of virus entry. EMBO J *24*, 4144-4153.

Laquerre, S., Argnani, R., Anderson, D.B., Zucchini, S., Manservigi, R., and Glorioso, J.C. (1998). Heparan sulfate proteoglycan binding by herpes simplex virus type 1 glycoproteins B and C, which differ in their contributions to virus attachment, penetration, and cell-to-cell spread. J Virol *72*, 6119-6130.

Li, W., Minova-Foster, T.J., Norton, D.D., and Muggeridge, M.I. (2006). Identification of Functional Domains in Herpes Simplex Virus 2 Glycoprotein B. J Virol *80*, 3792-3800.

Linehan, M.M., Richman, S., Krummenacher, C., Eisenberg, R.J., Cohen, G.H., and Iwasaki, A. (2004). In Vivo Role of Nectin-1 in Entry of Herpes Simplex Virus Type 1 (HSV-1) and HSV-2 through the Vaginal Mucosa. J Virol *78*, 2530-2536.

Lopez, M., Cocchi, F., Menotti, L., Avitabile, E., Dubreuil, P., and Campadelli-Fiume, G. (2000). Nectin2α (PRR2α or HveB) and nectin2δ are low-efficiency mediators for entry of herpes simplex virus mutants carrying the Leu25Pro substitution in glycoprotein D. J Virol *74*, 1267-1274.

Manoj, S., Jogger, C.R., Myscofski, D., Yoon, M., and Spear, P.G. (2004). Mutations in herpes simplex virus glycoprotein D that prevent cell entry via nectins and alter cell tropism. PNAS *101*, 12414-12421.

Martinez, W.M., and Spear, P.G. (2001). Structural features of nectin-2 (HveB) required for herpes simplex virus entry. J Virol *75*, 11185-11195.

McGeoch, D.J., Dalrymple, M.A., Davison, A.J., Dolan, A., Frame, M.C., McNab, D., Perry, L.J., Scott, J.E., and Taylor, P. (1988). The complete DNA sequence of the long unique region in the genome of herpes simplex virus type 1. J Gen Virol *69*, 1531-1574.

Mettenleiter, T.C. (2004). Budding events in herpesvirus morphogenesis. Virus Res *106*, 167-180.

Mizoguchi, A., Nakanishi, H., Kimura, K., Matsubara, K., Osaki-Kuroda, K., Katata, T., Honda, T., Kiyohara, Y., Heo, K., Higashi, M.*, et al.* (2002). Nectin: an adhesion molecule involved in formation of synapses. J Cell Biol *156*, 555-565.

Modis, Y., Ogata, S., Clements, D., and Harrison, S.C. (2004). Structure of the dengue virus envelope protein after membrane fusion. Nature *427*, 313-319.

Montgomery, R.I., Warner, M.S., Lum, B.J., and Spear, P.G. (1996). Herpes simplex virus-1 entry into cells mediated by a novel member of the TNF/NGF receptor family. Cell *87*, 427-436.

Murphy, K.M., Nelson, C.A., and Sedy, J.R. (2006). Balancing co-stimulation and inhibition with BTLA and HVEM. Nat Rev Immunol *6*, 671-681.

Norton, D.D., Dwyer, D.S., and Muggeridge, M.I. (1998). Use of a neural network secondary structure prediction to define targets for mutagenesis of herpes simplex virus glycoprotein B. Virus Res *55*, 37-48.

Novotny, M.J., Parish, M.L., and Spear, P.G. (1996). Variability of herpes simplex virus 1 gL and anti-gL antibodies that inhibit cell fusion but not viral infectivity. Virology *221*, 1-13.

Ogita, H., and Takai, Y. (2006). Nectins and nectin-like molecules: Roles in cell adhesion, polarization, movement, and proliferation. IUBMB Life *58*, 334-343.

Okuma, K., Nakamura, M., Nakano, S., Niho, Y., and Matsuura, Y. (1999). Host range of human T-cell leukemia virus type 1 analyzed by a cell fusion-dependent reporter gene activation assay. Virology *254*, 235-244.

Papaioannou, V.E., and Fox, J.G. (1993). Efficacy of tribromoethanol anesthesia in mice. Lab Animal Sciences *43*, 189-192.

Para, M.F., Parish, M.L., Noble, A.G., and Spear, P.G. (1985). Potent neutralizing activity associated with anti-glycoprotein D specificity among monoclonal antibodies selected for binding to herpes simplex virions. JVirol *55*, 483-488.

Parr, M.B., Kepple, L., McDermott, M.R., Drew, M.D., Bozzola, J.J., and Parr, E.L. (1994). A mouse model for studies of mucosal immunity to vaginal infection by herpes simplex virus type 2. Lab Invest *70*, 369-380.

Parr, M.B., and Parr, E.L. (2003). Intravaginal administration of herpes simplex virus type 2 to mice leads to infection of several neural and extraneural sites. J Neurovirol *9*, 594-602.

Peng, T., Ponce de Leon, M., Novotny, M.J., Jiang, H., Lambris, J.D., Dubin, G., Spear, P.G., Cohen, G.H., and Eisenberg, R.J. (1998). Structural and antigenic analysis of a truncated form of herpes simplex virus glycoprotein gH-gL complex. JVirol *72*, 6092-6103.

Pertel, P., Fridberg, A., Parish, M.L., and Spear, P.G. (2001). Cell fusion induced by herpes simplex virus glycoproteins gB, gD, and gH-gL requires a gD receptor but not necessarily heparan sulfate. Virology *279*, 313-324.

Rey, F.A. (2006). Molecular gymnastics at the herpesvirus surface. EMBO Reports *7*, 1000-1005.

Richart, S.M., Simpson, S.A., Krummenacher, C., Whitbeck, J.C., Pizer, L.I., Cohen, G.H., Eisenberg, R.J., and Wilcox, C.L. (2003). Entry of herpes simplex virus type 1 into primary sensory neurons in vitro Is mediated by nectin-1/HveC. J Virol *77*, 3307-3311.

Roche, S., Bressanelli, S., Rey, F.A., and Gaudin, Y. (2006). Crystal structure of the low-pH form of the vesicular stomatitis virus glycoprotein G. Science *313*, 187-191.

Roche, S., Rey, F.A., Gaudin, Y., and Bressanelli, S. (2007). Structure of the Prefusion Form of the Vesicular Stomatitis Virus Glycoprotein G 10.1126/science.1135710. Science *315*, 843-848.

Roop, C., Hutchinson, L., and Johnson, D.C. (1993). A mutant herpes simplex virus type 1 unable to express glycoprotein L cannot enter cells, and its particles lack glycoprotein H. JVirol *67*, 2285-2297.

Ruel, N., Zago, A., and Spear, P.G. (2006). Alanine substitution of conserved residues in the cytoplasmic tail of herpes simplex virus gB can enhance or abolish cell fusion activity and viral entry. Virology *346*, 229-237.

Sakisaka, T., Taniguchi, T., Nakanishi, H., Takahashi, K., Miyahara, M., Ikeda, W., Yokoyama, S., Peng, Y.F., Yamanishi, K., and Takai, Y. (2001). Requirement of interaction of nectin-1 alpha / HveC with afadin for efficient cell-cell spread of herpes simplex virus type 1. JVirol *75*, 4734-4743.

Schibli, D.J., and Weissenhorn, W. (2004). Class I and class II viral fusion protein structures reveal similar principles in membrane fusion. Mol Membr Biol *21*, 361-371.

Shukla, D., Liu, J., Blaiklock, P., Shworak, N.W., Bai, X., Esko, J.D., Cohen, G.H., Eisenberg, R.J., Rosenberg, R.D., and Spear, P.G. (1999). A novel role for 3-*O*-sulfated heparan sulfate in herpes simplex virus 1 entry. Cell *99*, 13-22.

Shukla, D., and Spear, P.G. (2001). Herpesviruses and heparan sulfate: an intimate relationship in aid of viral entry. J Clin Invest *108*, 503-510.

Simmons, A., and Nash, A. (1984). Zosteriform spread of herpes simplex virus as a model of recrudescence and its use to investigate the role of immune cells in prevention of recurrent disease. J Virol *52*, 816-821.

Simpson, S.A., Manchak, M.D., Hager, E.J., Krummenacher, C., Whitbeck, J.C., Levin, M.J., Freed, C.R., Wilcox, C.L., Cohen, G.H., Eisenberg, R.J.*, et al.* (2005). Nectin-

1/HveC mediates herpes simplex virus type-1 entry into primary human sensory neurons and fibroblasts. J Neurovirol *11*, 208-218.

Skehel, J.J., and Wiley, D.C. (2000). Receptor binding and membrane fusion in virus entry: the influenza hemagglutinin. Annu Rev Biochem *69*, 531-569.

Smith, J.S., and Robinson, N.J. (2002). Age-specific prevalence of infection with herpes simplex virus types 2 and 1: a global review. J Infect Dis *186 Suppl 1*, S3-28.

Spear, P.G. (2004). Herpes simplex virus: receptors and ligands for cell entry. Cell Microbiol *6*, 401-410.

Spear, P.G., Eisenberg, R.J., and Cohen, G.H. (2000). Three classes of cell surface receptors for alphaherpesvirus entry. Virology *275*, 1-8.

Spear, P.G., Manoj, S., Yoon, M., Jogger, C.R., Zago, A., and Myscofski, D. (2006). Different receptors binding to distinct interfaces on herpes simplex virus gD can trigger events leading to cell fusion and viral entry. Virology *344*, 17-24.

Stiasny, K., Allison, S.L., Mandl, C.W., and Heinz, F.X. (2001). Role of metastability and acidic pH in membrane fusion by tick-borne encephalitis virus. J Virol *75*, 7392-7398.

Subramanian, R.P., and Geraghty, R.J. (2007). Herpes simplex virus type 1 mediates fusion through a hemifusion intermediate by sequential activity of glycoproteins D, H, L, and B

10.1073/pnas.0608374104. PNAS *104*, 2903-2908.

Suzuki, K., Hu, D., Bustos, T., Zlotogora, J., Richieri-Costa, A., Helms, J.A., and Spritz, R.A. (2000). Mutations of *PVRL*1, encoding a cell-cell adhesion molecule/herpesvirus receptor, in cleft lip/palate-ectodermal dysplasia. Nature Genetics *25*, 427-430.

Takai, Y., Shimizu, K., and Ohtsuka, T. (2003). The roles of cadherins and nectins in interneuronal synapse formation. Curr Opin Neurobiol *13*, 520-526.

Tong, S., Li, M., Vincent, A., Compans, R.W., Fritsch, E., Beier, R., Klenk, C., Ohuchi, M., and Klenk, H.-D. (2002). Regulation of Fusion Activity by the Cytoplasmic Domain of a Paramyxovirus F Protein. Virology *301*, 322-333.

Wahlberg, J.M., Boere, W.A., and Garoff, H. (1989). The heterodimeric association between the membrane proteins of Semliki Forest virus changes its sensitivity to low pH during virus maturation. J Virol *63*, 4991-4997.

Wahlberg, J.M., Bron, R., Wilschut, J., and Garoff, H. (1992). Membrane fusion of Semliki Forest virus involves homotrimers of the fusion protein. J Virol *66*, 7309-7318.

Wahlberg, J.M., and Garoff, H. (1992). Membrane fusion process of Semliki Forest virus. I: Low pH-induced rearrangement in spike protein quaternary structure precedes virus penetration into cells. J Cell Biol *116*, 339-348.

Wang, Y., Subudhi, S.K., Anders, R.A., Lo, J., Sun, Y., Blink, S., Wang, J., Liu, X., Mink, K., Degrandi, D.*, et al.* (2005). The role of herpesvirus entry mediator as a negative regulator of T cell-mediated responses. J Clin Invest *115*, 711-717.

Warner, M.S., Geraghty, R.J., Martinez, W.M., Montgomery, R.I., Whitbeck, J.C., Xu, R., Eisenberg, R.J., Cohen, G.H., and Spear, P.G. (1998). A cell surface protein with herpesvirus entry activity (HveB) confers susceptibility to infection by mutants of herpes simplex virus type 1, herpes simplex virus type 2 and pseudorabies virus. Virology *246*, 179-189.

Westmoreland, D., and Rapp, F. (1976). Host range temperature-sensitive mutants of herpes simplex virus type 2. J Virol *18*, 92-102.

Yamada, H., Jiang, Y.M., Oshima, S., Wada, K., Goshima, F., Daikoku, T., and Nishiyama, Y. (1998). Characterization of the UL4 gene product of herpes simplex virus type 2. Arch Virol *143*, 1199-1207.

Yamada, H., Jiang, Y.M., Zhu, H.Y., Inagaki-Ohara, K., and Nishiyama, Y. (1999). Nucleolar localization of the UL3 protein of herpes simplex virus type 2. J Gen Virol *80*, 2157-2164.

Yoon, M., Zago, A., Shukla, D., and Spear, P.G. (2003). Mutations in the N termini of herpes simplex virus type 1 and 2 gDs alter functional interactions with the entry/fusion receptors HVEM, nectin-2 and 3-O-sulfated heparan sulfate but not with nectin-1. J Virol *77*, 9221-9231.

APPENDIX 1: Alternative Entry Receptors for Herpes Simplex Virus and Their Roles in Disease. *

Joann M. Taylor,[1,6] Erick Lin,[1,6] Nanette Susmarski,[1] Miri Yoon,[1] Anna Zago,[1] Carl F. Ware,[2] Klaus Pfeffer,[3] Jun Miyoshi,[4] Yoshimi Takai,[5] and Patricia G. Spear[1],*

[1] Department of Microbiology-Immunology, Feinberg School of Medicine, Northwestern University, Chicago, IL 60611, USA

[2] Division of Molecular Immunology, La Jolla Institute for Allergy and Immunology, La Jolla, CA 92037, USA

[3] Institute of Medical Microbiology, Heinrich-Heine-Universität, Düsseldorf, Düsseldorf, Germany

[4] Department of Molecular Biology, Osaka Medical Center for Cancer and Cardiovascular Diseases, Osaka 537-8511, Japan

[5] Department of Molecular Biology and Biochemistry, Osaka University Graduate School of Medicine/Faculty of Medicine, Suita 565-0871, Japan

[6] These authors contributed comparably to this work.

SUMMARY

Either herpesvirus entry mediator (HVEM, TNFRSF14) or nectin-1 (PVRL1) is sufficient for herpes simplex virus (HSV) infection of cultured cells. The contribution of individual receptors to infection in vivo and to disease is less clear. To assess this, *Tnfrsf14* -/- and/or *Pvrl1* -/- mice were challenged intravaginally with HSV-2. Infection of the vaginal epithelium occurred in the absence of either HVEM or nectin-1, but was virtually undetectable when both receptors were absent, indicating that either HVEM or nectin-1 was necessary. Absence of nectin-1 (but not HVEM) reduced efficiency of infection of the vaginal epithelium and viral spread to the nervous system, attenuating neurological disease and preventing external lesion development. While nectin-1 proved not to be essential for infection of the nervous system, it is required for the full manifestations of disease. This study illustrates the value of mutant mice for understanding receptor contributions to disease caused by a human virus.

INTRODUCTION

Viral entry can be mediated by multiple alternative receptors that are expressed in many cell types and tissues, making it difficult to assess the roles of each receptor in disease. Mice with gene disruptions have been of limited use for studying this problem with human viruses because mice are often resistant to these viruses. However, mice are susceptible to HSV infection and disease, and mouse entry receptors are encoded by genes orthologous to the genes for the human entry receptors (Spear et al., 2000). Here we describe the use of mutant mice to explore the roles in HSV disease of two cell surface proteins that can mediate the entry of HSV-2 into cells.

Manifestations of disease caused by HSV infection of children or adults range from none to mucocutaneous lesions to meningitis and encephalitis. The virus replicates in cells of the mucosal or cutaneous epithelium, causing blisters or lesions often confined to the epithelium. HSV also enters neurons and is transported to sensory and autonomic ganglia to establish latent infections. Reactivation of HSV in neurons results in transport of virus to the body surface and in recurrent mucocutaneous lesions, permitting seeding of additional neurons. Occasionally, the virus can spread to the CNS to cause life-threatening disease.

HSV is an enveloped DNA virus, the prototype of the neurotropic alphaherpesviruses. Of the dozen or more envelope glycoproteins in the HSV virion, five have a role in viral entry. Glycoproteins gB and/or gC can mediate the binding of virus to cell surface heparan sulfate or related glycosaminoglycans (Shukla and Spear,

2001). This binding is not sufficient for entry, which requires the interaction of envelope glycoprotein gD with any one of several cell surface molecules. These include HVEM (Montgomery et al., 1996), a member of the tumor necrosis factor receptor family; nectin-1 (Cocchi et al., 1998; Geraghty et al., 1998) and nectin-2 (Warner et al., 1998), cell adhesion molecules belonging to the immunoglobulin superfamily; and specific sites in heparan sulfate (3-O-S-HS) generated by particular 3-O-sulfotransferases (Shukla et al., 1999). Interaction of any of these receptors with gD is thought to trigger conformational changes in gD that result in activation of the fusogenic activity of trimeric gB and/or the heterodimer gH-gL (Carfi et al., 2001; Fusco et al., 2005; Heldwein et al., 2006; Krummenacher et al., 2005; Rey, 2006; Spear et al., 2006), resulting in entry by envelope-membrane fusion.

HVEM and nectin-1 are efficient entry and cell fusion receptors for both serotypes of HSV whereas nectin-2 and 3-O-S-HS appear to be less efficient (Lopez et al., 2000; Shukla et al., 1999). Also, nectin-2 preferentially mediates entry of HSV-2 and certain mutants of HSV-1 (Lopez et al., 2000; Martinez and Spear, 2001; Warner et al., 1998) whereas 3-O-S-HS preferentially mediates entry of HSV-1 (Shukla and Spear, 2001). Mouse forms of these receptors resemble the human forms in their entry and fusion activities with both HSV-1 and HSV-2 (Yoon et al., 2003) except that it has been difficult to document entry activity for mouse nectin-2 (Martinez and Spear, 2001; Shukla et al., 1999). Thus, the best candidates for efficient HSV-2 entry receptors in the mouse are HVEM and nectin-1.

Mice in which the gene encoding HVEM (*Tnfrsf14*) was disrupted displayed no evident developmental abnormalities but did exhibit enhanced lethal responses to the mitogen, concanavalin A, and increased susceptibility to autoimmune encephalomyelitis (Wang et al., 2005). HVEM has two natural ligands. One is a member of the tumor necrosis factor family and its binding to HVEM on T cells, B cells, neutrophils, macrophages, and possibly dendritic cells can enhance activation and/or differentiation of these cells (Croft, 2005; Murphy et al., 2006). The other is B and T lymphocyte attenuator (BTLA) and the binding of HVEM to BTLA on T cells can repress T cell proliferation and activation (Murphy et al., 2006). Although physiological roles of HVEM have been associated mainly with cells of the lymphoid system, HVEM is widely expressed in a number of other cell types, including epithelial, stromal and endothelial cells (Spear, 2004). Its expression in the nervous system has not been studied, in part because initial screens for transcripts revealed little or no expression in the brain (Hsu et al., 1997; Montgomery et al., 1996).

Mice in which the gene encoding nectin-1 (*Pvrl1*) was disrupted were fertile and developed normally, for the most part, but exhibited delays in attaining adult size and abnormalities such as microphthalmia (Inagaki et al., 2005). There are four nectins and five nectin-like molecules, all of which participate in cell junctions of various kinds, including adherens junctions (Ogita and Takai, 2006). It seems likely that there is redundancy in functionality of the members of this family because disruptions in expression of specific nectins have deleterious effects on only a limited subset of the junctions in which each molecule can be detected. Gene disruptions have shown that

nectin-1 and nectin-3 are both required for a specific junction between pigmented and non-pigmented cell layers in the ciliary epithelia and for normal development of the ciliary body of the eye (Inagaki et al., 2005). Moreover, both nectin-1 and nectin-3 contribute to the formation of puncta adherentia junctions in the mouse hippocampus and influence mossy fiber trajectories (Honda et al., 2006; Mizoguchi et al., 2002). Nectin-1 is widely expressed in a variety of cell types, including epithelial, stromal, endothelial and lymphoid cells, and also in many neurons of the mouse peripheral and central nervous systems (PNS and CNS) (Haarr et al., 2001). Moreover, antibodies specific for nectin-1 have been shown to inhibit entry of virus into cultured human and rodent neurons (Richart et al., 2003; Simpson et al., 2005).

Mice can be infected by HSV-1 or HSV-2 and provide useful models for several aspects of HSV disease in humans. Mice are susceptible to infection via the intravaginal route during the diestrous stage of the estrous cycle, when the vaginal epithelium is only a few cell layers thick and not cornified, but not during other stages when there is extensive cornification. Diestrous can be induced artificially by an injection of progesterone, so that mice do not have to be staged prior to inoculation. This model of HSV infection and disease (Parr et al., 1994) is widely used. Virus replicates in the vaginal epithelium, causing lesions, and then spreads via autonomic and sensory nerves to peripheral ganglia, including dorsal root ganglia (DRG), paracervical ganglia and other autonomic ganglia in the bladder and rectal walls (Parr and Parr, 2003). Secondary lesions occur externally, on the perineal skin and surrounding areas. Clinical symptoms resemble, in some respects, what humans may experience during severe

primary genital infection with HSV-2. For example, both mice and humans may experience urinary retention, constipation and paraparesis, as well as internal and external lesions. In mice, virus is more likely to spread also to the CNS causing death, particularly at the doses of virus used in experimental studies.

To investigate the roles of HVEM and nectin-1 in HSV-2 infection and acute disease, we inoculated $Tnfrsf14^{-/-}$ and $Pvrl1^{-/-}$ mice, double mutants and wild-type controls with virus via the intravaginal route and monitored both clinical signs of disease and the spread of virus from the portal of entry to the PNS and CNS. The results showed that either nectin-1 (most efficiently) or HVEM could mediate the infection of cells in the vaginal epithelium and that neither receptor was required for spread of virus to the PNS and CNS or for lethal consequences of disease. Nectin-1 was required, however, for the appearance of secondary external lesions, which may result from horozontal cell-to-cell transmission of infection between mucosal and skin epithelia or zosteriform transmission from neurons to skin cells.

RESULTS

Effects of mouse gene disruptions on clinical signs of disease after HSV-2 inoculation

Two virus strains were used for inoculation: virulent HSV-2(333) and a recombinant form of HSV-2(333) in which a *lacZ* expression cassette was inserted into an intergenic region, so that presence of virus in cells and tissues could be assessed by staining with the β-galactosidase substrate, X-gal. Unless otherwise indicated, the inoculating dose for each virus, designated here HSV-2 and HSV-2/Gal, was 6 x 10^5 plaque-forming units (PFU) per mouse delivered intravaginally.

The mice were examined daily after inoculation and clinical symptoms recorded, including the appearance of external signs of infection such as hair loss, inflammation and lesions around the vaginal and rectal openings, around the tail base and down the legs. Symptoms also included signs of lethargy, abdominal distention, dehydration and (rarely) hind-limb paralysis, which were indicative of impending death. Mice showing these latter signs in severe form were euthanized. The results are summarized in the Kaplan Meier survival plots shown in Figure A1.1. The top panels show days without external signs of disease and the bottom panels show days remaining alive.

Absence of HVEM in the *Tnfrsf14*$^{-/-}$ mice had little or no effect on the course of acute disease, assessed either by the appearance of external lesions or by mortality, after wild-type HSV-2 inoculation. Absence of nectin-1 in the *Pvrl*$^{-/-}$ mice had significant

effects, however. In contrast to the wild-type control mice or $Pvrl^{+/-}$ mice, which were

statistically indistinguishable in terms of disease symptoms, none of the $Pvrl^{-/-}$ mice

inoculated with HSV-2 showed any signs of external lesions (P <0.001), despite more

than half eventually dying from the infection. The survival curve (mortality) for the $Pvrl^{-/-}$

mice also differed significantly from that for the wild-type mice (P <0.01), indicating

some attenuation of disease in the absence of nectin-1.

HSV-2/Gal is less virulent than HSV-2 (Figure A1.1 and statistical analysis given

in the Experimental Procedures). The mutation that abrogates nectin-1 expression ($Pvrl^{-/-}$) had the expected effect of further attenuating disease caused by HSV-2/Gal. For the

mutation abrogating HVEM expression ($Tnfrsf14^{-/-}$), the somewhat unexpected result

was attenuation of disease with HSV-2/Gal but not with HSV-2. There was a statistically

significant difference between wild-type and Tnfrsf14-/- mice in the timing of external

lesion appearance and number of mice eventually showing such lesions (P <0.001).

Figure A1.1. Appearance of external lesions and mortality after intravaginal inoculation of wild-type (+/+), *Tnfrsf14*$^{-/-}$, *Pvrl*$^{+/-}$ and *Pvrl*$^{-/-}$ mice with HSV-2/Gal or HSV-2. All mice were injected with Depo-Provera 6 days prior to inoculation of virus (6 x 10^5 PFU per mouse). The mice were examined daily for external lesions. They were also examined for severe morbidity requiring euthanasia. The day on which external lesions were first noted and the day of death or sacrifice were recorded for each animal (n = 16-20 mice for each experimental group). In A, C57BL/6 (+/+) mice are compared with *Tnfrsf14*$^{-/-}$ mice, in which the gene expressing HVEM was disrupted; in B, littermate controls (both +/+ and *Pvrl*$^{+/-}$) are compared with *Pvrl*$^{-/-}$ mice, in which the gene expressing nectin-1 was disrupted. Kaplan-Meier survival analysis was performed using the Gehan-Breslow test. Statistically significant differences between mice of different genotypes are noted on the relevant panels. In B, the P values shown apply to comparisons of *Pvrl*$^{-/-}$ mice with either +/+ or *Pvrl*$^{+/-}$ mice except for the survival curves for mice inoculated with HSV-2. In the latter case, a significant difference was noted only for the comparison between *Pvrl*$^{-/-}$ and +/+ mice (curves linked by line). The closed circles on each survival curve indicate censored data due to death of mice during the experiment or sacrifice of mice at the conclusion of the experiment. Mice were monitored for at least 21 days but no changes in status were noted between 18 and 21 days.

Figure A1.1. Appearance of external lesions and mortality after intravaginal inoculation of wild-type (+/+), *Tnfrsf14*$^{-/-}$, *Pvrl*$^{+/-}$ and *Pvrl*$^{-/-}$ mice with HSV-2/Gal or HSV-2.
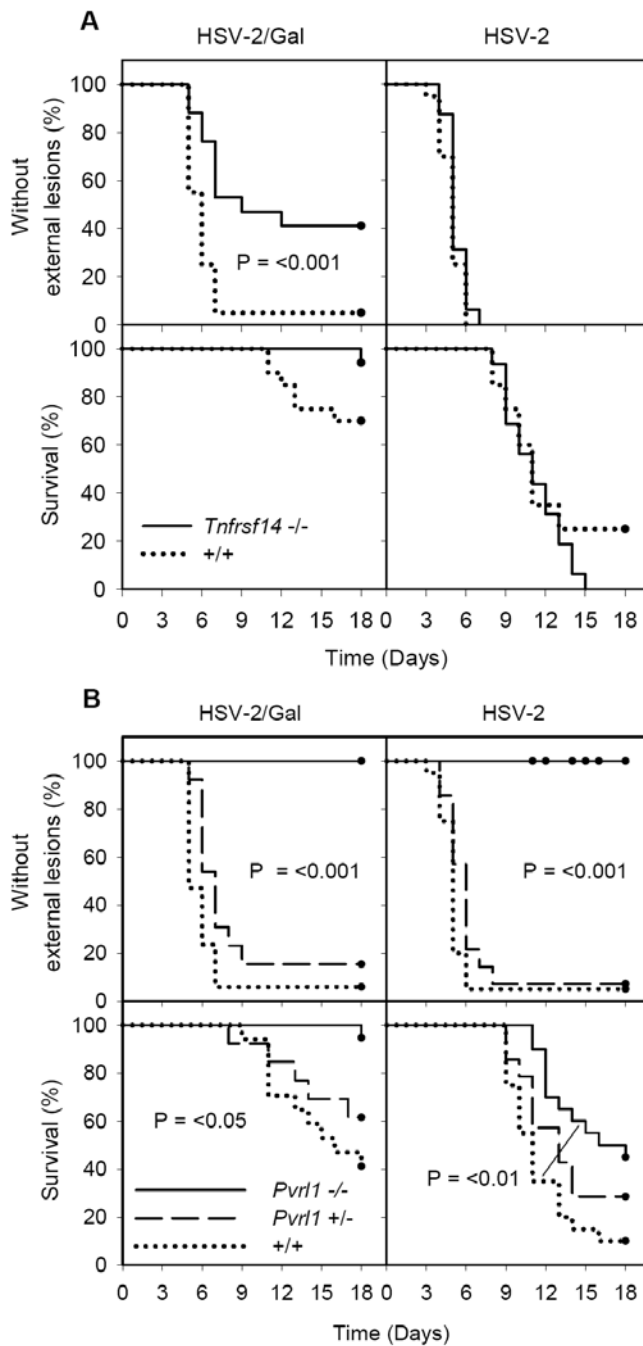
Mice expressing nectin-1 but not HVEM ($Tnfsfr14^{-/-}Pvrl1^{+/-}$), HVEM but not

nectin-1 ($Pvrl1^{-/-}$) and neither ($Tnfrsf14^{-/-}Pvrl^{-/-}$) were also challenged with HSV-2 at a

10-fold higher dose than that used in Figure A1.1 (6 x 10^6 PFU per mouse instead of 6 x

10^5). The higher dose of virus did not significantly alter the timing or manifestations of

clinical symptoms for the HVEM-expressing and nectin-1-expressing mice (except that

one $Pvrl1^{-/-}$ mouse exhibited some inflammation at the vaginal opening without the hair

loss and lesions typically observed around the vaginal and rectal openings, tail base

and down the legs). None of the double-mutant mice (n=9) showed any signs of disease

for more than 21 days (Figure A1.2).

The results of these challenge experiments demonstrate that neither nectin-1 nor

HVEM is essential for HSV-2 infection of mice via the intravaginal route, as evidenced

by symptoms or mortality in 50-100% of the mice inoculated. Expression in mice of at

least one of these entry receptors appears to be necessary for disease, based on

absence of any clinical symptoms in the double-mutant mice after virus challenge.

Absence of nectin-1 alone delayed death and reduced its incidence, but did not prevent

it, whereas absence of HVEM alone had little effect on disease caused by HSV-2.

Strikingly, absence of nectin-1 completely abrogated external lesions in mice inoculated

with either HSV-2/Gal or HSV-2. For mice that expressed nectin-1, mortality was never

observed in the absence of external lesions. HVEM-deficient mice inoculated with HSV-

2/Gal, but not HSV-2, were partially protected from the development of external lesions.

Figure A1.2. Appearance of external lesions and mortality after intravaginal inoculation with HSV-2 of nectin-1-expressing *Tnfrsf14$^{-/-}$Pvrl1$^{+/-}$* mice, HVEM-expressing *Pvrl1$^{-/-}$* mice and double-mutant mice. The experiment was done as in Figure A1.1 except that the mice were inoculated with 10 times the dose of HSV-2 (6 x 10^6 PFU/mouse). The single *Pvrl1$^{-/-}$* mouse that exhibited an external sign of disease showed some inflammation at the vaginal opening but no hair loss or external lesions around the vagina, rectum or tail or down the legs, as was typical for mice that express nectin-1. Kaplan-Meier survival analysis was performed using the Gehan-Breslow test. Statistically significant differences were noted for all pair-wise comparisons (P <0.02) except *for Pvrl1$^{-/-}$* mice vs *Tnfrsf14$^{-/-}$Pvrl1$^{-/-}$* mice in the % remaining free of external lesions (n = 4--*Tnfrsf14$^{-/-}$Pvrl$^{+/-}$*; n=13--*Pvrl1$^{-/-}$*; N=9--*Tnfrsf14$^{-/-}$Pvrl1$^{-/-}$*).

Figure A1.2. Appearance of external lesions and mortality after intravaginal inoculation with HSV-2 of nectin-1-expressing *Tnfrsf14*$^{-/-}$*Pvrl1*$^{+/-}$ mice, HVEM-expressing *Pvrl1*$^{-/-}$ mice and double-mutant mice.
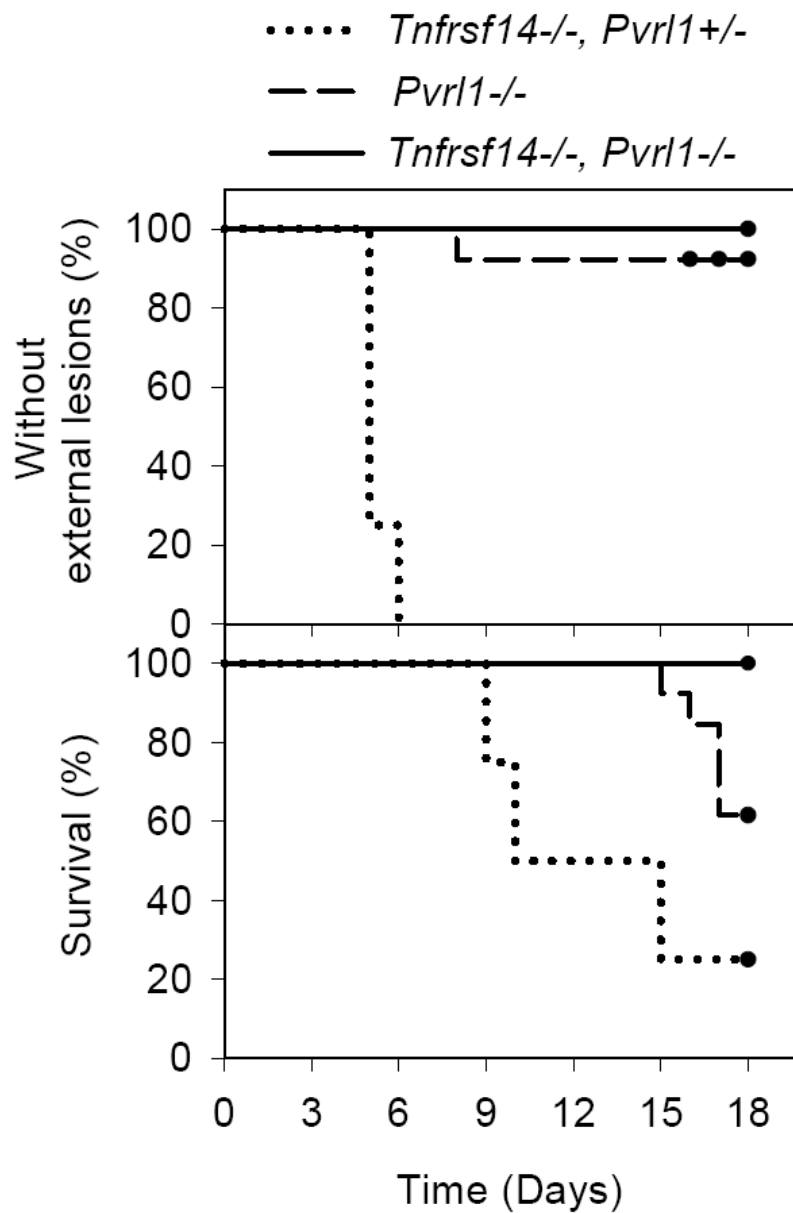
Tracking of virus infection and spread by monitoring expression of β-galactosidase from HSV-2/Gal

The question arises from Figures A1.1 and A1.2 as to whether mice failing to show any symptoms of disease had actually become infected by the inoculated virus. As one measure of the efficiency of infection of the vaginal epithelium and spread to the nervous system, wild-type and mutant mice were inoculated with HSV-2/Gal and sacrificed at various times after inoculation for the dissection of vaginas, DRG, spinal cords and perivaginal skin, followed by staining of these tissues with the β-galactosidase substrate, X-gal. The extent of lesion development on the vaginal luminal surface and in nervous system tissue was scored as described in Experimental Procedures.

Figure A1.3 shows examples of stained vaginas photographed at 24 hrs after inoculation with two different doses of HSV-2/Gal: 6×10^5 and 6×10^6 PFU/mouse. At the lower dose of virus (Figure A1.3A and A1.3B), the viral lesions were numerous and extensive for wild-type and $Tnfrsf14^{-/-}$ mice but were reduced in number and size for the $Pvrl^{-/-}$ mice. However, mice of all three genotypes invariably had detectable lesions on the vaginal epithelium (no lesion scores of 0). For the double-mutant mice ($Tnfrsf14^{-/-}Pvrl^{-/-}$), only rare blue spots (<5 per vagina) were observed, if at all, at either dose of inoculated virus (Figure A1.3A and A1.3C) whereas there were significantly increased numbers of lesions for the $Pvrl^{-/-}$ mice at the higher dose. These results show that nectin-1 expression is associated with efficient infection of the vaginal epithelium

but, in its absence, HVEM expression permits infection, albeit less efficiently. When

neither nectin-1 nor HVEM is expressed, infection of the vaginal epithelium was

extremely limited or not detectable even at high doses of inoculated virus. These results

also indicate that the failure of some wild-type, $Tnfrsf14^{-/-}$ or $Pvrl^{-/-}$ mice to show

symptoms of disease in Figure A1.1 was probably not due to failure of the inoculated

virus to initiate infection of the vaginal epithelium. On the other hand, failure of double-

mutant $Tnfrsf14^{-/-}Pvrl^{-/-}$ mice to show any clinical signs of disease might be accounted

for by failure of the virus to establish infection via the intravaginal route of inoculation.

Figure A1.3. Development of lesions on the vaginal epithelium at 24 hrs after inoculation of C57BL/6 (+/+), *Tnfrsf14*$^{-/-}$, *PvrI*$^{-/-}$ or double mutant *Tnfrsf14*$^{-/-}$*PvrI*$^{-/-}$ mice with HSV-2/Gal. The mice were injected with Depo-Provera as in Figure A1.2 and then inoculated with HSV-2/Gal at 6 x 10^5 PFU per mouse (A and B) or 6 x 10^6 PFU per mouse (C). At 24 hrs after virus inoculation, the mice were sacrificed. The vaginas were removed and split open longitudinally and then fixed and stained with X-gal to detect β-galactosidase expressed from an insert in the viral genome. The extent of staining and therefore of virus infection was scored on a scale from 0 (no blue lesions noted) to 5 (greater than 80% of vaginal epithelium infected) as described in the text. A - Representative pictures of vaginas from mice of the indicated genotypes inoculated with 6 x 10^5 PFU per mouse. B - Scores assigned for vaginas from mice of the genotypes noted, after inoculation with HSV-2/Gal at 6 x 10^5 PFU/mouse. The values shown are means plus standard deviation (n = 8-11). Only the mean for the *PvrI*$^{-/-}$ mice was significantly different from that for the wild-type (+/+) mice (*t* test). C – *PvrI*$^{-/-}$ and double-mutant mice (*Tnfrsf14*$^{-/-}$*PvrI*$^{-/-}$) were inoculated with HSV-2/Gal at 6 x 10^6 PFU per mouse and treated as in A. A total of 8 double-mutant mice have been inoculated with either 6 x 10^5 or 6 x 10^6 PFU and none have exhibited staining scores other than 0 or 1.

Figure A1.3. Development of lesions on the vaginal epithelium at 24 hrs after inoculation of C57BL/6 (+/+), *Tnfrsf14*$^{-/-}$, *Pvrl*$^{-/-}$ or double mutant *Tnfrsf14*$^{-/-}$ *Pvrl*$^{-/-}$ mice with HSV-2/Gal.
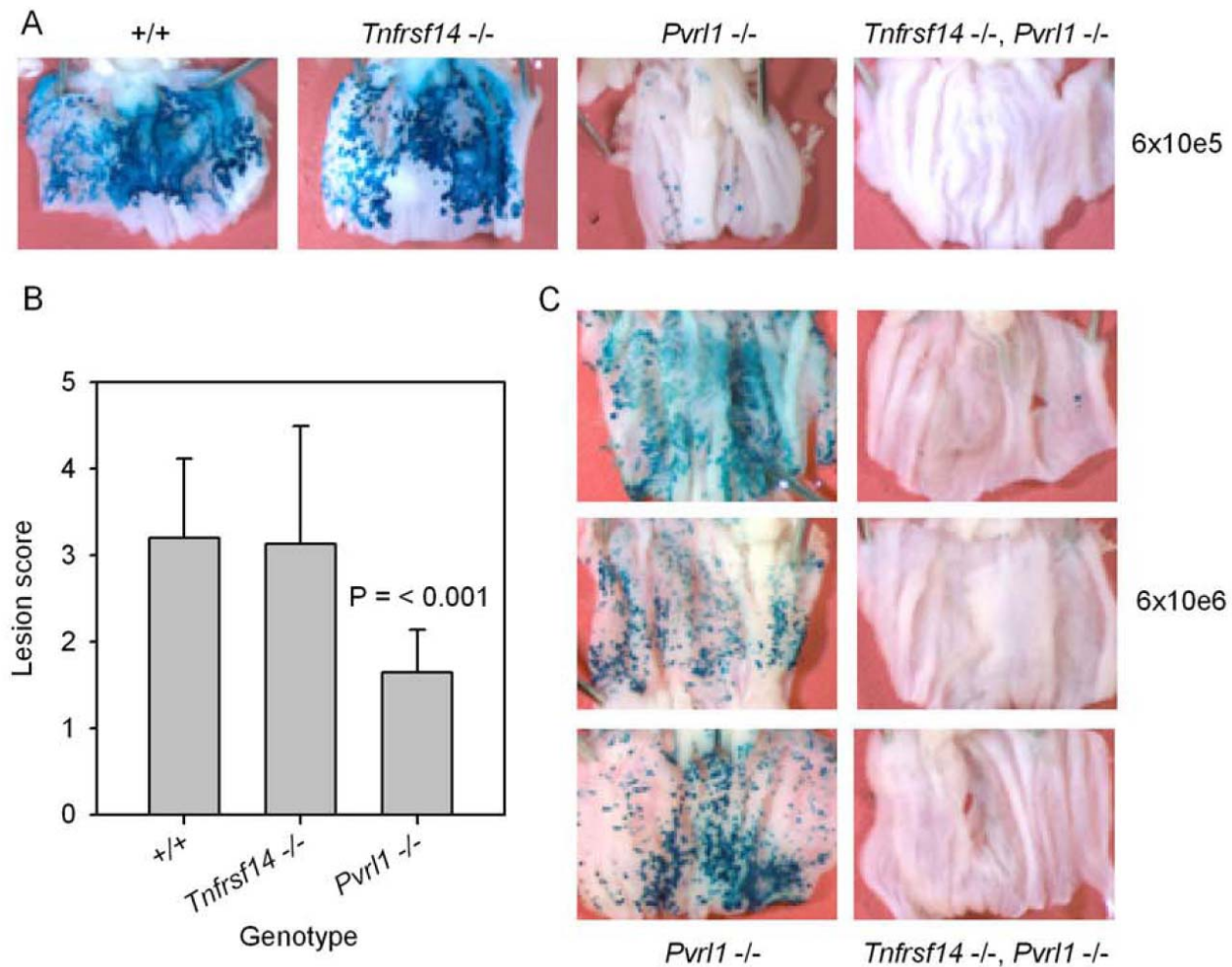
Figure A1.4A shows an example of an X-gal-stained spinal column from a wild-type mouse inoculated with HSV-2/Gal. A portion of the image was enlarged to show the staining of DRG. At several timepoints following HSV-2/Gal inoculation, infection of the nervous system (DRG, attached nerves and spinal cord) was scored. There was a significant difference between wild-type littermate controls and $Pvrl^{-/-}$ mice in the lesion scores for days 3, 5, 7 and 9 after virus inoculation (Figure A1.4B; P < or = 0.003). Moreover, spread of virus infection to the PNS and CNS was detectable by X-gal staining for only a subset of mice in each $Pvrl^{-/-}$ experimental group (numbers in parentheses in Figure A1.4B) whereas this spread of infection was readily detectable in all wild-type mice. $Tnfrsf14^{-/-}$ mice (n = 3 for each time point) had scores indistinguishable from those of the wild-type mice on days 3, 5 and 9 following inoculation (data not shown).

Figure A1.4. Development of lesions in DRG and the spinal cord after inoculation of *Pvrl*$^{-/-}$ mice and littermate wild-type (+/+) mice with HSV-2/Gal. Depo-Provera-treated mice were inoculated with HSV-2/Gal at 6 x 10^5 PFU per mouse and sacrificed at days 3, 5, 7 and 9 after inoculation. The spinal columns were then dissected out (A), the vertebra cut and the entire tissue stained with X-gal. After staining, the spinal cords with attached ganglia and nerves were teased away from other tissue so that blue foci of infection in these tissues could be scored on a scale from 0 (no blue stain observed) to 5 (most ganglia in sacral and lumbar region positive, attached nerves positive and spinal cord positive in several regions) as described in the text. A - Representative picture of a stained spinal column from a +/+ mouse sacrificed at day 9. The magnified inset shows two heavily stained and two lightly stained ganglia in the lumbar region. B - Scores assigned for infected mice of the genotypes indicated at the days indicated. The values shown are means plus standard deviation (n = 5-7 for the wild-type (+/+) littermate control groups and n = 7 for all *Pvrl*$^{-/-}$ groups). Shown in parentheses beside each point in the lower curve is the number of *Pvrl*$^{-/-}$ mice in each group for which lesions could be detected in nervous tissue (score greater than 0). On each day the values for the *Pvrl*$^{-/-}$ mice were significantly different from those for the +/+ mice (P < or = 0.003, Mann Whitney rank-sum test). Scale bar divisions in A are 0.1 cm.

Figure A1.4. Development of lesions in DRG and the spinal cord after inoculation of *Pvrl*[^-/-] mice and littermate wild-type (+/+) mice with HSV-2/Gal.
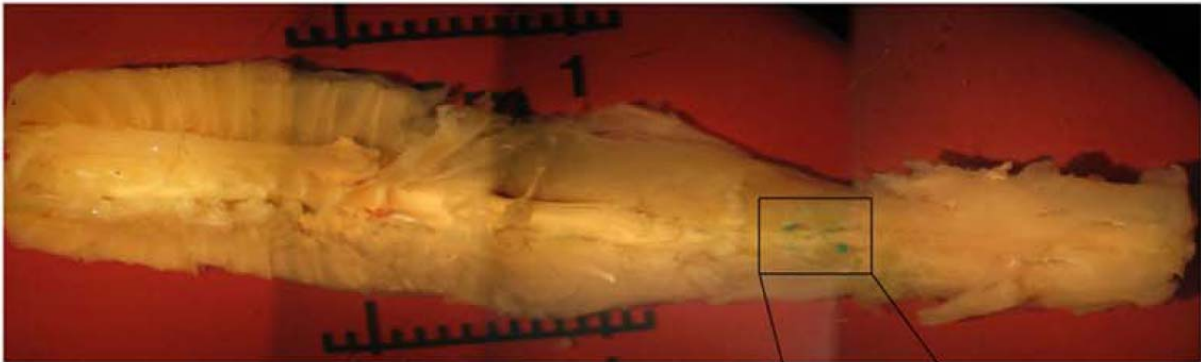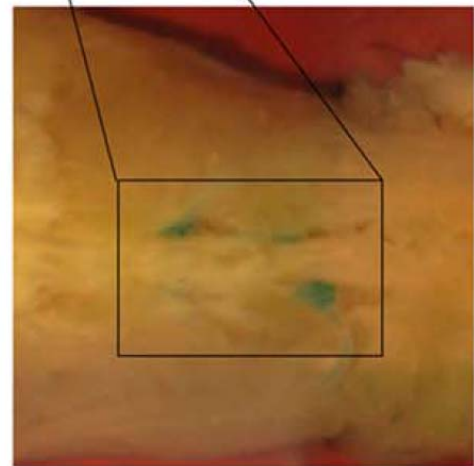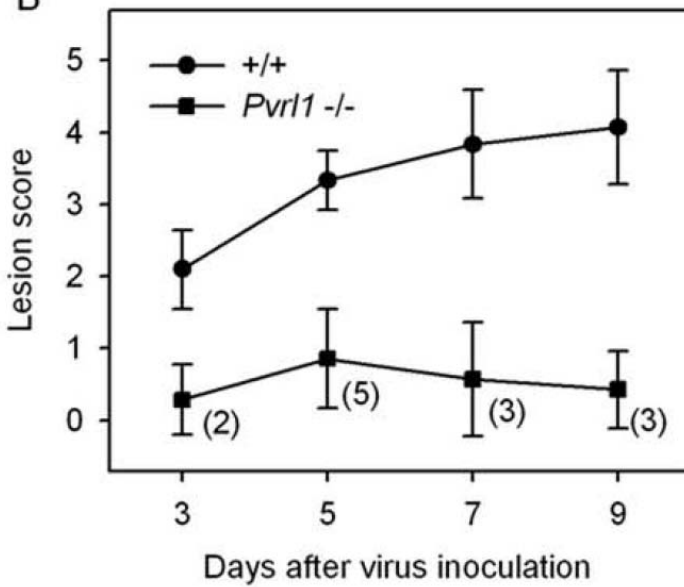
An example of the typical external lesions caused by HSV-2 is shown in Figure A1.5A. Samples of perivaginal skin were dissected from wild-type mice infected with HSV-2/Gal to assess the spread of virus infection and distribution of lesions at the gross (Figure A1.5B) and histological (Figure A1.5C-F) levels. We failed to observe indications that infection spread directly and contiguously from the vaginal epithelium itself to external perivaginal regions but, instead, noted isolated X-gal stained lesions, some quite distant from the vaginal opening (Figure A1.5B). Serial sections of external skin also provided evidence for isolated microscopic viral lesions, often extending into hair follicles (Figure A1.5C-F), as previously observed (Parr and Parr, 2003).

Figure A1.5. Development of external lesions on skin at sites non-contiguous with the vaginal opening and involvement of hair follicles. A - A mixed-strain wild-type mouse was treated with Depo-Provera, inoculated with 6 x 10^5 PFU of HSV-2 and photographed on day 15 to show external hair loss, inflammation and lesions around the vagina and rectum. B-F – A C57BL/6 mouse was treated with Depo-Provera, inoculated with 6 x 10^5 PFU of HSV-2/Gal and sacrificed 7 days later. Skin was dissected from the area ventral to the vaginal orifice (vo), fixed and stained with X-gal. Areas of skin around the vo suffered hair loss and had been inflamed. B - Isolated lesions (blue foci) at sites distant from the vo. The urethral orifice (uo) is indicated by the arrow. C - F Serial sections, after H&E staining, of paraffin-embedded tissue from the same mouse. The dark blue insoluble product generated by action of β-galactosidase on X-gal identifies infected cells on the epithelial surface of the skin and extending along the hair follicle toward a sebaceous gland (sg). Scale bar in C represents 20 μm for panels C-F.

Figure A1.5. Development of external lesions on skin at sites non-contiguous with the vaginal opening and involvement of hair follicles.
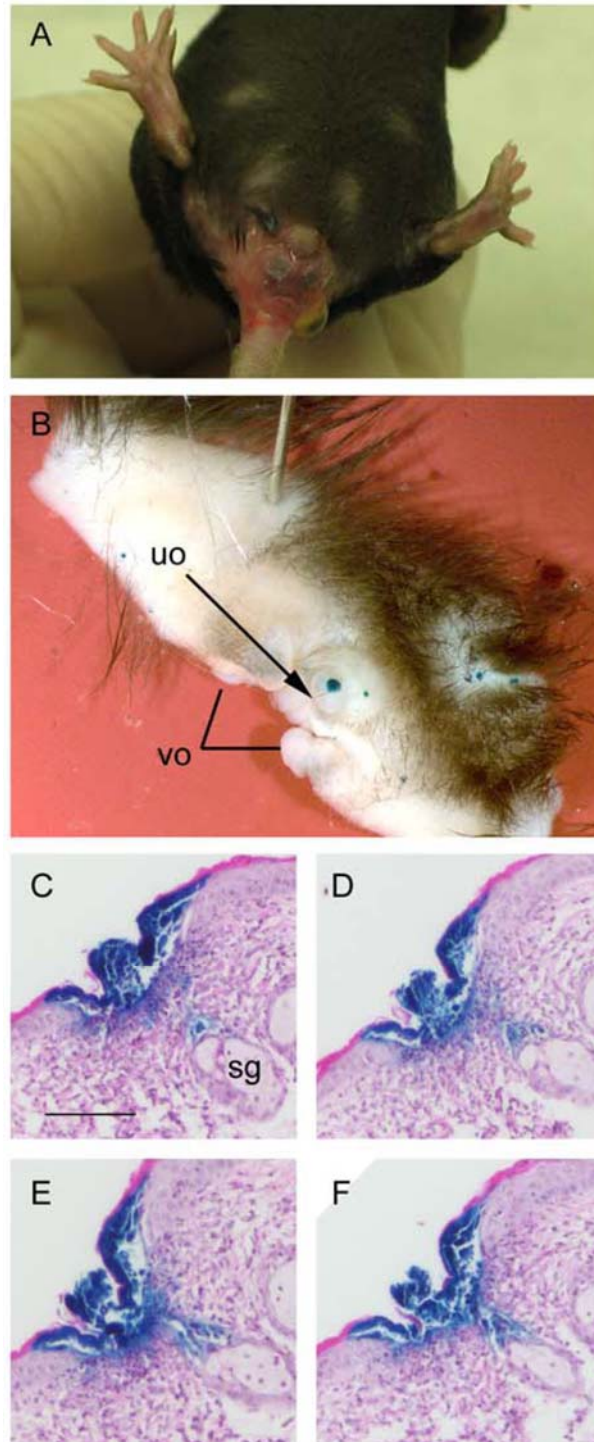
**Tracking of virus infection and spread by titration of infectious HSV-2 in various organs**

Groups of wild-type, *Tnfrsf14*$^{-/-}$ and *Pvrl*$^{-/-}$ mice were inoculated with HSV-2 at 6 x 10^5 PFU per mouse and sacrificed at intervals following inoculation for removal of the tissues indicated in Figure A1.6. Each organ was weighed, homogenized and serial dilutions prepared for quantification of PFU. On day 1, virus was detected only in the vaginal samples, with significantly lower mean titers for the *Pvrl*$^{-/-}$ mice than for wild-type controls or *Tnfrsf14*$^{-/-}$ mice. Viral loads declined in the vaginal samples thereafter. On day 3, maximal mean titers of virus were detected in the DRG of wild-type and *Tnfrsf14*$^{-/-}$ mice whereas maximal titers were not detected until day 5 for the *Pvrl*$^{-/-}$ mice. By day 5, maximal titers of virus were detected in the spinal cords of mice of all three genotypes but at significantly lower levels for the *Pvrl*$^{-/-}$ mice. Finally, virus could be detected in the hindbrains of most wild-type and *Tnfrsf14*$^{-/-}$ mice by day 7 and 9 but not in any of the *Pvrl*$^{-/-}$ mice. For the DRG and spinal cords and at timepoints where infectious virus could be detected in these organs for all wild-type and *Tnfrsf14*$^{-/-}$ mice, there were one or more *Pvrl*$^{-/-}$ mouse in which virus could not be detected. This study was also done with *Pvrl1*$^{+/-}$ mice. Mean titers of virus detected in various organs of the *Pvrl*$^{+/-}$ mice at each timepoint were usually not statistically different from those obtained for the wild-type mice but were nevertheless usually less than those obtained for the

wild-type mice, suggesting gene dosage effects (data not shown), as did Figure A1.1.

Thus, absence of HVEM expression was without effect on the replication of HSV-2 in

the organs tested whereas absence of nectin-1 resulted in reduced titers in all organs.

To determine whether replication of HSV-2 could be detected in double-mutant

mice, groups of these mice and control nectin-1-expressing $Tnfrsf14^{-/-}Pvrl1^{+/-}$ mice

were inoculated with the higher dose of HSV-2 (6×10^6 PFU). Five days after virus

inoculation, the mice were sacrificed for quantification of progeny virus in homogenates

of vaginas, DRG and spinal cords. The 5-day time point was selected because, by this

time, input virus that failed to initiate infection would have been inactivated and, at this

time, mice of all other genotypes had significant levels of virus in the organs tested

(Figure A1.6). Table A.1 shows that, while significant levels of virus were present in all

three organs of the nectin-1-expressing mice, no virus could be detected in the double-

mutant mice (except for a few PFU near the lower limit of detection in one vaginal

sample). Thus, double-mutant mice may support very low levels of HSV-2 replication in

the vagina (as was noted also with HSV-2/Gal) but infection did not spread to the

nervous system and did not lead to disease (Figure A1.2).

Figure A1.6. Viral loads in various tissues of wild-type (+/+), *Tnfrsf14$^{-/-}$* and *Pvrl$^{-/-}$*

mice at the days indicated after inoculation with HSV-2. The mice were treated with

Depo-Provera, inoculated with HSV-2 at 6 x 10^5 PFU per mouse, sacrificed on the day

indicated after inoculation and various tissues removed for preparation of extracts and

virus titrations by plaque assay. Each symbol represents PFU per g of tissue from an

individual mouse. Geometric means for each experimental group are indicated by

horizontal black lines (n = 5-6 for all three genotypes). Symbols in the hatched regions

of each panel represent the lower limit of virus detection; values for these samples were

recorded as the actual low number of PFU detected or assigned as 0.5 PFU per g of

tissue when no PFU were detected. Brackets marked by an asterisk indicate that means

of the viral loads detected in the +/+ mice were statistically different from those in the

mutant mice (P <0.05, *t* test).

Figure A1.6. Viral loads in various tissues of wild-type (+/+), Tnfrsf14-/- and Pvrl-/- mice at the days indicated after inoculation with HSV-2.
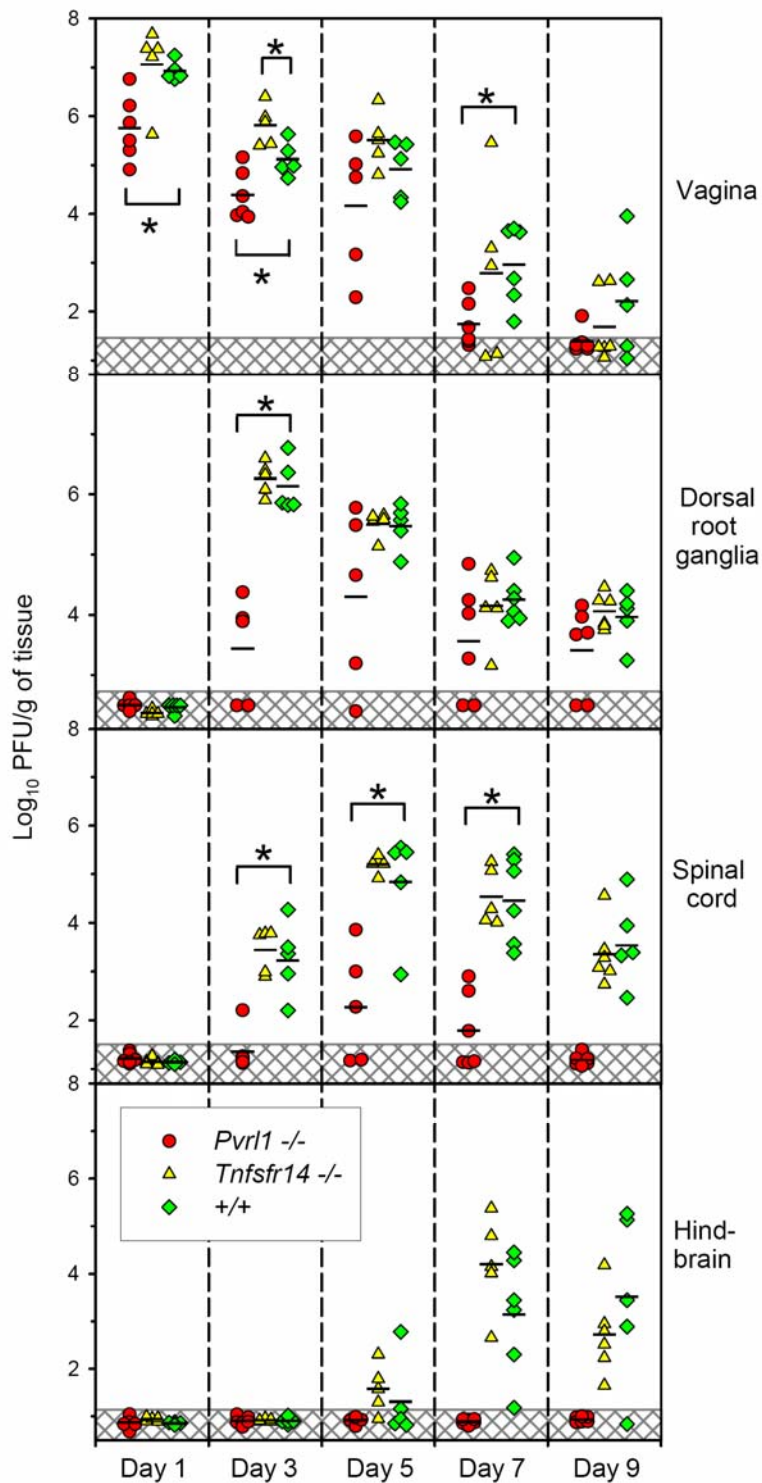
Table A1.1. No infectious virus detected in dorsal root ganglia or cords of double-mutant mice at 5 days after HSV-2 inoculation

Mouse genotype	Mouse number	Log_{10} PFU/g of tissue (lower limit of detection)*		
		Vagina	Dorsal root ganglia	Spinal cord
$Tnfrsf14^{-/-} Pvrl1^{+/-}$	2438	3.57	4.86	3.40
	2439	3.22	4.62	3.67
	2441	3.60	4.59	2.62
$Tnfrsf14^{-/-} Pvrl1^{-/-}$	2440	1.89 (1.42)	none (2.49)	none (1.17)
	2546	none (1.40)	none (2.40)	none (1.17)
	2547	none (1.23)	none (2.40)	none (1.11)

* Mice of the genotypes indicated were treated with DepoProvera and 6 days later were inoculated with 6 x 10^6 PFU of HSV-2. Five days after virus inoculation the mice were sacrificed and the organs indicated taken to prepare homogenates for titrations of infectious virus. Virus was undetectable in nervous system tissues of the double-mutant mice and in vaginal tissues of 2/3 of these mice. For all three organs the mean virus titers detected in mice expressing nectin-1 were statistically different from the actual titer or limits of detection in the double-mutant mice (P < 0.005, *t* test).

DISCUSSION

A major conclusion emerging from this study is that HSV-2 infection of the vaginal epithelium of mice requires expression of either nectin-1 or HVEM, based on findings that double-mutant $Tnfrsf14^{-/-} Pvrl^{-/-}$ mice were largely resistant to infection via the vaginal route of inoculation whereas both $Tnfrsf14^{-/-}$ and $Pvrl^{-/-}$ mice were susceptible. Absence of nectin-1 expression reduced the efficiency of infection of the vaginal epithelium whereas absence of HVEM expression appeared to be without effect. Possibly, nectin-1 is normally more accessible or efficient as an entry receptor than HVEM, at least in the stratified mouse vaginal epithelium. It was previously reported that nectin-1 mediated infection of the vaginal epithelium in mice, based on finding that a soluble form of nectin-1 could reduce or abolish infection (Linehan et al., 2004). However, this soluble nectin-1 would also be expected to abolish infection mediated by HVEM. Although nectin-1 and HVEM bind to different interfaces on gD (Spear et al., 2006), binding of either soluble receptor to HSV can inhibit infection of cells bearing either receptor (Geraghty et al., 1998).

A second major conclusion is that neither HVEM nor nectin-1 is essential for the spread of HSV-2 infection from the vaginal epithelium to the nervous system in mice, based on the detection of infectious HSV-2 and/or β-galactosidase expressed by HSV-2/Gal in DRG and spinal cords of wild-type, $Tnfrsf14^{-/-}$ and $Pvrl^{-/-}$ mice. Virus produced by non-neuronal cells in the vaginal epithelium could directly enter the endings of neurons that extend to the epithelium, leading to viral replication in DRG, whereas

replication of virus in the spinal cord would probably require neuron-to-neuron transmission.

Since replication of HSV-2 in the vaginal epithelium of double-mutant mice was extremely limited, and therefore HSV-2 access to neurons would be limited, it was not possible to assess whether HSV-2 could infect neurons via the vaginal route in these mice. Therefore, a possible role for another as-yet-unrecognized entry receptor that is expressed in the nervous system, but not on the vaginal epithelium, cannot be ruled out. Use of mutant mice in which receptor expression is knocked out only in neurons could address this issue.

Clearly, absence of nectin-1, but not HVEM, delayed and reduced the efficiency of HSV-2 spread to DRG and the spinal cord and also delayed and reduced the incidence of mortality. These comparisons were made at an input dose of virus (6×10^5 PFU) sufficient to infect virtually 100% of wild-type, $Tnfrsf14^{-/-}$ and $Pvrl^{-/-}$ mice, but a dose that resulted in reduced involvement of the vaginal epithelium in $Pvrl^{-/-}$ mice. A 10-fold higher dose of HSV-2/Gal caused greater involvement of the vaginal epithelium in $Pvrl^{-/-}$ mice (Figure A1.3) but inoculation of HSV-2 at this higher dose did not enhance disease (Figure A1.2) or increase viral loads in the nervous system (Figure A1.6 and Table A1.1).

A third conclusion is that the formation of external lesions, as depicted in Figure A1.5A, depended on expression of nectin-1, as these typical lesions were not observed in $Pvrl^{-/-}$ mice. In wild-type or $Tnfrsf14^{-/-}$ mice, external hair loss, inflammation and

lesions were invariably noted prior to any signs of lethal disease although not all mice exhibiting external lesions experienced lethal disease. In the $Pvrl^{-/-}$ mice, on the other hand, the typical external signs of disease were never observed, at either dose of virus, even in mice who succumbed to disease and despite levels of virus in various tissues of individual mice that were comparable to those observed in wild-type mice (Figure A1.6). Since the secondary external lesions in nectin-1-expressing mice are associated with the spread of virus to perineal skin and surrounding areas, it seems likely that this spread is somehow blocked in nectin-1-deficient mice.

It has been established in a flank (zosteriform) model of HSV disease in mice that secondary lesions occur, beginning about 4 days after inoculation of virus at the primary site, and that these secondary lesions result from viral spread via neural pathways and are prevented by neurotomy (Simmons and Nash, 1984). In the vaginal model of disease, the secondary lesions occurring on the external skin after primary lesion development in the vaginal epithelium could also depend in part on neural routes of spread. The isolated microscopic and gross lesions containing HSV-2/Gal at sites non-contiguous to the perivaginal opening (Figure A1.5) and occurring 5-9 days after virus inoculation are consistent with a neural route of spread but do not rule out horizontal cell-cell spread in epithelial cell layers contiguous from the vaginal mucosa to external skin (Parr and Parr, 2003). Expression of nectin-1 has been shown to promote cell-to-cell spread of HSV in non-neuronal cultured cells (Sakisaka et al., 2001). Consistent with this finding, our results show that (i) lesions on the vaginal epithelium of nectin-1-deficient mice are smaller than normal at 24 h and (ii) absence of nectin-1

expression prevents external lesions that are likely to depend on long-range cell-to-cell spread of infection whether this spread is via neural routes or between contiguous mucosal and skin epithelia or both.

Whereas absence of nectin-1 expression prevented the typical external lesions caused by either HSV-2/Gal or HSV-2, absence of HVEM reduced the incidence of these lesions, but only for HSV-2/Gal, at least at the virus dose used in Figure A1.1. Adoptive transfer of immune cells has been shown to block zosteriform spread in the mouse flank model (Simmons and Nash, 1984). Possibly, enhanced immune responses to an attenuated virus expressing a bacterial antigen, i.e. HSV-2/Gal, could explain the reduced incidence of external lesions in the $Tnfrsf14^{-/-}$ mice, compared with wild-type control mice, inasmuch as absence of HVEM expression has been associated with enhanced immune responses (Wang et al., 2005).

To what extent are these results relevant to human genital disease? The three known human entry receptors for HSV-2 are nectin-1, nectin-2 and HVEM. Human mutations affecting expression of functional HSV entry receptors have been described only for nectin-1. Chain-terminating mutations in the $Pvrl1$ gene have been linked to an autosomal recessive cleft lip/cleft palate-ectodermal dysplasia syndrome in a few families from the Margarita Islands, Brazil and Israel (Suzuki et al., 2000). Unfortunately, access to persons with disruptions in the nectin-1 gene has been limited and it has not been determined whether these people are resistant to HSV infection and disease. The results presented here suggest that they would not be totally resistant, especially since nectin-2 as well as HVEM could be functional *in situ* as entry receptors. Nectin-1 is

expressed in the human vaginal epithelium throughout the menstrual cycle (Linehan et al., 2004) and is also expressed in human neurons (Simpson et al., 2005; Takai et al., 2003). The patterns of expression of HVEM and nectin-2 have not been well-defined in the tissues of relevance to this study. It seems safe to predict that, as in the mouse, multiple entry receptors could permit infection via the vaginal epithelium and spread to the nervous system. If, as in the mouse, nectin-1 is required for secondary mucocutaneous lesions, it may also be required for recurrent lesions, one of the most troublesome aspects of HSV disease. Possibly, new approaches to blocking the interaction of HSV with nectin-1 could be effective for preventing recurrent disease.

EXPERIMENTAL PROCEDURES

Cells and Virus strain

Vero cells cultured in Dulbecco's modification of Eagle's (DME) medium plus 10% fetal bovine serum (FBS) were used for the propagation of virus. Plaque titrations were performed on Vero cells by standard methods. HSV-2 strain 333 was isolated from a genital lesion and underwent limited passage in human cells (Westmoreland and Rapp, 1976). The virus was plaque-purified and passaged no more than 3 times in Vero cells.

Construction of HSV-2/Gal

HSV-2/Gal has a *lacZ* expression cassette inserted between the convergently transcribed genes, UL3 and UL4. This virus was generated by co-transfecting Vero cells with genomic DNA from wild-type HSV-2(333) and plasmid pUL3UL4-CMVlacZ, followed by isolation and plaque-purification of a recombinant virus that expresses β-galactosidase. The insert in the plasmid used for recombination contains the following elements: nucleotides 11002-11911 from the HSV-2(333) genome, including the entire UL3 ORF and all but 20 nucleotides of the downstream UL3-UL4 intergenic region; the immediate-early promoter from human cytomegalovirus (CMV); the *lacZ* gene; nucleotides 11663-11823 from the HSV-1(KOS) genome, including the entire UL3-UL4 intergenic region from HSV-1; nucleotides 11932-12531 from the HSV-2(333) genome, including all but the first few codons of the UL4 ORF. The intergenic regions, one from HSV-2 and the other from HSV-1 (different in sequence from the HSV-2 version), were placed upstream and downstream of the inserted CMV-*lacZ* cassette to ensure that polyadenylation signals would function properly for the UL3, *lacZ* and UL4 transcripts

and to avoid homologous recombination between these repeats. The nucleotide sequences given are from the published sequences for HSV-1(17) (McGeoch et al., 1988) and HSV-2(HG52) (Dolan et al., 1998). HSV-2/Gal and HSV-2 were indistinguishable in levels of UL3 and UL4 expression, as determined by western blot analysis using antibodies previously described (Yamada et al., 1998; Yamada et al., 1999). Also, HSV-2/Gal was indistinguishable from parental HSV-2 in its ability to replicate in Vero cells, with respect to the kinetics of progeny production and yields of progeny virus during a single replicative cycle. In wild-type mice, the spread of HSV-2/Gal to various target organs was similar to that of HSV-2 but HSV-2/Gal was less virulent than HSV-2 (Figure A1.1). The survival plots for days without lesions and days remaining alive differed significantly (Gehan-Breslow test: P = 0.004 and <0.001, respectively, for the C57BL/6 mice used as controls for the back-crossed $Tnfrsf14^{-/-}$ mice and P = 0.018 and 0.003, respectively, for the wild-type littermate mice used as controls for the $Pvrl^{-/-}$ mice).

Mouse lines

Animal care and use were in accordance with institutional and NIH guidelines and all studies were approved by the Animal Care and Use Committee of Northwestern University. Mice were maintained in specific-pathogen-free conditions until infection and then were transferred to a containment facility.

Generation of the $Tnfrsf14^{-/-}$ mice and back-cross to the C57BL/6 background have been described (Wang et al., 2005). The mice used here were obtained from

homozygous mutant breeding pairs and their genotypes checked by PCR analysis of

genomic DNA using forward primer HVEM1 (5'ACTCACAGACACCTACTATGG) and

reverse primers HVEM2 (5'GGAGATGAGTGCTGGAGGAGA) and HVEM KO

(5'CTGAAGAGGAGTTTACGTCCAG). Female C57BL/6 mice, purchased from Jackson

Labs, served as wild-type controls for the $Tnfrsf14^{-/-}$ mice.

The generation and properties of $Pvrl^{-/-}$ mice were also previously described

(Inagaki et al., 2005). Frozen heterozygous embryos (genetic background 50% 129/SV,

25% C57BL/6 and 25% DBA) at the two-cell stage were implanted into pseudopregnant

C57BL/6 mothers. The mice obtained were genotyped by PCR analysis of genomic

DNA as previously described (Inagaki et al., 2005). The colony was maintained by

heterozygous mating. Wild-type and $Pvrl^{+/-}$ mice were used as littermate controls for the

$Pvrl^{-/-}$ mice. $Tnfrsf14^{-/-}$ and $Pvrl^{-/-}$ mice and their progeny were crossed to obtain

double-mutant mice.

Infection of mice and post-infection procedures

Female mice ranging in age from 11-18 weeks were injected with 0.1 ml of Depo-

Provera diluted to 25 mg/ml with phosphate-buffered saline (PBS) (Parr et al., 1994).

Histology performed on the vaginas of mice sacrificed 6 days after injection showed

that, in both wild type and mutant mice, Depo-Provera altered the vaginal epithelium,

causing remodeling to non-cornified thinned epithelia as described (Parr et al., 1994). At

6 days after DepoProvera injection, experimental mice were anesthetized with

tribromoethanol (Papaioannou and Fox, 1993) and then inoculated intravaginally, using

a positive-displacement micropipettor, with 20 µl of HSV-2 or HSV-2/Gal diluted in PBS

containing 1% inactivated calf serum and 0.1% glucose. The virus solution remaining

after inoculation was re-titered to ensure proper dosage (6×10^5 or 6×10^6 PFU/mouse).

The lower dose was chosen because, in pilot experiments, 6×10^5 PFU/mouse was

shown to cause 100% incidence of vaginal infection in +/+ mice, as assessed by

staining the vaginal epithelium 24 hrs after HSV-2/Gal inoculation, and >90% incidence

of external lesions in +/+ mice after inoculation with either HSV-2 or HSV-2/Gal. The 10-

fold higher dose was the highest practical dose that could be administered in attempts

to enhance or detect disease in some of the mutant mice.

Some mice were maintained after inoculation with HSV-2 or HSV-2/Gal solely to

observe and document clinical signs of disease for 21 days or until death or sacrifice.

These mice were examined daily for external lesions (hair loss, inflammation, and skin

lesions around the vaginal opening, the rectum, tail base and down the legs) and

neurological signs of disease (abdominal distention indicative of fecal or urine retention

or, rarely, hind-limb paralysis) or other signs of morbidity (hunched posture, lethargy,

dehydration, chills). Those exhibiting severe morbidity were sacrificed. The recorded

day of death was when the mouse was found dead or had to be sacrificed.

Other mice were sacrificed at specific times after virus inoculation to assess the

spread of virus infection to various tissues. For mice inoculated with HSV-2/Gal, the

vagina and the entire spinal column, as shown in Figure A1.4, were removed after

sacrifice. The vagina was split open longitudinally and the vertebrae of the spinal

column were cut to expose the spinal cord. These organs were fixed in 2%

paraformaldehyde/0.02% Nonidet-P40 in PBS for 4-6 hrs and then stained overnight

with X-gal (solution: 1 mg/ml 5-bromo-4-chloro-3-indolyl-β-D-galactopyranoside, 3 mM

potassium ferrous cyanide, 3 mM ferric cyanide, 2 mM magnesium chloride, 0.1 mM

EGTA, 0.01% sodium deoxycholate and 0.02% Nonidet P40). With the aid of a

dissecting microscope, staining of the vaginal luminal surfaces was scored as follows: 0

= no blue staining; 1 = <5 blue foci; 2 = >5 foci; <30% of surface covered in blue

lesions; 3 = >30%, <50%; 4 = >50%, <80%; 5 = >80% covered in lesions, cervical area

infected. Staining of the ganglia, attached nerves and spinal cords was scored as

follows: 0 = no staining; 1 = 2-3 positive ganglia in sacral region only; 2 = 3-5 positive

ganglia in sacral region, nerves positive or negative; 3 = >30% of ganglia positive in

lumbar/sacral region, nerves positive, spinal cord positive or negative; 4 = >50% of

ganglia positive in lumbar/sacral region, nerves positive, spinal cord positive; 5 = >80%

of ganglia positive in lumbar/sacral region, thoracic ganglia positive or negative, nerves

positive, spinal cord positive in multiple areas.

For mice inoculated with HSV-2, after sacrifice several organs were removed,

weighed, snap-frozen and stored at -80°C for virus titration by plaque assay. The

organs were homogenized in 2.5 ml of cold PBS-1% calf serum-0.1% glucose, using

disposable homogenizers, sonicated briefly, centrifuged at low speed to remove tissue

debris and the supernatant serially diluted for PFU quantification on Vero cells. Results

are presented as PFU per g of tissue.

Histology

C57BL/6, *Tnfrsf14*$^{-/-}$ and *Pvrl*$^{-/-}$ mice (n=3) were injected with Depo-Provera as

described in the preceding section and control mice of each genotype (n=3) were left

untreated. Six days after the injection, the mice were sacrificed and vaginas removed

for fixation, embedding in paraffin, and sectioning. The sections were stained with H&E.

Tissues from mice infected with HSV-2/Gal, including external skin stained with X-gal

(Figure A1.5), were also taken for histology to localize the X-gal stained cells in H&E-

stained sections.

Statistical tests

Kaplan-Meier survival analysis was performed using the Gehan-Breslow test. Means of

scores recorded for X-gal-stained tissues and geometric means of values for viral

infectious units in tissues were compared using the unpaired *t* test or Mann Whitney

rank-sum test.

ACKNOWLEDGMENTS